THE UNIVERSITY OF MICHIGAN
COLLEGE OF ENGINEERING

Scientific Report

EXCITATION OF SURFACE CURRENTS ON A PLASMA-IMMERSED CYLINDER BY ELECTROMAGNETIC AND ELECTROKINETIC WAVES

Edmund K. Miller

Department of Aerospace Engineering
High Altitude Engineering Laboratory

under contract with:
NATIONAL AERONAUTICS AND SPACE ADMINISTRATION
WASHINGTON, D. C.

initial research supported by:
NATIONAL AERONAUTICS AND SPACE ADMINISTRATION
GRANT NsG - 472
Langley Research Center, Hampton, Virginia

ORA project 05627
administered through:
OFFICE OF RESEARCH ADMINISTRATION, ANN ARBOR

September 1966

Acknowledgement

This report is a condensed version of the author's doctoral dissertation, which was completed while he was a member of the Radiation Laboratory of the Electrical Engineering Department. The thesis was submitted to the University of Michigan in 1965 in partial requirement for the degree of Doctor of Philosophy in Electrical Engineering. The author wishes to express his thanks to the members of his doctoral committee, Prof. Andrejs Olte, Chao-Min Chu, John S. King, Herschel Weil and Dr. Raymond F. Goodrich, for their help and guidance during this study. Special thanks are due to the committee chairman, Andrejs Olte, who suggested the problem, and who gave invaluable support throughout the course of the investigation.

The author also expresses his gratitude to Prof. Leslie M. Jones and Mr. Hal F. Schulte of the High Altitude Engineering Laboratory at the University of Michigan, who have encouraged and made this report possible under NASA Contract No. NASr-54(05), Washington, D. C.

The research was supported in part by NASA under Grant NsG-472 with the Langley Research Center at Hampton, Virginia. The numerical computations were supported by the University of Michigan Computing Center.

TABLE OF CONTENTS

LIST OF FIGURES

LIST OF FIGURES (continued)

LIST OF FIGURES (continued)

LIST OF FIGURES (continued)

Abstract

A theoretical investigation of the surface currents excited by plane electromagnetic (EM) and electrokinetic (EK) waves on a metal cylinder immersed in a uniform, collisionless isotropic plasma is described. The formulation is based on a linearized treatment which proceeds from velocity moments of the Boltzmann equation for electrons together with Maxwell's equations. The sheath which forms about the cylinder, assumed to be at floating potential, is represented by two models, both of which take the sheath to be of finite thickness and the plasma outside the sheath to be uniform. In the first model, the sheath is approximated by a free-space layer called the vacuum sheath. Analytic solutions are given for the fields, for an arbitrary angle of wave incidence. It is found from the numerical calculations that the vacuum sheath tends to screen the EK wave from the cylinder, and produces a large attenuation of the surface currents excited by the EK wave. The sheath and EK wave are found on the other hand to negligibly affect the currents excited by the EM wave.

In the second, the inhomogeneous sheath model, the actual sheath is included in the formulation. Some results of numerical calculations carried out for normal wave incidence are presented. The effects of varying the sheath thickness and static potential are examined. In addition, numerical calculations are performed assuming either complete reflection or absorption of the electrons at the cylinder surface. It is found that the surface currents for EK wave incidence are substantially in agreement with results obtained from the vacuum sheath model. In particular, the inhomogeneous sheath model which was used has the effect of decreasing

the currents excited by the EK wave compared with the case where the plasma is uniform everywhere. For EM wave incidence on the other hand, the surface currents are found to be negligibly affected, both by the inhomogeneous sheath and plasma compressibility.

EXCITATION OF SURFACE CURRENTS ON A PLASMA-IMMERSED CYLINDER BY ELECTROMAGNETIC AND ELECTROKINETIC WAVES

I. The Vacuum Sheath

I. 1 Introduction

Considerable attention has been devoted in recent years to the influence of plasma compressibility on electromagnetic (EM) fields in a plasma. The usual method of accounting for the plasma compressibility is to introduce a scalar pressure term for the electrons in the electron equation of motion. The effect of this term for the uniform plasma, as was shown by Field (1956), is to introduce a longitudinal electron pressure wave, which we will refer to as the electrokinetic (EK) wave. This name was introduced by Hok (1958) since the energy in the wave is shared between the electric field due to charge separation and the kinetic energy of the electrons.

Small amplitude EM and EK waves can be shown to propagate independently in a uniform plasma, but they are coupled by plasma inhomogeneity, boundary effects, magnetic fields and non-linear effects. The coupling of these waves is of interest in such diverse studies as astrophysics, radar and antennas. Radio waves emitted by stars have been attributed to EK waves converted to EM radiation in the outer regions of the star. Studies relating to this aspect of the problem have been performed by Field (1956), Kritz and Mintzer (1960), and Tidman and Boyd (1962).

The influence of the EK wave on the scattering and radiating properties of plasma-immersed bodies has also been rather extensively investigated. Cohen (1962), Hessel and Shmoys (1962), Wait (1964a, 1964b, 1965a) and Seshadri (1965a, 1965b) have looked into the radiation problem, while Cohen (1962), Yildiz (1963), Seshadri et. al. (1964) and Wait (1965b) have explored the scattering problem. Parker et. al. (1964) have analyzed a related problem, the scattering of EM waves from a cylinder of plasma in free space. Results obtained so far indicate that the impedance of a filamentary current source in the plasma will be dominated by the effect of the EK wave, but it is unsafe to extrapolate this result to the case of a physical antenna in the plasma. This is due to the fact the antenna boundary and sheath effects are ignored in the current filament analysis. Recent analyses due to Wait (1965a) and Seshadri (1965b) indicate that an antenna more than a few electron Debye lengths in diameter is much less affected by the plasma compressibility. A similar result was obtained by Seshadri (1965a) for current filament located in a cylindrical column of insulation surrounded by an infinite, uniform, compressible plasma.

The present study is concerned with the scattering properties of a plasma-immersed obstacle for plane EM and EK waves, taking into account the sheath which forms about an object immersed in a plasma. In particular, we will investigate the surface currents excited by the incident waves on an infinitely-long, perfectly-conducting, circular metal cylinder. There are two reasons for this interest in the currents.

(1) we wish to determine the feasability of detecting the presence of the EK wave in a plasma by a measurement of the surface currents it may excite on such a cylinder; and (2) it is of interest to establish the effect of the plasma compressibility and sheath on the currents excited by the EM wave. This investigation will involve examining the contribution to the surface currents excited by the EK wave of both the cylinder surface and sheath-uniform plasma interface (boundary coupling), and the inhomogeneous sheath (inhomogeneity coupling).

It is assumed in the analysis that the cylinder is drawing zero net current from the plasma, so that the sheath is a region with a deficiency of electrons. In Part I of this report, the actual sheath is replaced by a free space layer, which we call the vacuum sheath model. In Part II, the actual inhomogeneous sheath will be accounted for. In both cases, the sheath is taken to extend only a finite distance from the cylinder surface and the plasma outside the sheath region is considered to be uniform. A summary of extensive numerical results will be presented relating to the surface currents excited on the cylinder by the EM and EK waves.

The incorporation of a free-space layer or vacuum sheath in place of the real physical sheath is a rough physical approximation, primarily because the coupling effect of the sheath inhomogeneity is ignored. However, there are some important advantages to be gained from the vacuum sheath analysis. First, the solution obtained from the vacuum sheath analysis can be used to serve as a numerical check on the results obtained from the inhomogeneous sheath analysis. Second, if a comparison of the results

obtained from the two models shows them to be in approximate agreement, a wider range of parameter variation can be studied using the vacuum sheath analysis, since its numerical solution requires considerably less computer time. Third, we should be able to infer the relative importance of the sheath innomogeneity and boundary coupling from a comparison of results obtained with the two models.

I. 2. Formulation

We take the plasma to be infinite in extent, and to consist of positive ions, electrons and neutrals. It is of uniform temperature throughout, and only slightly ionized, with the electrons and ions present in equal numbers on the average when the plasma is uniform. Electron collisions are ignored and the ions are neglected insofar as their effect on the collective plasma oscillations is concerned.

Upon taking velocity moments of the collisionless Boltzmann equation to second order in velocity, setting the heat flux tensor equal to zero and assuming a scalar electron pressure, there is obtained

$$\frac{\partial n}{\partial t} + \nabla \cdot (n\vec{v}) = 0 \qquad (1)$$

$$mn \left(\frac{\partial}{\partial t} + \vec{v} \cdot \nabla\right)\vec{v} = -en\vec{E} - \nabla P , \qquad (2)$$

m and -e are the electron mass and charge, and n and v are the macroscopic electron number density and vleocity. E is the electric field in the plasma and P is the electron pressure. In obtaining (1) and (2) we have neglected magnetic and gravitational force effects on the electrons. We also require Maxwell's equations, which are:

$$\nabla \times \vec{E} = -\mu_o \frac{\partial}{\partial t} \vec{H} \qquad (3)$$

$$\nabla \times \vec{H} = \epsilon_o \frac{\partial}{\partial t} \vec{E} - en\vec{v} \qquad (4)$$

where ϵ_o and μ_o are the permittivity and permeability of free space and H is the total magnetic field.

This set of equations is completed by introducing a relationship between the electron pressure and electron number density. The non-time varying or static pressure is taken to be related to the number density by

$$P = nkT$$

where T is the electron temperature and k is Boltzmann's constant. When the electron velocity distribution function is Maxwellian, as is assumed here, then

$$T = mv_r^2/3$$

where v_r is the electron root-mean-square velocity. For the time varying or dynamic pressure, we take, with subscript 1 denoting a dynamic quantity,

$$P_1 = \gamma n_1 kT$$

where γ is the ratio of the specific heats, and for one-dimensional adiabatic compression, $\gamma = 3$. It may be noted here that ignoring the dynamic plasma compressibility is equivalent to having $\gamma = 0$.

The final approximation which we introduce is the usual one of linearizing (1) to (4) by dividing the macroscopic variables into static and dynamic parts, where products in the dynamic terms may be neglected.

We thus use the following scheme to linearize (1) to (4),

$$n = n_o + n_1 \tag{5a}$$

$$\vec{E} = \vec{E}_1 \tag{5b}$$

$$\vec{H} = \vec{H}_1 \tag{5c}$$

$$\vec{v} = \vec{v}_1 \tag{5d}$$

where the subscript o denotes a static quantity and 1 denotes a dynamic quantity. Note that the inhomogeneous sheath analysis will require static electric field and static electron velocity terms in addition to those corresponding dynamic terms of (5), in the inhomogeneous sheath itself. Outside the sheath in the uniform plasma, the same equations apply in the vacuum sheath and inhomogeneous sheath analyses. Upon using (5) in (1) to (4), we obtain with a harmonic time dependence $e^{i\omega t}$,

$$i\omega n_1 + \nabla \cdot (n_o \vec{v}_1) = 0 \tag{6}$$

$$i\omega n_o \vec{v}_1 = -(e/m) n_o \vec{E}_1 - v_r^2 \nabla n_1 \tag{7}$$

$$\nabla \times \vec{E}_1 = -i\mu_o \omega \vec{H}_1 \tag{8}$$

$$\nabla \cdot \vec{E}_1 = -en_1/\epsilon_o \tag{9}$$

$$\nabla \times \vec{H}_1 = i\omega\epsilon_o \vec{E}_1 - en_o \vec{v}_1 \tag{10}$$

Following Field (1956), we can decompose the total electric field and the average electron velocity into solenoidal and irrotational parts, denoted respectively by the subscripts E and P, as

$$\vec{E}_1 = \vec{E}_E + \vec{E}_P$$

$$\vec{v}_1 = \vec{v}_E + \vec{v}_P$$

It is easy to show that

$$(\nabla^2 + K_E^2)\vec{E}_E = 0 \tag{11}$$

$$(\nabla^2 + K_P^2)\vec{E}_P = 0 \tag{12}$$

where E_E represents the usual EM wave electric field and E_P the EK wave electric field. K_E and K_P are given by

$$K_E = K_{Eo}\sqrt{\epsilon_r}$$

$$K_P = K_E\, v_\ell / v_r$$

$$\epsilon_r = 1 - N^2$$

$$N = \omega_P/\omega = f_P/f$$

$$\omega_P^2 = e^2 n_o/(\epsilon_o m)$$

v_ℓ is the velocity of light in free space, and K_{Eo} is the free space EM plane wave propagation constant.

It is instructive to rewrite (11) and (12) as

$$(\nabla^2 + K_E^2)\vec{H}_1 = 0 \tag{13}$$

$$(\nabla^2 + K_P^2)n_1 = 0 \tag{14}$$

These forms for (11) and (12) emphasize the independence of the magnetic field H_1, associated with the EM wave, and the dynamic electron density n_1, associated with the EK wave, in a uniform plasma. When there are inhomogeneities in the plasma such as temperature or density, then (13) and (14) no longer hold, and instead variations in H_1 and n_1 are coupled. Note also, that the wavelengths of the EM and EK waves at the same frequency are in the ratio (v_ℓ / v_r), a result which leads to some interesting consequences which will be discussed below.

We are now in a position to complete the specification of the boundary value problem for the analysis of the vacuum sheath. The infinitely-long, circular cylinder is oriented with its axis coincident with the z-axis of a cylindrical coordinate system (ρ, φ, z). The cylinder radius is denoted by c, and the concentric free-space layer which forms the vacuum sheath has the radius s at the vacuum sheath-uniform plasma interface (plasma interface) . A uniform plasma is taken to exist in the region $\rho>s$. Equations (13) and (14) serve to describe wave propagation in the uniform plasma outside the vacuum sheath, while only (13) is required (with $\omega_P = 0$) in the vacuum sheath since the EK wave cannot propagate there.

The incident plane wave fields of the EM or EK wave type can be generated from a potential, which is in the cylindrical coordinate system,

$$\Phi_-^i = V_-^i e^{i\beta z} e^{i\lambda\rho\cos\varphi} = V_-^i e^{i\beta z} \sum_{n=-\infty}^{n=\infty} i^n e^{-in\varphi} J_n(\lambda_-\rho) \qquad (15)$$

where V_-^i is the amplitude, $\varphi = 0$ defines the front of the cylinder as viewed by the incident plane wave, and

$$\beta = K_- \cos\theta^i$$

$$\lambda_- = K_- \sin\theta^i = \sqrt{K_-^2 - \beta^2}$$

where K_- is the propagation constant of the incident wave, and θ^i is the angle of incidence measured from the positive z-axis. If the subscripts p, e and m respectively indicated above by dashes on λ , V^i, K, and Φ denote quantities associated with the EK wave and the transverse electric ($E_z = 0$) and transverse magnetic ($H_z = 0$) polarizations of the EM waves, then the incident electric fields are obtained from

$$\vec{E}_p = \nabla\Phi_p^i \qquad (16)$$

$$\vec{E}_e = \nabla \times (\Phi_e^i \hat{z}) \qquad (17)$$

$$\vec{E}_m = \frac{1}{K_E} \nabla \times \nabla \times (\Phi_m^i \hat{z}) \qquad (18)$$

The field quantities produced by the scattering of the incident wave can be similarly generated from potentials given by

$$\Phi_{-}^{-} = e^{i\beta z} \sum_{n=-\infty}^{n=\infty} A_{n--}^{-} H_n^{(1,2)} (\lambda_{-}\rho)\, e^{-in\varphi} \qquad (19)$$

where

$$\lambda_{-} = \sqrt{K_{-}^2 - \beta^2}$$

$K_{-} = K_P$ for the scattered EK fields, while $K_{-} = K_E$ for the EM fields in the plasma and $K_{-} = K_{Eo}$ for the EM fields in the vacuum sheath. The subscript on λ and Φ indicates the mode type, in accordance with K_{-}. Hankel functions of the first and second kind are used respectively for inward and outward traveling fields in the radial direction. The superscripts S, T, and R will be used respectively to denote fields scattered at the plasma interface, those transmitted through the sheath to the cylinder and those reflected at the cylinder surface. The subscripts on the Fourier coefficients A_{n--}^{-} denote in order, the mode number, the incident wave type and the mode type produced by the incident wave.

A solution to the problem now requires that all the Fourier coefficients A_{n--}^{-} be found for each kind of incident wave. Since there are seven A_{n--}^{-}'s for a given incident wave type, seven boundary conditions are needed to complete the boundary value problem for the vacuum sheath. In accordance with other analyses of EM and EK wave propagation (Wait, 1964b and Seshadri et. al, 1964) and others we require continuity of the tangential electric and magnetic fields at the plasma interface, and vanishing of the tangential electric field on the cylinder surface, which gives six scalar boundary conditions.

The one remaining boundary condition is generally taken to involve the electron motion at the plasma boundary, in this case, the plasma interface. Wait (1964b), for the case of vacuum sheath enclosing the spherical dipole antenna, used the condition that the normal electron velocity vanish at the plasma interface. This same condition has been employed by Hessel et. al. (1962), Yildiz (1963), and Seshadri (1965a, 1965b). Cohen (1962) on the other hand, proposed a boundary condition on the normal electron velocity at a metal surface which relates it to the electric field and electron number density, as

$$\hat{\rho} \cdot \vec{v}_1 = Y_A \hat{\rho} \cdot \vec{E}_1 + Y_B n_1 \qquad (20)$$

Y_A and Y_B are surface admittances relating the electron velocity, number density and electric field. Thus we see that the usual condition taking the normal electron velocity to vanish is equivalent to having both Y_A and Y_B zero, for the interface at which (20) is applied. It should be noted that the usual boundary condition used in acoustics is a relationship between velocity and pressure alone, through the surface admittance Y_B. An impenetrable boundary is characterized by $Y_B = 0$ (this will be called the hard boundary) and a completely permeable boundary by $Y_B = \infty$ (this is called the soft boundary).

Because the numerical computations which are required to evaluate the quantities of interest in this study are quite lengthy, and for want of a meaningful way to specify Y_A (Cohen, 1962), we choose to set $Y_A = 0$ here. Further, we restrict the value of Y_B to either zero or infinity, so that both the hard and soft boundaries are investigated, but no consideration is given to boundaries with surface admittances between these two extremes. It is

obvious that this choice for Y_B is on firmer physical grounds when the vacuum sheath is of zero thickness, (the sheathless case), since then there is a real physical boundary in contact with tne uniform plasma, which is not the case for non-zero sheath thickness.

The boundary conditions may be summarized as

$$\rho = s: \quad \hat{\rho} \times [(\vec{E}_1)_{plasma} - (\vec{E}_1)_{sheath}] = 0 \qquad (21a)$$

$$\hat{\rho} \times [(\vec{H}_1)_{plasma} - (\vec{H}_1)_{sheath}] = 0 \qquad (21b)$$

$$\hat{\rho} \cdot (\vec{v}_1)_{plasma} = 0 \text{ or } (n_1)_{plasma} = 0 \qquad (21c)$$

$$\rho = c: \quad \hat{\rho} \times (\vec{E}_1)_{sheath} = 0 \qquad (21d)$$

where the subscripts plasma and sheath refer to field quantities evaluated in the uniform plasma and vacuum sheath respectively.

Upon application of the boundary conditions for the hard boundary, there is obtained for the determination of the Fourier coefficients, the following set of equations.

$$\begin{bmatrix} \\ \\ \\ \\ \Delta \\ \\ \\ \\ \\ \end{bmatrix} \begin{bmatrix} A^S_{n-p} \\ A^S_{n-m} \\ A^S_{n-e} \\ A^T_{n-m} \\ A^T_{n-e} \\ A^R_{n-m} \\ A^R_{n-e} \end{bmatrix} = \begin{bmatrix} -i\beta S_p - (\lambda_E^2/K_E)S_m \\ (in/s)S_p - (\beta n/K_E s)S_m + S'_e \\ -(\lambda_E^2/\eta K_E)S_e \\ (1/\eta)S'_m - (\beta n/\eta s K_E)S_e \\ - 1/N^2\, S'_p - (i\beta/K_E)S'_m + (in/s)S_e \\ 0 \\ 0 \end{bmatrix} \qquad (22)$$

where the prime denotes differentiation with respect to ρ, and

$$S_p = V_p^i \, i^n \, J_n(\lambda_P s) \tag{23a}$$

$$S_m = V_m^i \, i^n \, J_n(\lambda_E s) \tag{23b}$$

$$S_e = V_e^i \, i^n \, J_n(\lambda_E s) \tag{23c}$$

$$[\Delta] =$$

$$\begin{vmatrix}
i\beta H_n^{(2)}(\lambda_P s) & \frac{\lambda_E^2}{K_E} H_n^{(2)}(\lambda_E s) & 0 & -\frac{\lambda_{Eo}^2}{K_{Eo}} H_n^{(1)}(\lambda_{Eo} s) & 0 & -\frac{\lambda_{Eo}^2}{K_{Eo}} H_n^{(2)}(\lambda_{Eo} s) & 0 \\
-\frac{in}{s} H_n^{(2)}(\lambda_P s) & \frac{\beta n}{K_E s} H_n^{(2)}(\lambda_E s) & -H_n^{(2)'}(\lambda_E s) & -\frac{\beta n}{K_{Eo} s} H_n^{(1)}(\lambda_{Eo} s) & H_n^{(1)'}(\lambda_{Eo} s) & -\frac{\beta n}{K_{Eo} s} H_n^{(2)}(\lambda_{Eo} s) & H_n^{(2)'}(\lambda_{Eo} s) \\
0 & 0 & \frac{\lambda_E^2}{K_E \eta} H_n^{(2)}(\lambda_E s) & 0 & -\frac{\lambda_{Eo}^2}{K_{Eo} \eta_o} H_n^{(1)}(\lambda_{Eo} s) & 0 & -\frac{\lambda_{Eo}^2}{K_{Eo} \eta_o} H_n^{(2)}(\lambda_{Eo} s) \\
0 & -\frac{1}{\eta} H_n^{(2)'}(\lambda_E s) & \frac{\beta n}{K_E s \eta} H_n^{(2)}(\lambda_E s) & \frac{1}{\eta_o} H_n^{(1)'}(\lambda_{Eo} s) & -\frac{\beta n}{K_{Eo} s \eta_o} H_n^{(1)}(\lambda_{Eo} s) & \frac{1}{\eta_o} H_n^{(2)'}(\lambda_{Eo} s) & -\frac{\beta n}{K_{Eo} s \eta_o} H_n^{(2)}(\lambda_{Eo} s) \\
\frac{1}{N^2} H_n^{(2)'}(\lambda_P s) & \frac{i\beta}{K_E} H_n^{(2)'}(\lambda_E s) & -\frac{in}{s} H_n^{(2)}(\lambda_E s) & 0 & 0 & 0 & 0 \\
0 & 0 & 0 & \frac{\lambda_{Eo}^2}{K_{Eo}} H_n^{(1)}(\lambda_{Eo} c) & 0 & \frac{\lambda_{Eo}^2}{K_{Eo}} H_n^{(2)}(\lambda_{Eo} c) & 0 \\
0 & 0 & 0 & \frac{\beta n}{K_{Eo} c} H_n^{(1)}(\lambda_{Eo} c) & -H_n^{(1)'}(\lambda_{Eo} c) & \frac{\beta n}{K_{Eo} c} H_n^{(2)}(\lambda_{Eo} c) & -H_n^{(2)'}(\lambda_{Eo} c)
\end{vmatrix}$$

(Equation 24)

When the soft boundary condition is considered, then the fifth rows of and the source vector on the right hand side of (22) are replaced by

$$\Delta_{5,1} \cdots \Delta_{5,7} = H_n^{(2)}(\lambda_P s),\ 0,\ \ldots,\ 0 \tag{25a}$$

$$S_5 = -S_P \tag{25b}$$

It is evident that there is no coupling of EK to EM waves (or vice versa) when the soft boundary condition is used. Subsequent discussion is consequently limited, for EK wave incidence, to the hard boundary only.

Note that the boundary conditions at the plasma interface ($\rho = s$) lead to the requirement that the scattered, transmitted and reflected fields exhibit the same z-direction variation, so that for an incident EK wave, there is explicitly obtained.

$$\lambda_P = K_P \sin\theta^i \tag{26a}$$

$$\lambda_E = K_E \sqrt{1 - (v_\ell/v_r)^2 \cos^2\theta^i} \tag{26b}$$

$$\lambda_{Eo} = K_{Eo} \sqrt{1 - (v_\ell/v_r)^2 (1-N^2)\cos^2\theta^i} \tag{26c}$$

Since for a typical plasma, $v_r \approx 10^{-3} v_\ell$, we observe that λ_{Eo} and λ_E become imaginary for θ^i slightly different from normal, and the EM fields produced by the EK wave are evanescent in the radial direction. We also observe that λ_E becomes imaginary before λ_{Eo} as θ^i is decreased from normal, so that there can exist trapped waves in the vacuum sheath for a small range of θ^i. For $T = 10^4\ ^oK$, a typical value for a laboratory plasma, λ_E becomes imaginary for $\theta^i < 89.87^o$. When the Hankel function arguments become imaginary, then

$$H_n^{(2)}(-iz) = \frac{2}{\pi} i^{n+1} K_n(z) \tag{27a}$$

$$H_n^{(1)}(-iz) = 2(-1)^n I_n(z) + \frac{2}{\pi} i^{n-1} K_n(z) \tag{27b}$$

where I_n and K_n are modified Bessel Functions and the -square root is used to ensure the proper behavior of the fields as $\rho \to \infty$.

When the incident EM wave is considered, then

$$\lambda_P = K_P \sqrt{1 - (v_r/v_\ell)^2 \cos^2\theta^i} \tag{28a}$$

$$\lambda_E = K_E \sin\theta^i \tag{28b}$$

$$\lambda_{Eo} = K_{Eo} \sqrt{1 - (1-N^2)\cos^2\theta^i} \tag{28c}$$

In this case, it is observed that $\lambda_P \approx K_P$ for all θ^i, and there is no possibility for the excitation of evanescent waves.

A solution for the Fourier coefficients of the various scattered, transmitted and reflected fields is tedious, but straightforward. We include here only expressions for $A^S_{n\text{-}p}$, $A^R_{n\text{-}m}$, and $A^R_{n\text{-}e}$. The others can be obtained from the expressions given in appendix A.

The three sets of coefficients obtained for each of the three types of incident wave, the EK wave and the transverse electric (TE wave) and transverse magnetic (or TM wave) polarizations of the EM wave, are given below. For purpose of shortening these expressions, the following abbreviations are used.

$$W(c,s) = H_n^{(1)}(\lambda_{Eo}c)H_n^{(2)}(\lambda_{Eo}s) - H_n^{(1)}(\lambda_{Eo}s)H_n^{(2)}(\lambda_{Eo}c) \tag{29a}$$

$$W(c',s) = H_n^{(1)'}(\lambda_{Eo}c)H_n^{(2)}(\lambda_{Eo}s) - H_n^{(1)}(\lambda_{Eo}s)H_n^{(2)'}(\lambda_{Eo}c) \tag{29b}$$

$$W(c,s') = H_n^{(1)}(\lambda_{Eo}c)H_n^{(2)'}(\lambda_{Eo}s) - H_n^{(1)'}(\lambda_{Eo}s)H_n^{(2)}(\lambda_{Eo}c) \tag{29c}$$

$$W(c',s') = H_n^{(1)'}(\lambda_{Eo}c)H_n^{(2)'}(\lambda_{Eo}s) - H_n^{(1)'}(\lambda_{Eo}s)H_n^{(2)'}(\lambda_{Eo}c) \tag{29d}$$

$$H_P = H_n^{(2)}(\lambda_P s) \tag{30a}$$

$$J_P = J_n(\lambda_P s) \tag{30b}$$

$$H_E = H_n^{(2)}(\lambda_E s) \tag{30c}$$

$$H_{Eo} = H_n^{(1)}(\lambda_{Eo} c) \tag{30d}$$

The determinant D_n of the matrix Δ can then be written

$$D_n = \frac{1}{H_{Eo}\, H'_{Eo}\, H_E\, H'_E} \left\{ \left(\frac{n}{s}\right)^2 H_E\, W(c',s) \left[K_{Eo} H_P \left(\frac{1}{\epsilon_r} H'_E\, W(c,s) \right.\right.\right.$$

$$\left. - \left(\frac{\lambda_{Eo}}{\lambda_E}\right)^3 H_E\, W(c,s') \right) + \left(\frac{\beta\omega_P}{v_\ell} \right)^2 \frac{\lambda_P}{\epsilon_r K_{Eo} \lambda_E^3}\, H_E H_P'\, W(c,s) \Bigg]$$

$$+ \left[\frac{\lambda_{Eo}}{\lambda_E} H'_E\, W(c',s) - H_E\, W(c',s') \right] \left[\frac{\lambda^2_{Eo}}{\epsilon_r K_{Eo}} W(c,s') \left(\beta^2 H_P H'_E \right.\right.$$

$$\left.\left. + \frac{\lambda_P}{N^2} \lambda_E\, H_E\, H'_P \right) - \frac{\lambda_P}{N^2} \frac{\lambda^3_{Eo}}{K_{Eo}} H'_E\, H'_P\, W(c,s) \right] \Bigg\} \tag{31}$$

where the prime denotes differentiation now with respect to argument.

The Fourier coefficients A^S_{n-p}, A^R_{n-m}, and A^R_{n-e} are:

Incident EK wave -

$$D_n A^S_{npp} = \frac{i^n V_p^i}{H_{Eo} H_{Eo}'} \left\{ \left(\frac{n}{s}\right)^2 W(c',s) \left[K_{Eo} \left(\frac{\lambda_{Eo}^3 H_E}{\lambda_E^3 H_E'} W(c,s') - \frac{1}{\epsilon_r} W(c,s) \right) J_P - \left(\frac{\beta\omega_P}{v_\ell}\right)^2 \frac{\lambda_P H_E / H_E'}{K_{Eo}\epsilon_r \lambda_E^3} J_P' W(c,s) \right] + \frac{(\beta\lambda_{Eo})^2}{\epsilon_r K_{Eo} \lambda_E} W(c,s') J_P \left[\lambda_E W(c',s') - \lambda_{Eo} \frac{H_E'}{H_E} W(c',s) \right] + \frac{\lambda_P}{N^2} \frac{\lambda_{Eo}^2}{K_{Eo}} J_P' \left[\left(\frac{\lambda_E H_E}{\epsilon_r H_E'} W(c,s') - \lambda_{Eo} W(c,s) \right) W(c',s') - \frac{\lambda_{Eo}}{\lambda_E} W(c',s) \left(\frac{\lambda_E}{\epsilon_r} W(c,s') - \lambda_{Eo} \frac{H_E'}{H_E} W(c,s) \right) \right] \right\} \quad (32a)$$

$$D_n A^R_{npm} = \frac{2\beta i^n V_p^i}{\pi s N^2 H_{Eo}'} \left\{ \lambda_{Eo} W(c',s') + W(c',s) \left(\left[\frac{n\omega_P}{v_\ell s} \right]^2 \frac{H_E}{\lambda_E^3 H_E'} - \frac{\lambda_{Eo}^2}{\lambda_E} \frac{H_E'}{H_E} \right) \right\} \quad (32b)$$

$$D_n A^R_{npe} = - \frac{2K_{Eo} n i^n V_p^i}{(Ns)^2 \pi H_{Eo}} \left\{ \frac{\lambda_{Eo}}{\lambda_E} \frac{H_E}{H_E'} W(c,s') - W(c,s) \right\} \quad (32c)$$

Incident TM wave -

$$D_n A^S_{nmp} = - \frac{2\beta i^n V_m^i}{\pi s \lambda_E K_E} \frac{1}{H_{Eo} H_{Eo}' H_E'} \left\{ \left(\frac{n\omega_P}{v_\ell s}\right)^2 \frac{1}{\epsilon_r K_{Eo}} W(c',s) W(c,s) + \frac{(\lambda_{Eo}\lambda_E)^2}{K_{Eo}\epsilon_r} W(c,s') \left[W(c',s') - \frac{\lambda_{Eo}}{\lambda_E} \frac{H_E'}{H_E} W(c',s) \right] \right\} \quad (33a)$$

$$D_n A^R_{nmm} = - \frac{2i^{n+1} V_m^i}{\pi s \lambda_E} \frac{1}{H_{Eo}' H_E'} \left\{ \left(\frac{n}{s}\right)^2 \frac{K_E}{\epsilon_r} W(c',s) H_P \right.$$

$$+ \frac{\lambda_P}{N^2} \frac{\lambda_{Eo}}{K_E} \lambda_E^2 \left[W(c',s') - \frac{\lambda_{Eo}}{\lambda_E} \frac{H_E'}{H_E} W(c',s) \right] H_P' \Bigg\}$$

$$D_n A^R_{nme} = - \frac{2\beta n i^{n+1} V_m^i}{\pi s^2 K_E \lambda_E H_{Eo} H_E'} \Bigg\{ \lambda_{Eo} K_{Eo} H_P W(c,s')$$

$$+ \frac{\lambda_P}{N^2} \left(\frac{\omega_P}{v_\ell} \right)^2 \frac{1}{K_{Eo}} H_P' W(c,s) \Bigg\} \qquad (33c)$$

Incident TE wave -

$$D_n A^S_{nep} = \frac{2\lambda_{Eo}^3 n i^n V_e^i W(c',s)}{\pi s^2 \epsilon_r \lambda_E K_{Eo} H_E H_E' H_{Eo} H_{Eo}'} \left[H_E W(c\, s',) - \frac{\lambda_E}{\lambda_{Eo}} H_E' W(c,s) \right] \qquad (34a)$$

$$D_n A^R_{nem} = - \frac{2\beta n\, i^{n+1} V_e^i}{\pi s^2 \epsilon_r H_E H_E' H_{Eo}'} W(c',s) \left[H_P H_E' - \frac{\lambda_P}{\lambda_E} H_E H_P' \right] \qquad (34b)$$

$$D_n A^R_{nee} = - \frac{2 \lambda_{Eo} i^{n+1} V_e^i}{\pi s \epsilon_r K_{Eo} H_E H_{Eo}} \Bigg\{ W(c,s') \left[\beta^2 H_P \right.$$

$$\left. + \frac{\lambda_P}{N^2} \lambda_E \frac{H_E}{H_E'} H_P' \right] - \frac{\lambda_P}{N^2} \lambda_{Eo} \epsilon_r W(c,s) H_P' \Bigg\} \qquad (34c)$$

It is interesting to observe that the TM field components decouple from the TE and EK components for normal incidence, as has been previously pointed out by Seshadri et. el. (1964) and Wait (1965b). The expressions obtained for the Fourier coefficients for TE and TM wave incident may be specialized to the situation where the plasma compressibility is neglected, insofar as the EK wave is concerned, by setting terms not involving λ_P

in these expressions equal to zero. This is equivalent to ignoring the dynamic electron pressure variations in the plasma, or as was mentioned previously, to $\gamma = 0$. The same result is obtained by use of the soft boundary condition, since there is then no coupling from the EM to EK waves, and the incident EM wave does not see the plasma compressibility. Note that this neglect of the dynamic plasma compressibility is not the same as the cold plasma limit, where $T \to 0$, as long as a sheath effect is taken into account, since a sheath does not form when in the limit $T \doteq 0$.

The surface currents excited by the incident wave are obtained from

$$\underline{K}^{(z)} = -\frac{4\, e^{i\beta z}}{\pi c \lambda_{Eo} \eta_o} \sum_{n=-\infty}^{n=\infty} e^{-in\varphi} \left[\frac{\beta n}{c K_{Eo}} \frac{A^R_{n-e}}{H'_{Eo}} + \frac{\lambda_{Eo}}{H_{Eo}} A^R_{n-m} \right] \tag{35a}$$

$$\underline{K}^{(\phi)} = \frac{4\, \lambda_{Eo} e^{i\beta z}}{\pi\, c\, K_{Eo} \eta_o} \sum_{n=-\infty}^{n=\infty} e^{-in\varphi} \frac{A^R_{n-e}}{H'_{Eo}} \tag{35b}$$

where the dash subscript indicates the kind of incident wave. Due to the behavior of the Fourier coefficients with a change in sign of the mode number n, the currents can be shown to depend upon φ as

$$K^{(z)}_p,\ K^{(z)}_m,\ K^{(\phi)}_e \ \alpha \sum_{n=0}^{n=\infty} (\ )_n \cos n\phi$$

$$K^{(\phi)}_p,\ K^{(\phi)}_m,\ K^{(z)}_e \ \alpha \sum_{n=1}^{n=\infty} (\ )_n \sin n\phi$$

It is interesting to note that the TM and EK induced currents exhibit the same symmetry on φ, a reasonable result since the electric fields of each lie in the plane of incidence.

I. 3. Numerical Results

The surface currents were obtained in phase and magnitude as a function of azimuthal angle ϕ for the following values of the parameters:

Incident wave frequency : f = 1 Gc/s

Electron temperature : $T = 10^4\ ^oK$

Ratio of plasma frequency to incident wave frequency: N = 0.7 to 0.99

Angle of incidence : θ^i = 0.05 to 0.5π

Cylinder radius : c = 0.005 to 1.0 cm

Sheath thickness :X=s-c= 0 to 20 electron Debye lengths

This choice for the parameter values was determined in part by a knowledge of typical values for a laboratory plasma, in anticipation of a possible experiment, and partly by practical considerations involved in performing the calculations and displaying the results. For example, with N = 0.7, i.e. f_P = 700 Mc/s, $K_P \tilde{=} 66.5\ cm^{-1}$, so that with c=1 cm on the order of 100 tems were required to sum the Fourier series for the current excited by the EK wave. While this summation can be carried out with reasonable accuracy, the current fluctuates so rapidly with changing azimuthal angle φ that it cannot be plotted on $8\frac{1}{2}$ by 11 inch graph paper. Thus, the graphs which present the current magnitude as a function of ϕ are for c = 0.2 cm only. In addition, since the current magnitude is symmetric about φ = 0 degrees (the front of the cylinder) and φ = 180 degrees, results are shown for φ = 0 to 180 degrees only. The current phase is not shown; it was found that rapid changes in phase were associated with minima in the current magnitude.

The sheath thickness was varied between 0 and 20 electron Debye lengths (0 to 0.177 cm) since some theoretical studies by Self (1963), Parker (1963) and Laframbois (1964) for various geometries indicate that charge neutrality is obtained to within a few percent to 10 at 20 electron Debye lengths from a bounding surface of the plasma. The representation of the real inhomogeneous sheath by an equivalent vacuum sheath of the thickness used is thus suggested. The sheath thickness s-c, in units of the electron Debye length (D_ℓ), is given by X. Note that $D_\ell = v_r / (\sqrt{3}\,\omega_P)$ The current magnitude on the vertical axis of the graph is amperes/cm.

The most interesting and significant results obtained for the surface currents from the calculations performed are shown below, first for EK wave incidence, and then EM wave incidence, for $V_-^i = 1$. When subsequently, the currents excited by the two kinds of waves are compared, then V_-^i will be so chosen as to make the power flow densities in the incident plane waves equal. A more detailed presentation of the condensed results, which follow is given by Miller (1965). There are also included in Appendix C additional graphs of surface current excited by the EM and EK waves for the vacuum sheath model, which supplement the following discussion.

I. 3.1 Incident EK wave

The magnitude of the φ -component of current excited by the EK wave, $K_p^{(\varphi)}$, is shown in figure 1 for N = 0.7, $\theta^i = \pi/4$, c = 0.2 cm and with X, the sheath thickness in electron Debye lengths, a parameter. It is obvious that the sheath has a very strong influence over the current. Both its magnitude, and to a less extent its fluctuation as a function of φ, are decreased with

increasing sheath thickness. This attenuation by the sheath of the surface current excited by the EK wave is due to the fact that when $\theta^i = \pi/4$, radially evanescent EM fields are excited at the plasma interface by the EK wave, as discussed above. As a result, the fields at the cylinder surface, and hence the currents excited there, are attenuated compared with those for the sheathless case. Since the z-component of current exhibits the same general characteristics as the φ-component, it is not shown here.

When the maximum value of the current magnitude as a function of φ (this will be referred to as the maximum current magnitude) was observed for several values of the sheath thickness and angles of incidence, it was found to be an exponentially decreasing function of the sheath thickness, with a scale factor dependent upon the angle of incidence. The attenuation is a minimum at $\theta^i = \pi/2$; at this angle, the EM fields produced by the EK wave are radially propagating.

A summation of the first few terms in the Fourier series for the current $K_p^{(\varphi)}$ shows that the sheath attenuation A_s is proportional to

$$A_s \alpha \exp \left[- \sqrt{1-N^2} \cos\theta^i \; X/ (\sqrt{3}N) \right] \qquad (36)$$

for $\theta^i \leq 85^o$, $X \geq 2$ and $c \geq 0.1$ cm. This expression is in approximate agreement with the curves of figure 1, as well as with other results presented in Appendix C. We observe that the attenuating effect of the sheath is dependent upon the sheath thickness measured in terms of the incident planewave EK wavelength in the direction of incidence.

In figures 2 and 3 are presented the maximum current magnitudes for both the and z-components of the current as a function of N and c respectively, with $\theta^i =$ /4, X = 0 and 10. It may be observed that the

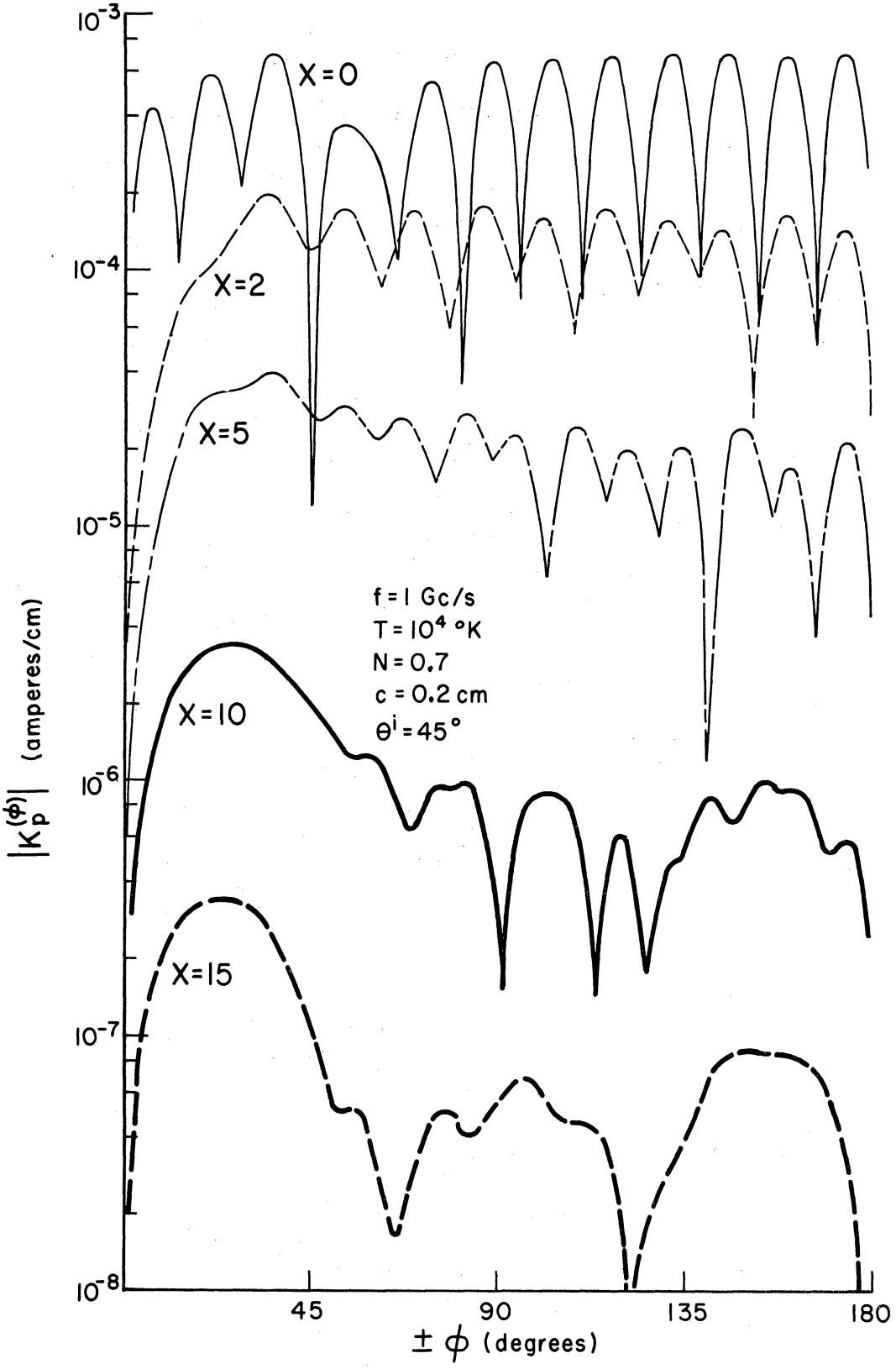

Figure 1. The magnitude of $K_p^{(\varphi)}$ as a function of azimuthal angle φ for the angle of incidence $\theta^i = \pi/4$ and the sheath thickness X in Debye lengths a parameter.

attenuating effect of the sheath is much more sensitive to variations in N than to variations in c. There is a general decrease in the maximum current magnitude with increasing N for the sheathless case, but no similar trend is observed when c is varied. When N approaches unity, the attentuation of the surface currents due to the sheath becomes small, in accordance with the expression for the sheath attenuation given by (36). In addition we note that when X = 10, the current reaches a maximum value when N is approximately 0.95.

There was found to be a regular decrease in the maximum current magnitudes for the cases X = 0 and X = 10 as θ^i was decreased from about 89^o to 9^o. However, a peaking in the z-component of current was observed as θ^i decreased from 90^o to the angle where the scattered EM fields in the plasma become evanescent, i.e. $\pi/2 - \theta^i \approx v_r/v_\ell$. The increase in the current magnitude for X = 0 was 2 to 3 orders of magnitude over the current values on either side of the peak. The peak is about 0.1^o wide at the points where the current falls to 0.1 of its maximum value.

I. 3. 2 Incident EM Wave

Since the value of $K_E c \ll 1$ for the parameter values primarily of interest here, the EM wave excited currents $K_m^{(\varphi)}$ and $K_e^{(z)}$ vary approximately as $\sin\varphi$ while $K_m^{(z)}$ and $K_e^{(\varphi)}$ are relatively independent of φ. Therefore their maximum magnitudes only are shown graphically while some of the parameters are varied. In cases where the current maximum magnitudes vary in a regular way with a parameter, the results are summarized rather than being presented graphically. Additional graphs of interest for EM wave incidence are included in Appendix C.

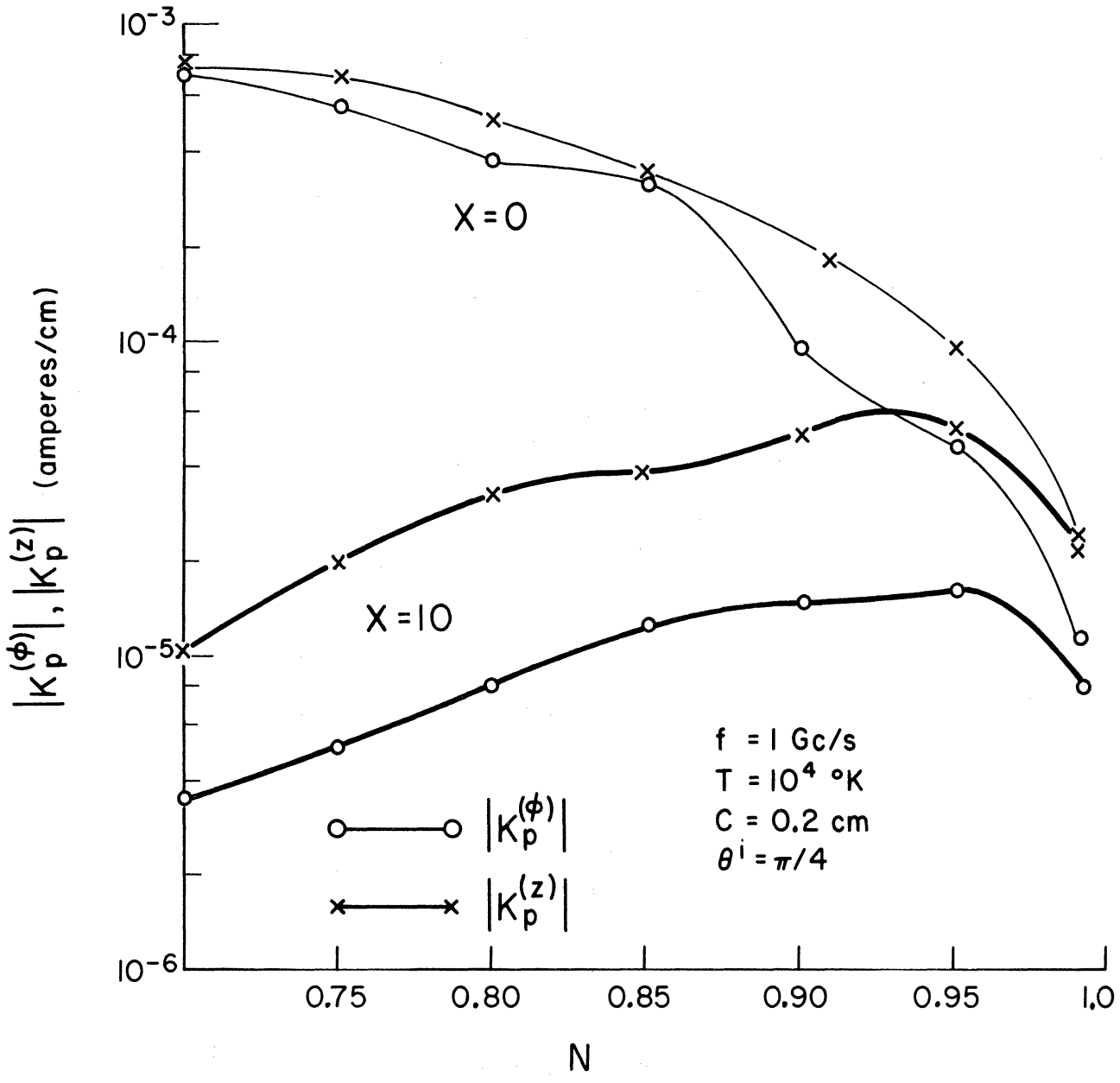

Figure 2. The maxi um values of $K_p^{(\varphi)}$ and $K_p^{(z)}$ as a function of the plasma frequency to incident wave frequency ratio N.

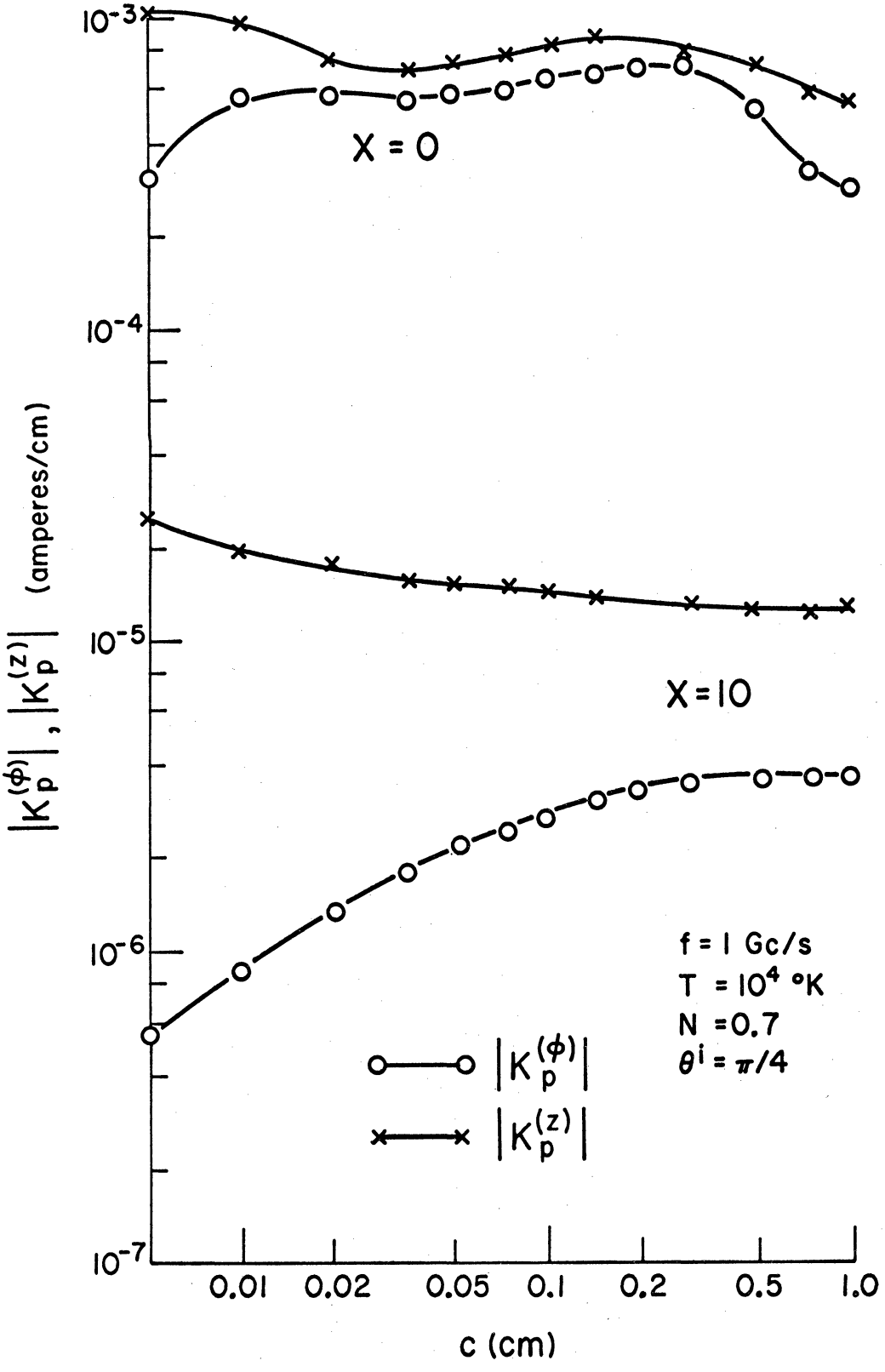

Figure 3. The maximum values of $K_p^{(\varphi)}$ and $K_p^{(z)}$ as a function of the cylinder radius c.

It was found that only the currents excited by the TM wave were for practical purposes dependent on the sheath thickness for X between 0 and 20. The z-component of current due to the TM wave, $K_m^{(z)}$, was found to decrease by a factor of about 3 in an exponential fashion, as X was increased from 0 to 20, with $\theta^i=9^o$ and c=0.2 cm. This dependence of $K_m^{(z)}$ on X decreased with increasing θ^i and c; for θ^i larger than 45^o, $K_m^{(z)}$ was practically independent of X. $K_m^{(\varphi)}$ was found to be increased by a factor of about 4 as X increased from 0 to 20, independent of θ^i. The currents excited by the TE wave changed less than 0.5% with X varying from 0 to 20. Now it is well known, that there is no conversion between the TM and TE polarizations when an EM wave is scattered from a perfectly conducting cylinder in free space (see Wait, 1965b). In the present study however, both the vacuum sheath and boundary coupling to the EK wave at the plasma interface are mechanisms which lead to conversion of TE to TM waves and TM to TE waves. That this is so may be verified by observing for example, that the coefficient A^R_{nme} which relates the reflected TE fields to the incident TM wave, is composed to two parts, one arising from the boundary coupling [the term with W(c, s')] and the other from the vacuum sheath [the term with W(c, s)]. This conversion of the incident wave polarization could be expected to have its maximum effect on the surface currents produced when a particular component of the current is determined by the TM or TE field alone. The only current component which has this property is $K_m^{(\varphi)}$, which is determined by A^R_{nme} alone. This explains the dependence of $K_m^{(\varphi)}$ upon X. Since the z-component of current is dependent upon both polarizations of the total field

at the cylinder surface, it is not so sensitive to X. By way of contrast, since there is no current component determined alone by A^R_{nem} as is the case of A^R_{nme}, we would not expect the TE wave currents to be as sensitive to the sheath thickness and plasma compressibility as are the TM wave currents, particularly $K_m^{(\varphi)}$.

The maximum current magnitudes were found to be monotonically decreasing functions with increasing N. This is to be expected since the impedance of the plasma increases as N increases, thereby decreasing the electric and magnetic fields for a constant value of V^i, and thus the currents excited.

In figure 4, where the maximum EM current magnitudes are plotted as a function of c, we observe results similar to those described above for the case of variable sheath thickness. Again, the currents due to the TE polarization are not dependent on the varying parameter, while those due to the TM polarization are. It is apparent also that the z-component of the current excited by the TM wave is much less affected by the sheath, than is the φ-component for the range of cylinder radii presented in figure 4. We further observe that for cylinder radii less than approximately 0.03 cm, the sheath exhibits an attenuating effect on $K_m^{(\varphi)}$, while for radii larger than this, the sheath leads to larger values for $K_m^{(\varphi)}$ than those obtained in the sheathless case.

The variation of the EM excited currents with varying angle of incidence was also examined. It was found that $K_m^{(\varphi)}$ and $K_e^{(z)}$ varied as $\sin\theta^i \cos\theta^i$. $K_e^{(\varphi)}$ was proportional to $\sin^2\theta^i$ and $K_m^{(z)}$ to $1/\log (K_F \sin\theta^i)$.

We may note here that the relative invariance of the currents due

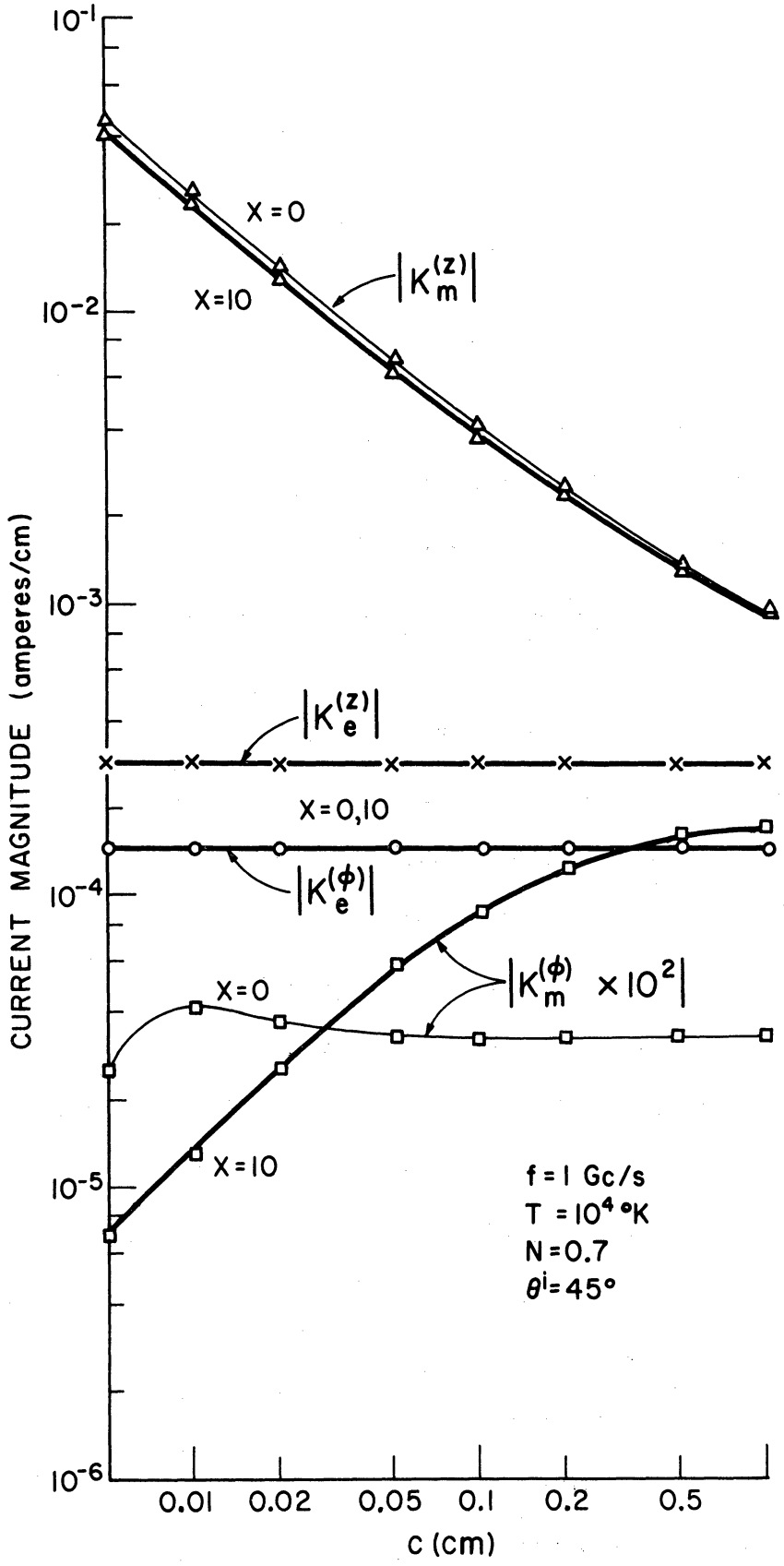

Figure 4. The maximum values of the current magnitudes excited by the incident EM wave as a function of cylinder radius c.

to the TE polarization with changing cylinder radius and sheath thickness is a demonstration of the Born approximation. That is of course that the total field near a scattering obstacle which is small in size in comparison with the EM wavelength in the direction of the electric field is approximately equal to the incident field. This is not the case for the TM polarization however, since then the electric field has a component along the axis of the infinitely long cylinder.

The currents for EM plane wave incidence were also calculated for the case where the dynamic plasma compressibility is neglected (i.e., $\gamma = 0$, or equivalently, the soft boundary condition). Except for $K_m^{(\varphi)}$, they were found to be changed by less than 5 per cent from the corresponding values obtained where the dynamic compressibility is taken into account, for cylinder radii of 0.005 cm to 60 cm ($K_E c \approx 7 \times 10^{-4}$ to 8.4).

$K_m^{(\varphi)}$ presents a special situation, since as remarked above, it is dependent upon the boundary coupling to the EK wave and the vacuum sheath for its excitation; in the absence of both, it is identically zero. When the sheath thickness X was greater than 2, $K_m^{(\varphi)}$ also was found to be changed by less than 5 per cent when the dynamic plasma compressibility was not accounted for. When however, X was decreased towards zero from a value of 2, the decrease in current caused by neglect of dynamic plasma compressibility became progressively greater, reaching a factor of about 2 for X = 1 and a factor of 3 at X = 0.5. Since $K_m^{(\varphi)}$ is quite sensitive to the sheath thickness and to a lesser extent, the boundary admittance Y_B, this suggests the possibility of determining the effective values of the sheath thickness and Y_B from an experimental determination of $K_m^{(\varphi)}$. It was also

found that for $X = 0$, the magnitude of $K_m^{(\varphi)}$ is proportional to the square root of the electron temperature T (i.e. proportional to v_r), for T less than $10^{4\,o}$ K. Since $K_m^{(\varphi)}$ is the only current component very sensitive to the dynamic plasma compressibility and electron temperature, and is generally 2 or more orders of magnitude less than the other current components caused by EM waves for a realistic range of electron temperature and other parameter values, it appears that the sheath and dynamic plasma compressibility may be neglected when considering the currents excited by the EM wave on a plasma-immersed obstacle.

We may also inquire as to the effect of the dynamic plasma compressibility and sheath on the fields scattered from the cylinder by an incident EM wave. From the current results and the scattering coefficients in Appendix A, we may infer that the scattered EM mode of the same polarization as the incident wave is negligibly affected by the dynamic plasma compressibility and sheath. The other polarization of the scattered EM mode, as well as the scattered EK mode are obviously determined by these two parameters. It appears, again from a consideration of the currents, that the scattering cross-section of the cylinder for scattering into either the cross-polarized EM mode or the EK mode would be small compared with that for scattering into the same polarization as the incident wave. Hence, it appears that the scattering properties of the cylinder for EM waves is only slightly affected by the dynamic plasma compressibility and sheath. However, since the production of cross-polarized components may give a practical method for measuring the importance of these effects, it seems that a calculation of the associated scattering cross-sections may be useful. This, however, is not taken up in this report.

I. 3.3 Comparison of EK and EM Excited Currents

We are now in a position to determine the feasibility of detecting the presence of the EK wave by the surface currents it produces. Since such a measurement would likely have to be carried out in a background of EM radiation, it is appropriate to compare the currents excited by both kinds of waves. The graphical results presented above show that for incident waves of unit potential amplitude, the EM waves generally produce currents of equal or greater magnitude than those due to the EK wave. This result can be misleading however, since there are two considerations to be taken into account before the comparison is meaningful. These are: (1) the power flow density in each incident wave, and (2) the satisfying of the linearity requirement upon which this analysis is based. The former point is important to the relative magnitudes of the induced currents while the latter places a limit on their absolute magnitudes in connection with a linearized analysis.

A reasonable comparison of the currents excited by the EM and EK waves is for equal power flow densities in the incident waves. This requirement together with a Poyntings vector for the EM and EK waves (Field 1956), leads to

$$V_p^i = N \sqrt{v_r / v_\ell}\ V_E^i \qquad (37)$$

where V_E^i represents either V_m^i or V_e^i. For an electron temperature of $10^4\ ^oK$, (37) reduces to

$$V_p^i = 4.74 \times 10^{-2}\ N\ V_E^i \qquad (38)$$

Thus, in order to compare the currents for EK wave incidence with those for EM wave incidence, the EK induced currents must be reduced by a factor of 0.0332 to 0.0470 for the range of N considered. This changes the picture considerably, since rather than there being currents on the same order of magnitude excited by both waves, the EK excited currents are now a minimum of 10 to 20 db less than the EM excited currents for the sheathless case (when the larger of the EM currents are considered).

The linearization requires that the dynamic electron number density be a small fraction **L** of the static number density, and likewise for the dynamic electron velocity in comparison with v_r, so that the plasma is not heated by the dynamic fields. These requirements for the incident waves can be stated

$$V_p^i \leq \frac{1}{L} \left[\frac{m}{e} \frac{v_r^2 N^2}{\sqrt{1-N^2}} \right] \tag{39a}$$

$$V_E^i \leq \frac{1}{L} \left[\frac{m}{e} \frac{v_r v_\ell}{\sqrt{1-N^2}} \right] \tag{39b}$$

With **L** = 10, N = 0.7 and T = 10^4 ^{o}K,

$$V_p^i \leq 0.178 \text{ volts} \tag{40a}$$

$$V_E^i \leq 159 \text{ volts} \tag{40b}$$

so that the results obtained with $V_E^i = 1$ and V_p^i determined by (38) will satisfy both the linearity requirement and equal power flow density criterion discussed above. Since the scattering of waves from the cylinder may give rise to local fields larger than those in the incident wave, (39) represents an upper limit on V_E^i and V_p^i.

With $V_E^i = 1$ and $V_p^i = 0.0332$ volts, and for the sheathless case only, the currents excited on the cylinder by the incident EM and EK waves for $\theta^i = \pi/4$ are shown together on figure 5. It can be seen that the z-component of current induced by the EK wave is about 0.003 that due to the TM wave and 0.05 that due to the TE wave. The φ - component of the EK current is about 0.1 that of the TE wave and 100 times that caused by the TM wave. Thus, apart from $K_m^{(\varphi)}$, the currents produced by the EK wave are 0.1 to 0.003 the corresponding currents due to the EM wave. When the attenuating effect of the vacuum sheath is considered, the EK induced currents are reduced by a further factor which may be as small as 10^{-6}, depending upon the angle of incidence and effective sheath thickness. It can thus be observed that the EK wave is considerably less efficient than the EM wave in producing surface currents on a plasma-immersed cylinder.

I. 4. Summary and Conclusions for Vacuum Sheath Analysis

The most significant finding of this investigation of the surface currents excited by EM and EK plane waves incident on a perfectly-conducting cylinder separated from a moderately-warm, ($T \leq 10^4\ ^oK$) uniform plasma by a vacuum sheath of variable thickness is the large attenuation which may be caused by the sheath of the surface currents excited on the cylinder by the EK wave. The attenuating effect of the vacuum sheath on the surface current was found to be approximately an exponential function of the sheath thickness. The currents excited by the EM wave on the other hand were found to be unaffected, for practical purposes, by the vacuum sheath or the dynamic compressibility. These results lead to the following conclusions, for a plasma with $T \leq 10^4\ ^oK$:

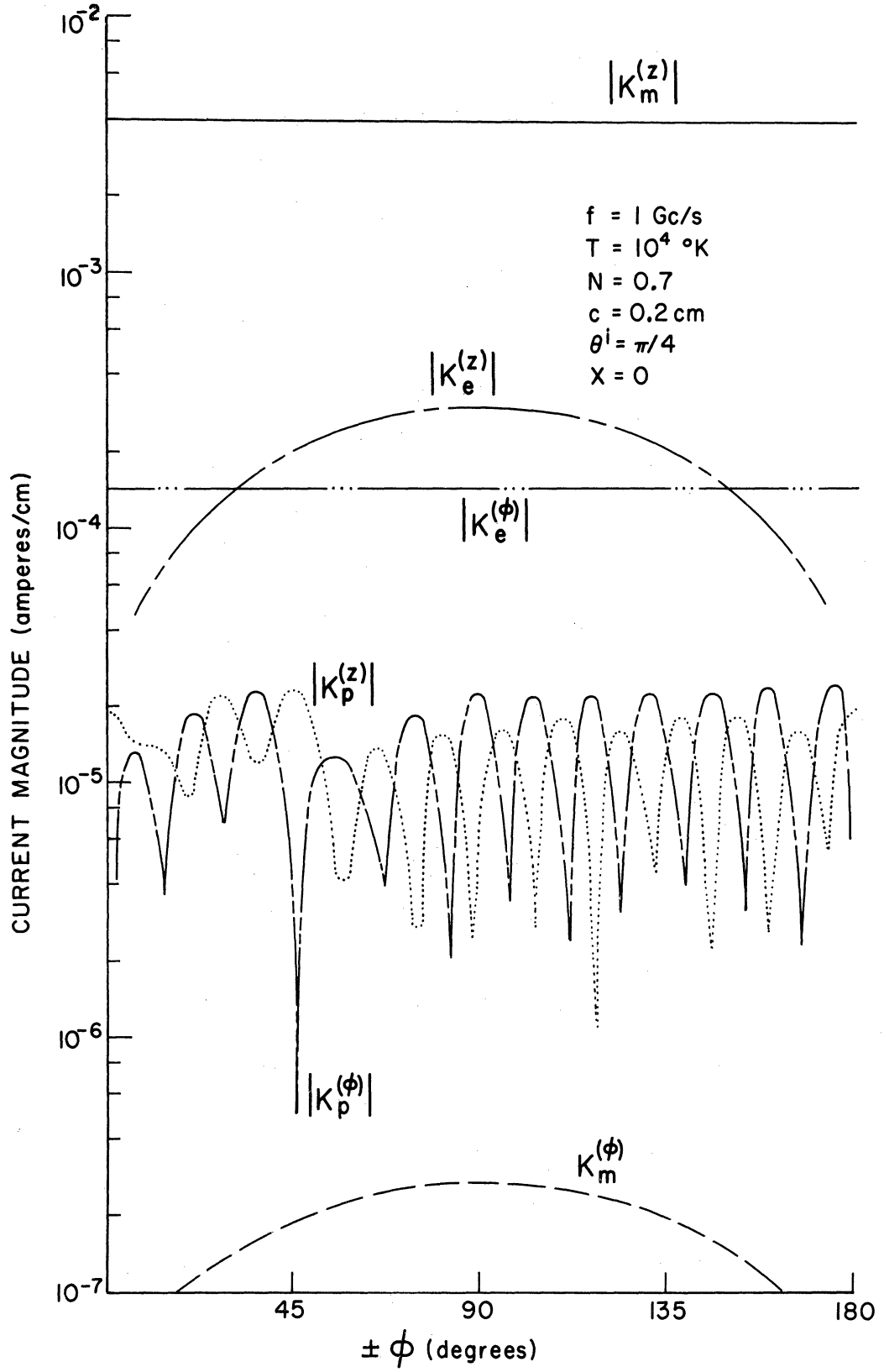

Figure 5. The maximum values of the current magnitudes excited by the incident EM and EK waves of equal power flow density ($V_e^i = V_m^i = 1$ V; $V_p^i = 0.0332$ V) as a function of azimuthal angle φ for an angle of incidence $\theta^i = \pi/4$.

(1) The sheath and dynamic plasma compressibility can be neglected when finding the currents excited on a plasma-immersed cylinder by EM waves.

(2) The EK wave is screened from the cylinder by the vacuum sheath, with the screening effect increasing with increasing sheath thickness and decreasing angle of incidence, measured from the cylinder axis.

(3) The EK wave is less efficient than the EM wave in exciting surface currents even when the screening effect of the sheath is not taken into account, by a factor of 10 to 500. It thus appears that the detection of the EK wave in a background of EM radiation by measuring the surface currents would be difficult to accomplish.

In addition, when we compare the results of this study for the scattering of EM waves from a plasma-immersed perfectly conducting cylinder with those of Parker et. al. (1964) for the scattering of EM waves from a plasma cylinder, an interesting observation can be made. For Parker's problem, both the dynamic plasma compressibility and sheath effects are required to account for the scattering properties of the plasma cylinder, whereas these effects have been shown here to negligibly affect the scattering of EM waves from the plasma-immersed cylinder. This implies that the treatment of EM wave scattering from obstacles in contact with plasmas requires accounting for sheath and dynamic plasma compressibility only if the geometry is such that standing EK waves may be excited in the plasma by the EM wave. We might similarly infer from the present results that the effect of the EK wave on the impedance characteristics of the plasma-immersed antenna would also be small, in contrast to the results of Cohen (1962) for a filamentary current source. Wait (1965a)

and Seshadri (1965b) have reached this conclusion for an infinitely long cylindrical antenna large in diameter compared with the EK wavelength.

Part II of this report, the vacuum sheath will be replaced by the actual inhomogeneous sheath, so that coupling due to both the boundary conditions and sheath inhomogeneity may be studied. The results presented here will be shown to be substantially in agreement with those obtained using the more physically realistic inhomogeneous sheath.

II The Inhomogeneous Sheath

II. 1 Introduction

In Part I of this report an investigation of the surface currents excited on an infinitely long, circular, plasma-immersed metal cylinder by electromagnetic (EM) and electrokinetic (EK) plane waves was described. The cylinder was assumed to be drawing no net current from the plasma, and the sheath surrounding it was replaced by a concentric free-space layer called the vacuum sheath. Some numerical results for the surface currents excited by both the EM and EK waves were presented.

The present section extends the analysis of I to take into account the actual inhomogeneous sheath which forms about the cylinder. The representation of the inhomogeneous sheath region with a spatially varying static electron number density and static electric field is obviously a more physically realistic approach than the vacuum sheath model of I. In particular, the inhomogeneous sheath treatment takes into account the coupling of the EK and EM fields due to both sheath inhomogeneity, and the boundary coupling, while the simpler approach used in I accounts only for the latter coupling mechanism. In addition, a comparison of results obtained from the inhomogeneous sheath analysis with those from the vacuum sheath analysis of I can establish the credibility of the vacuum sheath treatment. When equations which appeared in Part I are referred to, they will be preceded by I.

II. 2. Formulation

The formulation of I follows here also, through (I-4), i.e., the generation of a macroscopic continuity equation and equation of motion for the electrons from velocity moments of the Boltzmann equation, together with Maxwell's equations and an equation of state relating the scalar electron

pressure to the electron number density. Also, since we take the inhomogeneous sheath to extend out only a finite distance into the plasma from the surface of the cylinder, the uniform plasma outside the sheath is described by the same linearized equations used in I, i.e., (1-6) to (1-10). There are, however, static components of electric field and electron velocity in the inhomogeneous sheath which are zero in the uniform plasma, so that the set of linearized variables required for the linearization of (I-1) to (I - 4) for the inhomogeneous sheath, is now given by

$$n = n_o + n_1 \tag{1a}$$

$$\vec{E} = \vec{E}_o + \vec{E}_1 \tag{1b}$$

$$\vec{v} = \vec{v}_o + \vec{v}_1 \tag{1c}$$

$$\vec{H} = \vec{H}_1 \tag{1d}$$

where the subscripts o and 1 denote static and dynamic quantities respectively. Upon using (1) in (I-1) to (I-4), with a harmonic time dependence $e^{i\omega t}$, we obtain

$$i\omega n_1 + \nabla\cdot(n_o\vec{v}_1+n_1\vec{v}_o) = 0 \tag{2}$$

$$n_o[i\omega\vec{v}_1+(\vec{v}_1\cdot\nabla)\vec{v}_o+(\vec{v}_o\cdot\nabla)\vec{v}_1] + n_1(\vec{v}_o\cdot\nabla)\vec{v}_o = -\frac{e}{m}[n_o\vec{E}_1+n_1\vec{E}_o]-v_r^2\nabla n_1 \tag{3}$$

$$\nabla\times\vec{E}_1 = -i\omega\mu_o\vec{H}_1 \tag{4}$$

$$\nabla\cdot\vec{E}_1 = -\frac{e}{\epsilon_o}n_1 \tag{5}$$

$$\nabla\times\vec{H}_1 = i\omega\epsilon_o\vec{E}_1-en_o\vec{v}_1-en_1\vec{v}_o \tag{6}$$

ϵ_o and μ_o are the permittivity and permeability respectively of free space, and -e and m are the electron charge and mass.

Equations (2) to (6) differ from the corresponding equations of I, (I-6) to (I-10), due to the terms in $\vec{E}_o$ and $\vec{v}_o$ which constitute a coupling mechanism between the EM and EK waves in the inhomogeneous sheath. These terms arise from the interaction of the warm plasma with the cylinder. When the cylinder draws zero net current from the plasma, i.e. its potential is floating and determined by the plasma alone, it acquires a negative charge since the root-mean-square electron velocity is greater than that of the ions. The potential which results from the negative charge is just sufficient to balance the flow of electrons and ions to the cylinder, so the total net current is zero. Obviously then, there exists both a static potential and electron velocity near the cylinder as well as a gradient in static electron density. This non-uniform region is called a sheath, or as we refer to it here, the inhomogeneous sheath to distinguish it from the vacuum sheath of I. The sheath regions tends to shield the cylinder from the rest of the plasma, and to support the entire potential drop from the uniform plasma to the cylinder. For practical purposes, charge neutrality in the plasma is restored in a distance of 10 to 20 electron Debye lengths (D_ℓ) from the cylinder (Self, 1963; Parker, 1963; Laframbois, 1964).

The usual procedure followed is to neglect the terms containing $\vec{v}_o$ in (2) to (6) (for example, Parker et al., 1964, for a similar problem, Bernstein and Rabinowitz, 1959, for a static problem). It is not obvious that $\vec{v}_o$ may be neglected, however. Indeed, one would expect that under certain circumstances, it may constitute a more important coupling mechanism between EM and EK fields in the sheath than the static electric

field, as for example, when the cylinder is biased positive with respect to its floating potential. It is shown however in Appendix B that for the situation of interest here, where the cylinder draws no net current from the plasma, terms in $\vec{v}_o$ contribute negligibly on the average over the sheath to (2) to (6) in comparison with other terms arising from the sheath inhomogeneity. We thus set $\vec{v}_o = 0$ in the following development.

Since the discussion of the appendix as well as our subsequent consideration of wave propagation in the inhomogeneous sheath require a knowledge of the static sheath characteristics, we briefly here consider the properties of the static inhomogeneous sheath.

II. 2. 1 The Static Sheath

The basic information which is required to describe the static sheath is its static potential as a function of position. Since the problem under consideration has axial and azimuthal symmetry, this means that we desire the variation of the static potential with the radius variable ρ in a cylindrical coordinate system. The electron and ion number densities and fluxes (or static velocities) are obtained from this potential and appropriate integrations of their respective velocity distribution functions. The problem of course is to find the potential.

One method to obtain the potential is to use the Boltzmann equations for the ions and electrons, together with Poisson's equation. The Boltzmann equations are manipulated to obtain expressions for the electron and ion number densities in terms of the potential and their velocity distribution functions, which when used with Poisson's equation lead to an integro-differential equation for the potential. This equation is solved subject to boundary conditions on the ion and electron motion at the boundary

(generally complete absorption of both is assumed). The analysis used depends very strongly on the application and the justification for making certain assumptions, e.g., neglect of collisions and the form of the velocity distribution functions. Thus the approach used in the interior problem, where the plasma is confined to some container, and the exterior problem, where a body is surrounded by plasma, may be quite different. Our purpose here is not to discuss at length any of the analysis involved, but to briefly touch on the more pertinent aspects of some treatments currently in the literature.

An examination of theoretical results for the sheath potential given by Bernstein and Rabinowitz (1959), and Laframbois (1964) for the spherical and cylindrical probes, that of Self (1963) for the planar geometry and Parker (1963) for the interior problem in a cylindrical geometry show that the sheath potential Φ_o as a function of coordinate ρ in the sheath may be approximately represented by

$$\Phi_o(\rho) = \Phi_c \left[\frac{s-\rho}{s-c}\right]^M \qquad (7a)$$

where Φ_c is the wall potential, s the coordinate of the sheath-uniform plasma interface (or simply plasma interface) and c is the coordinate of the bounding surface. In the cylindrical coordinate system (ρ, φ, z) which we use here, s and c are the radii of the plasma interface and cylinder respectively, with the cylinder axis coincident with the z-axis of the coordinate system. M is an adjustable parameter, and is about 4 for the results quoted. We note that even in the exterior problem where the plasma is of infinite extent, the potential drop and hence the inhomogeneous sheath, is confined for practical purposes to a region on the order of a few D_ℓ thick, so that while (7a) is an approximation, it is a reasonable and convenient

form from which to obtain Φ_o. Some experimental investigations of the sheath by Gabor et. al. (1955), Gierke et. al. (1961) and Harp and Kino (1963) also tend to confirm the validity of (7a), but with M nearer to a value of 2. It should be observed that the most appropriate value of M is dependent upon the sheath thickness, s-c.

The cylinder potential Φ_c, will be calculated from

$$\Phi_c = -\frac{kT}{e} \ln \left[\sqrt{\frac{m_i}{m}} \frac{1}{1.22}\right] \qquad (7b)$$

with Boltzmann's constant denoted by k and where m_i is the ion mass, which is given in atomic mass units in the following. This form is due to Self (1963) for the planar geometry. An expression due to Chen et. al. (1961), derived for a planar geometry, but with assumptions very different from those used by Self yields nearly identical numerical results. Unfortunately, no similar closed form has been found in the literature for the wall potential in the cylindrical geometry. However, values of Φ_c obtained from (7b) and some graphical results given by Laframbois (1964) for a cylindrical probe 20 D_ℓ lengths in diameter, are in agreement to within 10 percent where Laframbois' graphs may be accurately read. In addition, Parker (1963) obtained some numerical values for the wall potential of a cylindrical envelope enclosing a plasma which agree with (7b) to within 10 percent for envelopes more than a few D_ℓ in diameter. The evidence indicates that the wall potential is almost independent of geometry so long as the dimensions of the probe or envelope sufficiently exceed D_ℓ, the situation in which we shall be interested, thus justifying the use of (7b). We will treat Φ_c as an adjustable parameter through

varying m_i, so that the effect of a reasonable variation in its magnitude can be observed.

Once the form of the potential is known, it is an easy matter to find the static electron number density in the sheath by application of the Boltzmann equation, which yields, with T the electron temperature,

$$n_o(\rho) = n_\infty \exp\left[\frac{e\Phi_o(\rho)}{kT}\right] \tag{8}$$

This form for the electron number density is known as the Boltzmann distribution. It neglects the flow of electrons to the cylinder due to the static velocity $\vec{v}_o$, which as discussed in appendix B, causes $n_o(\rho)$ to differ from that obtained using (8) by less than 5 percent over the outer 80 percent of the sheath. There is a maximum descrepancy in (8) due to neglect of $\vec{v}_o$ of a factor of 2 at the cylinder surface. This relatively small difference between the more exact experession for $n_o(\rho)$, given by (B3) and (8), in view of the fact that $n_o(\rho)$ varies by two to three orders of magnitude over the sheath, justifies, we feel, the use of (8), which has the additional advantage over (B3) of being more convenient to use in the numerical calculations.

The other static sheath quantity required for (2) to (6) in addition to n_o and Φ_o, is the electric field $\vec{E}_o$ which we obtain from

$$\vec{E}_o(\rho) = -\nabla \Phi_o(\rho) \tag{9}$$

$\vec{E}_o(\rho)$ of course, has a radial component only.

II. 2. 2 The Dynamic Sheath

Upon dropping terms in $\vec{v}_o$ from (2) to (6), an equation for $\vec{E}_1$ can be obtained as

$$\vec{E}_1 = \frac{1}{i\omega\epsilon} [\nabla x\vec{H}_1 + \nabla Q_1 + \vec{L}_o Q_1] \tag{10}$$

with

$$\epsilon_r = 1 - \omega_p^2/\omega^2 = 1 - N^2$$

$$\epsilon = \epsilon_r \epsilon_o$$

$$Q_1 = - \frac{e}{i\omega} v_r^2 n_1$$

$$\vec{L}_o = \frac{e}{m v_r^2} \vec{E}_o$$

If we let

$$\vec{P} = \frac{\nabla \epsilon}{\epsilon}$$

and successively take the curl and divergence of (10), then upon using (4) to (6) there is obtained

$$(\nabla^2 + K_E^2)\vec{H}_1 + \vec{P} x \nabla x \vec{H}_1 = \nabla Q_1 x (\vec{L}_o + \vec{P}) \tag{11}$$

$$(\nabla^2 + K_P^2) Q_1 - \vec{P} \cdot (\nabla Q_1 + \vec{L}_o Q_1) + \nabla \cdot (\vec{L}_o Q_1) = \vec{P} \cdot \nabla x \vec{H}_1 \tag{12}$$

The use of Q_1 in place of n_1 is convenient since $\vec{H}_1$ and Q_1 then have the same dimensions, amperes/unit length.

Equations (11) and (12) are useful in illustrating the coupling of the magnetic field H_1, with the dynamic electron pressure variation to which Q_1 is proportional, which are associated with independently propagating waves in a uniform plasma. The coupling terms contain $\vec{P}$ or $\vec{L}_o$, both of which are determined by the static sheath potential Φ_o. When Φ_o is zero (i.e., $\Phi_c = 0$) then (11) and (12) reduce to (1-13) and (1-14) of I, the equations for the homogeneous plasma.

Since a solution for the dynamic fields in the sheath must be obtained by numerical methods, as (11) and (12) do not admit of closed form solution as they now stand, we use instead the first order differential equations corresponding to (11) and (12), which are more convenient to deal with in a numerical analysis. We first separate the radial, angular and z-dependence of the field quantities in the form

$$\vec{E}_1 = e^{i\beta z} \sum_{n=-\infty}^{n=\infty} e^{-in\phi} \hat{\alpha} E_n^{(\alpha)}(\rho) \tag{13}$$

$$\vec{v}_1 = e^{i\beta z} \sum_{n=-\infty}^{n=\infty} e^{-in\phi} \hat{\alpha} V_n^{(\alpha)}(\rho) \tag{14}$$

$$\vec{H}_1 = e^{i\beta z} \sum_{n=-\infty}^{n=\infty} e^{-in\phi} \hat{\alpha} H_n^{(\alpha)}(\rho) \tag{15}$$

$$Q_1 = e^{i\beta z} \sum_{n=-\infty}^{n=\infty} e^{-in\phi} Q_n(\rho) \tag{16}$$

α is summed over the coordinates ρ, φ and z, to obtain the following set of first-order differential equations

$$Q_n' = i\omega\epsilon E_n^{(\rho)} + i\frac{n}{\rho} H_n^{(z)} + i\beta H_n^{(\varphi)} - L_o Q_n \tag{17}$$

$$H_n^{(\varphi)'} = i\omega\epsilon E_n^{(z)} - \frac{1}{\rho} H_n^{(\varphi)} - i\frac{n}{\rho} H_n^{(\rho)} - i\beta Q_n \tag{18}$$

$$H_n^{(z)'} = -i\omega\epsilon E_n^{(\varphi)} + i\beta H_n^{(\rho)} - i\frac{n}{\rho} Q_n \tag{19}$$

$$E_n^{(\rho)'} = -\frac{1}{\rho} E_n^{(\rho)} + i\frac{n}{\rho} E_n^{(\varphi)} - i\beta E_n^{(z)} + \frac{i\omega}{\epsilon_o v_r^2} Q_n \tag{20}$$

$$E_n^{(\varphi)'} = -\frac{1}{\rho} E_n^{(\varphi)} - i\frac{n}{\rho} E_n^{(\rho)} - i\omega\mu_o H_n^{(z)} \tag{21}$$

$$E_n^{(z)'} = i\beta E_n^{(\rho)} + i\omega\mu_o H_n^{(\varphi)} \tag{22}$$

$H_n^{(\rho)}$ is given by

$$H_n^{(\rho)} = \frac{n}{\omega\mu_o\rho} E_n^{(z)} + \frac{\beta}{\omega\mu_o} E_n^{(\varphi)}$$

while

$$\vec{V}_n = \frac{1}{en_o}\left[-\nabla x\vec{H}_n + i\omega\epsilon_o \vec{E}_n\right]$$

The prime indicates differentiation with respect to ρ. Note that no derivatives of $V_n^{(\alpha)}$ of $H_n^{(\rho)}$ appear in these equations.

The dynamic sheath behavior is thus specified by a system of six first-order ordinary differential equations. It is evident that if terms in $\vec{v}_o$ had been retained, then the system would be of eighth-order, since radial derivatives of $V_n^{(\varphi, z)}$ would also be required, as shown by (3). Our problem of finding the surface currents on the cylinder now involves solving (17) to (22) subject to certain boundary conditions at the plasma

interface and the cylinder surface, for incident plane EM or EK waves. Since the EM wave of arbitrary polarization may be decomposed into the transverse magnetic ($H_z = 0$) or TM wave, and the transverse electric ($E_z = 0$) or TE wave, there are essentially three polarizations of incident wave which concern us.

The boundary conditions on the electric and magnetic fields are the ordinary ones from EM theory and are: continuity of the tangential electric and magnetic field components at the plasma interface, and vanishing of the tangential electric fields at the cylinder surface. This produces six scalar boundary condition equations. Since there are three types of scattered field in the uniform plasma in addition to the sixth order system of differential equations which give the fields in the inhomogeneous sheath, a total of nine scalar boundary conditions are required. Two of the remaining boundary conditions follow from acoustics (Kritz and Mintzer, 1960 and Cohen, 1962) and are continuity of the normal dynamic electron velocity and dynamic electron pressure at the plasma interface. (Note that continuity of the tangential electric and magnetic fields and the dynamic electron pressure at the plasma interface leads also to continuity of the tangential dynamic electron velocity there.)

The one remaining boundary condition again involves a relationship between the normal dynamic electron velocity and dynamic electron pressure as in I, but now at the cylinder surface rather than at the plasma interface. We choose again to use

$$\hat{\rho} \cdot \vec{v}_1 = Y_B n_1 \qquad (23)$$

where Y_B is the surface admittance introduced by Cohen (1962). As in I, we let $Y_B = 0$ or ∞, corresponding to a perfectly reflecting (hard) boundary and a perfectly absorbing (soft) boundary respectively. It was pointed out in I that the soft boundary was of no interest as far as the coupling between the EM and EK waves was concerned, since the coupling in the absence of plasma inhomogeneity is then zero. In the present case however, the EK wave will excite surface currents when the soft boundary condition is used due to the inhomogeneity coupling in the sheath. Thus the currents excited by the EK wave due to the boundary coupling and the inhomogeneity coupling acting together are obtained from using the hard boundary condition and that of the inhomogeneity coupling alone is obtained from the soft boundary condition, so that we can obtain an idea of the relative importance of each coupling mechanism. The boundary conditions can be stated at $\rho = s$:

$$\hat{\rho} \times \left[(\vec{E}_1)_{\text{plasma}} - (\vec{E}_1)_{\text{sheath}}\right] = 0 \qquad (23a)$$

$$\hat{\rho} \times \left[(\vec{H}_1)_{\text{plasma}} - (\vec{H}_1)_{\text{sheath}}\right] = 0 \qquad (23b)$$

$$\hat{\rho} \times \left[(\vec{v}_1)_{\text{plasma}} - (\vec{v}_1)_{\text{sheath}}\right] = 0 \qquad (23c)$$

$$(Q_1)_{\text{plasma}} - (Q_1)_{\text{sheath}} = 0 \qquad (23d)$$

and at $\rho = c$:

$$\hat{\rho} \times (\vec{E}_1)_{\text{sheath}} = 0 \qquad (24a)$$

$$\hat{\rho} \cdot (\vec{v}_1)_{\text{sheath}} = 0 \text{ or } (Q_1)_{\text{sheath}} = 0 \qquad (24b)$$

We again represent the incident waves and the fields in the uniform plasma ($\rho > s$) scattered from the plasma interface, by a potential given in terms of a Fourier series of Bessel or Hankel functions, as in I,

and use the subscripts p, e, and m to denote quantities associated with the EK, TE and TM waves respectively. These boundary conditions may then be reduced to, at the plasma interface,

$$Q_n'(s)H_n^{(2)}(\lambda_p s) - Q_n(s)H_n^{(2)'}(\lambda_p s) = S_p \tag{25a}$$

$$H_n^{(z)'}(s) - i\beta H_n^{(\rho)}(s) + \frac{1}{\lambda_E^2} H_n^{(z)}(s) \left[\left(\frac{\beta n}{s}\right)^2 \frac{H_n^{(2)}(\lambda_E s)}{H_n^{(2)'}(\lambda_E s)} - K_E^2 \frac{H_n^{(2)'}(\lambda_E s)}{H_n^{(2)}(\lambda_E s)}\right] - \frac{\beta n}{s} \frac{H_n^{(2)}(\lambda_E s)}{H_n^{(2)'}(\lambda_E s)} H_n^{(\varphi)}(s) = S_e + \frac{\beta n}{\rho K_E} S_m \tag{25b}$$

$$H_n^{(\varphi)'}(s) + H_n^{(\varphi)}(s) \left[\frac{1}{s} + \lambda_E^2 \frac{H_n^{(2)}(\lambda_E s)}{H_n^{(2)'}(\lambda_E s)}\right] - \frac{\beta n}{s} \frac{H_n^{(2)}(\lambda_E s)}{H_n^{(2)'}(\lambda_E s)} H_n^{(z)}(s) + \frac{in}{s} H_n^{(\rho)}(s) = -\frac{\lambda_E^2}{K_E} S_m \tag{25c}$$

with $$S_p = -\frac{2\omega\epsilon}{\pi s} i^n V_p^i$$

$$S_e = \frac{-2\omega\epsilon}{\pi s H_n^{(2)}(\lambda_E s)} i^n V_e^i$$

$$S_m = -\frac{2\omega\epsilon}{\pi s H_n^{(2)'}(\lambda_E s)} i^n V_m^i$$

and at the cylinder surface

$$E_n^{(\varphi)}(c) = 0 \tag{26a}$$

$$E_n^{(z)}(c) = 0 \tag{26b}$$

$$Q_n(c) = 0 \quad \text{or} \quad i\beta H_n^{(\varphi)}(c) + \frac{in}{c} H_n^{(z)}(c) + i\omega\epsilon_o E_n^{(\rho)}(c) = 0 \tag{26c}$$

where the prime indicates differentiation with respect to the radial variable, after which the argument is set equal to the value indicated. The z-separation

variable is given by

$$\beta = K_{\_} \cos \theta^i$$

where $K_{\_} = K_P$ for the incident EK wave, $K_{\_} = K_E$ for the incident TE or TM wave and θ^i is the angle of incidence measured from the positive z-axis. The front of the cylinder as viewed by the incident wave is defined by $\varphi = 0$. Further,

$$\lambda_E = \sqrt{K_E^2 - \beta^2}$$

$$\lambda_P = \sqrt{K_P^2 - \beta^2}$$

and as in I, the EM fields produced by the EK wave may be evanescent. It will be assumed in using these equations, that there is only one wave type incident at a time, so that two of the three $V_{\_}^i$ are zero, while the $V_{\_}^i$ of the incident wave is taken to be unity.

The problem of finding the surface currents on the cylinder is now one of solving (17) to (22) subject to the boundary conditions (25) and (26). The surface currents are then obtained from

$$K_{\_}^{(z)} = H_1^{(\varphi)}(c) = \sum_{n=-\infty}^{n=\infty} e^{-in\varphi} H_n^{(\varphi)}(c) \qquad (27a)$$

$$K_{\_}^{(\varphi)} = -H_1^{(z)}(c) = -\sum_{n=-\infty}^{n=\infty} e^{-in\varphi} H_n^{(z)}(c) \qquad (27b)$$

where the dash subscript on K denotes the incident wave as TE, TM or EK, respectively. We can show from the relationship between cylindrical functions of positive and negative order n, and from the boundary conditions(25), that for TM and EK wave incidence, Q_1, $E_1^{(\rho)}$, $E_1^{(z)}$, and $H_1^{(\varphi)}$ are even functions of φ while $E_1^{(\varphi)}$, $H_1^{(\rho)}$, and $H_1^{(z)}$ are odd functions of φ. For TE wave incidence, the converse is true.

As a result, it follows that

$$K_e^{(\varphi)}, K_m^{(z)}, K_p^{(z)} \alpha \sum_{n=0}^{n=\infty} (\ )_n \cos n\varphi$$

$$K_e^{(z)}, K_m^{(\varphi)}, K_p^{(\varphi)} \alpha \sum_{n=1}^{n=\infty} (\ )_n \sin n\varphi$$

The problem of numerically solving a system of differential equations when the boundary conditions are applied at two boundaries is treated in detail by others (Fox, 1957; Collatz, 1960) and will not be discussed at length here. Parker et. al. (1964) also discussed this problem, in connection with the scattering of EM waves from a plasma column. The essential point is that in order to begin the numerical integration of (17) to (22), the starting values of the fields in these equations are required at one boundary. This information is contained in the boundary condition equations at both boundaries, one set of which cannot be utilized until the integration has been carried out from one boundary to the other. The difficulty is surmounted by successively setting equal to unity one of the unknown fields at the starting boundary, with the rest of the unknown fields at that boundary being set equal to zero, and performing the integration across the sheath. This procedure is repeated as many times as there are unknown starting values at the boundary where the integration is begun. A linear combination of these solutions is required to satisfy the boundary conditions at the second boundary, from which the coefficients of the linear combination are obtained, which are also the desired starting values. The procedure followed

was to begin the integration at the cylinder surface, using a Taylor series expansion to obtain the first point in the solution. Then a Runge-Kutta technique was used for the next four points in order to set up the values for the Milne predictor-corrector routine, which was used for the remainder of the integration. The number of integration points used was 25 with an accuracy on the order of 3 significant places being obtained for the total surface current.

II. 3. Numerical Results

It may be observed that (17) to (22) assume a particularly simple form for normal incidence, i.e., $\beta = 0$. In that case, the TE and EK waves decouple from the TM wave, a situation previously mentioned in I. Because of the time-consuming nature of the numerical computations required for the solution of (17) to (22), the numerical results presented here are restricted to the case of normal incidence only. While this has the effect of reducing by a factor of about two the computer time required to find the surface currents for EK wave incidence, the computations are still 20 times as lengthly as those for the vacuum sheath model of I. Consequently, the range of parameter variations which could be investigated was much more limited for the inhomogeneous sheath analysis. A further factor contributing to limiting the amount of parameter variation is the fact that there are additional parameters appearing in the inhomogeneous sheath analysis, such as M and Φ_c in (7) for the static potential, as well as the additional value for $Y_B = \infty$ (i.e., the soft boundary).

The calculations for the inhomogeneous sheath were performed for normally incident plane TE and EK waves of unit potential amplitude for

the following parameter values:

Incident wave frequency	: f = 1Gc/s
Electron temperature	: $T = 10^4\ ^oK$
Ratio of plasma frequency to incident wave frequency	: N = 0.7
Angle of incidence	: $\theta^i = \pi/2$
Cylinder radius	: c = 0.2cm
Sheath thickness	: X = s-c = 5, 20 electron Debye lengths
Cylinder potential	: Φ_c = -3.06, -5.34 volts (m_i = 1, 200 atomic mass units)
Exponent of potential variation	: M = 2, 4, 10

In most cases, the calculations were performed for both the hard and soft boundaries. The current magnitudes in amperes/cm are presented graphically for $\varphi = 0^o$ to $\varphi = 180^o$ only, since they are symmetric about these two points. The current phase is not shown; rapid phase changes were found to be associated with minima in the current magnitudes.

II. 3.1 Incident EK Wave

The magnitude of the φ-component of current for the incident EK wave, $K_p^{(\varphi)}$, is shown in figure 6 for the hard and soft boundaries, with M = 2 and Φ_c = -5.34 V (m_i = 200). The sheath thickness X measured in units of electron Debye length, is 20. We observe that the fluctuations of current magnitude with azimuthal angle φ are quite similar for both curves, but that the current obtained when the hard boundary condition is used is 5 to 10 times larger than that for the soft boundary. This result is quite significant in that the boundary appears to be more effective in producing a surface current than does the sheath inhomogeneity. This observation

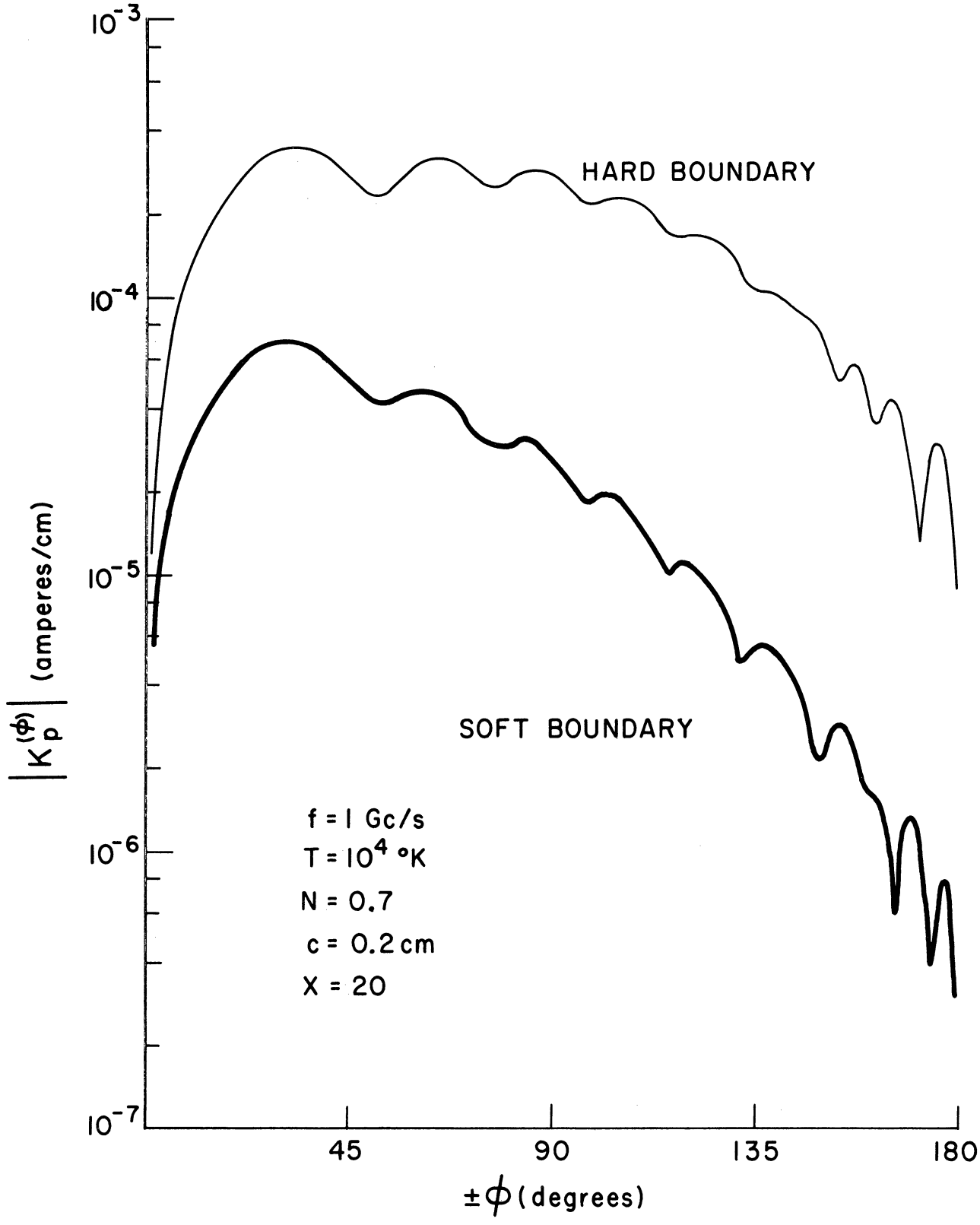

Figure 6. The magnitude of $K_p^{(\varphi)}$ as a function of azimuthal angle φ for normal EK wave incidence, with M = 2, Φ_c = - 5.34V and X = 20.

is based on the fact that when the soft boundary condition is used, there is no boundary coupling between the EK and EM fields, so that any surface currents produced by the EK wave then come as a result of the sheath inhomogeneity alone.

In order to compare the results of the inhomogeneous and vacuum sheath analyses, figure 7 presents the magnitude of $K_p^{(\varphi)}$ from the vacuum sheath results for normal EK wave incidence and the hard boundary condition, for several values of the vacuum sheath thickness X. We see that the X = 2 and X = 5 curves of figure 7 bracket the curve for the hard boundary of figure 6. In addition, the X = 20 curve of figure 7 bears a close resemblance to the soft boundary condition curve of figure 6. We also note that the current for the sheathless case of figure 7 is roughly 2 times that for the hard boundary and 20 times that of the soft boundary of figure 6. It might be inferred from these results that we can substitute a vacuum sheath with a surface admittance $Y_B = 0$ for the actual inhomogeneous sheath, and by the proper choice of vacuum sheath thickness, obtain surface currents excited by the EK wave which are in good quantitative agreement with those resulting from the inhomogeneous sheath.

In figure 8 are presented curves similar to those of figure 6, for the same parameter values except M which has been changed to a value of 4. We see that the fluctuation of the current magnitude with azimuthal angle φ is more pronounced in figure 8 than in figure 6. In addition, the current magnitude for the soft boundary of figure 8 has been increased by about 2 times over that of figure 6, while there is little change in the current mangitude for the hard boundary condition. This increase in the current

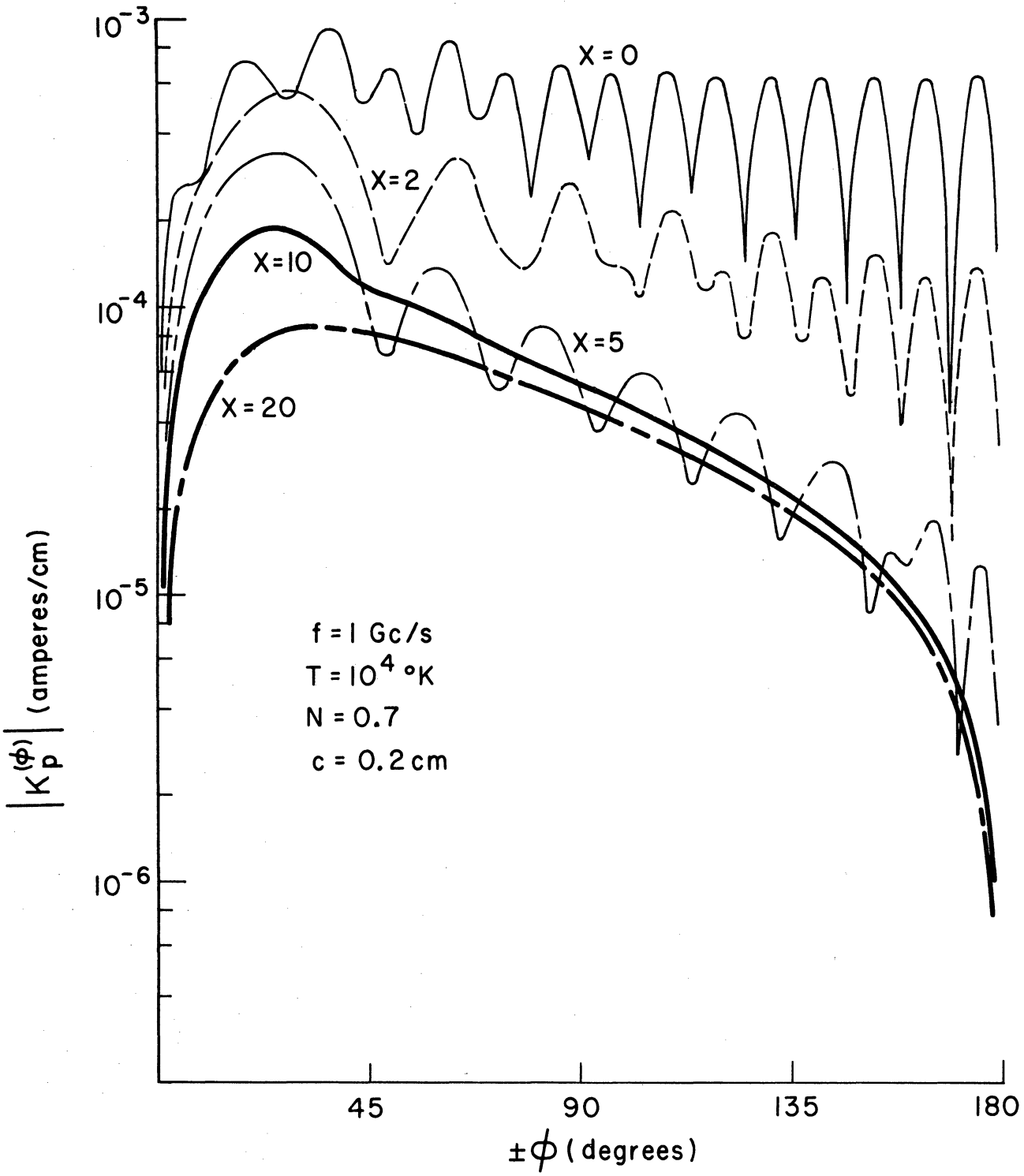

Figure 7. The magnitude of $K_p^{(\varphi)}$ as a function of azimuthal angle φ for the vacuum sheath model and normal EK wave incidence, with sheath thickness X a parameter.

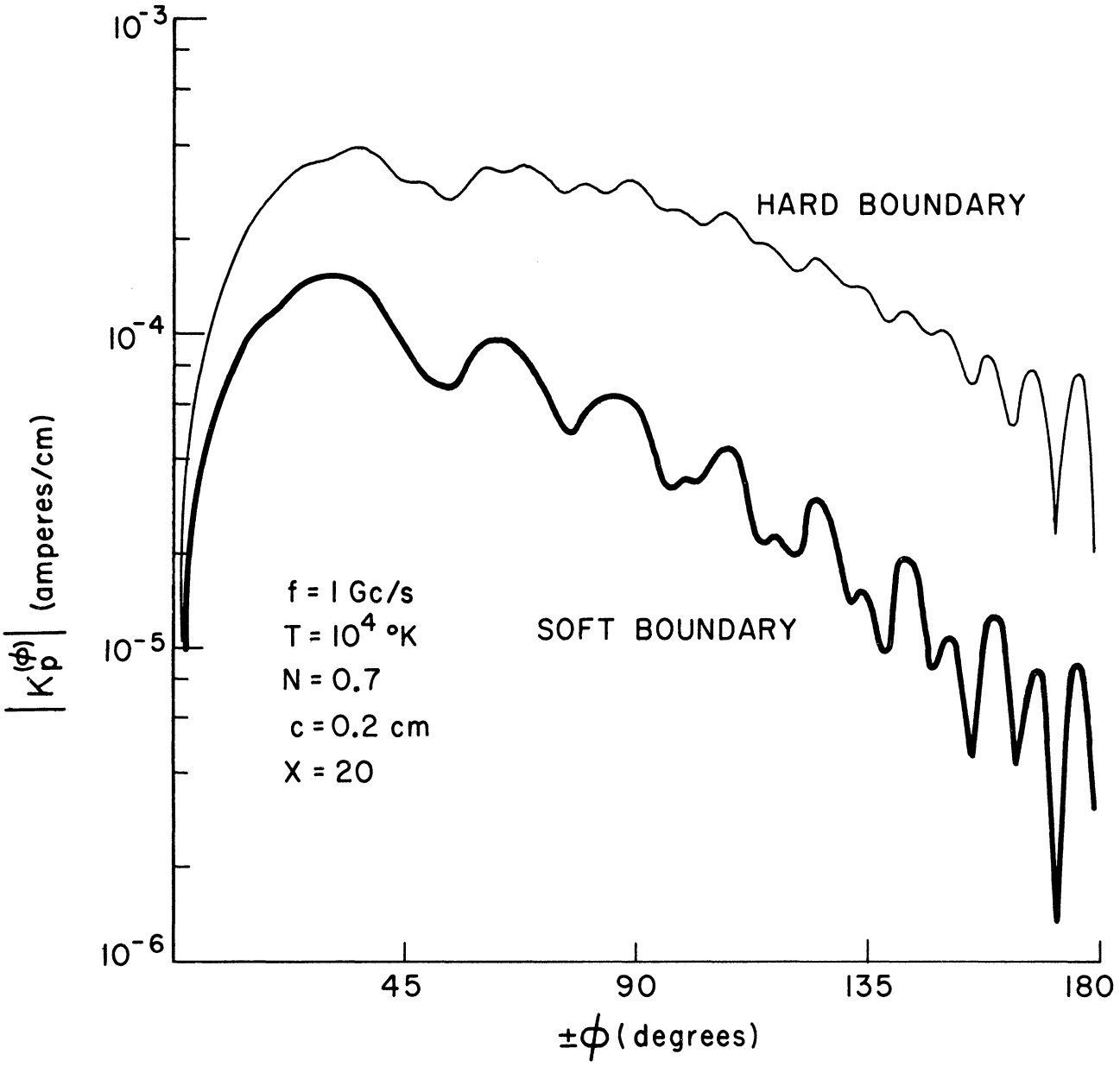

Figure 8. The magnitude of $K_p^{(\varphi)}$ as a function of azimuthal angle φ for normal EK wave incidence, with M = 4, Φ_c = - 5.34 V and X = 20.

magnitude for the soft boundary condition evidently arises from the greater degree of inhomogeneity in the sheath near the cylinder surface when M = 4. We may observe that the curves of figure 8 more closely resemble those for the vacuum sheath in figure 7 than do the curves of figure 6, in the fluctuation of the current magnitude as a function of azimuthal angle.

Figure 9 presents the current magnitude for the hard boundary condition only and the same parameter values as figure 8, but with Φ_c = -3.06 V (m_i = 1), and with M = 2 and M = 4. A comparison with the corresponding hard boundary condition curves of figures 6 and 8 shows that the inhomogeneous sheath current magnitudes are larger for the smaller value of Φ_c and in addition, bear a closer resemblance to the sheathless case current of figure 7. This seems reasonable, since the sheath inhomogeneity is proportional to the cylinder potential. The curves of figure 9 also show that the inhomogeneous sheath currents are closer to the sheathless case current of figure 7 for the larger value of M, a result which might be expected, since as M is made larger, the sheath inhomogeneity is confined to a progressively thinner area near the cylinder. This is further illustrated by figure 10 which shows the current magnitude for the hard boundary condition and the same parameter values as figure 9, but now with M = 10. The current shown in figure 10 is very similar to that for the sheathless case of figure 7.

The last graph of this series, figure 11, shows the current magnitudes for both the hard and soft boundary conditions, and the same parameter values as figure 6, but now the sheath thickness X = 5 rather than 20. Both curves are observed to exhibit greater fluctuation with changing azimuthal

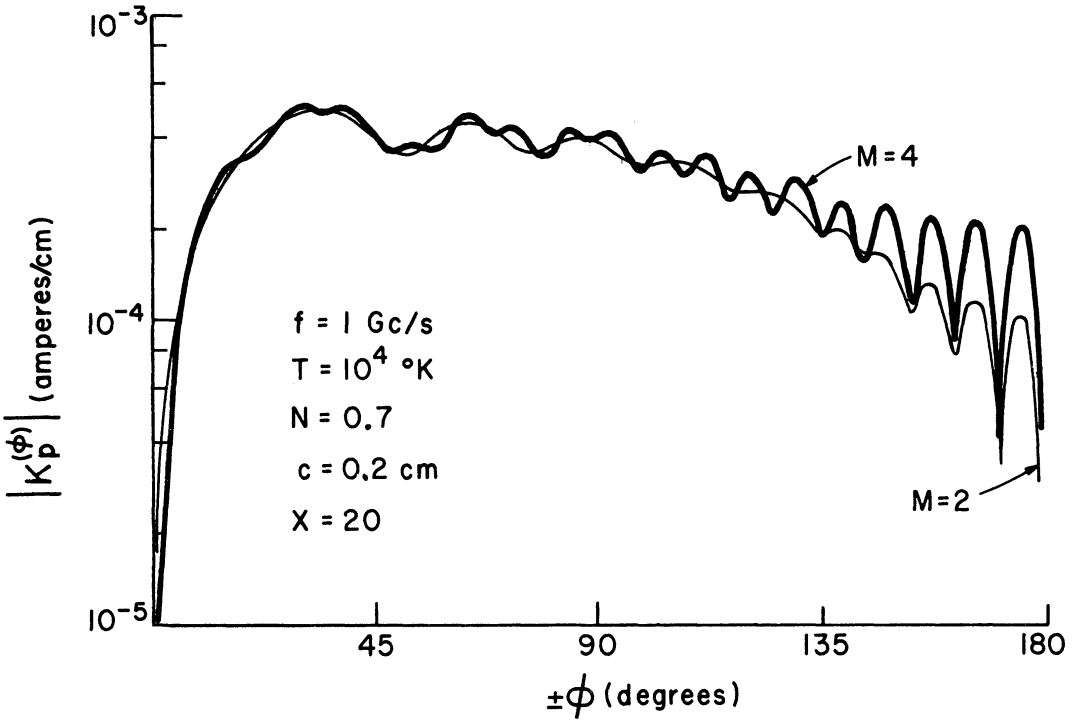

Figure 9. The magnitude of $K_p^{(\varphi)}$ as a function of azimuthal angle φ normal EK wave incidence, with Φ_c = - 3.06 V, M = 2, 4 and X = 20.

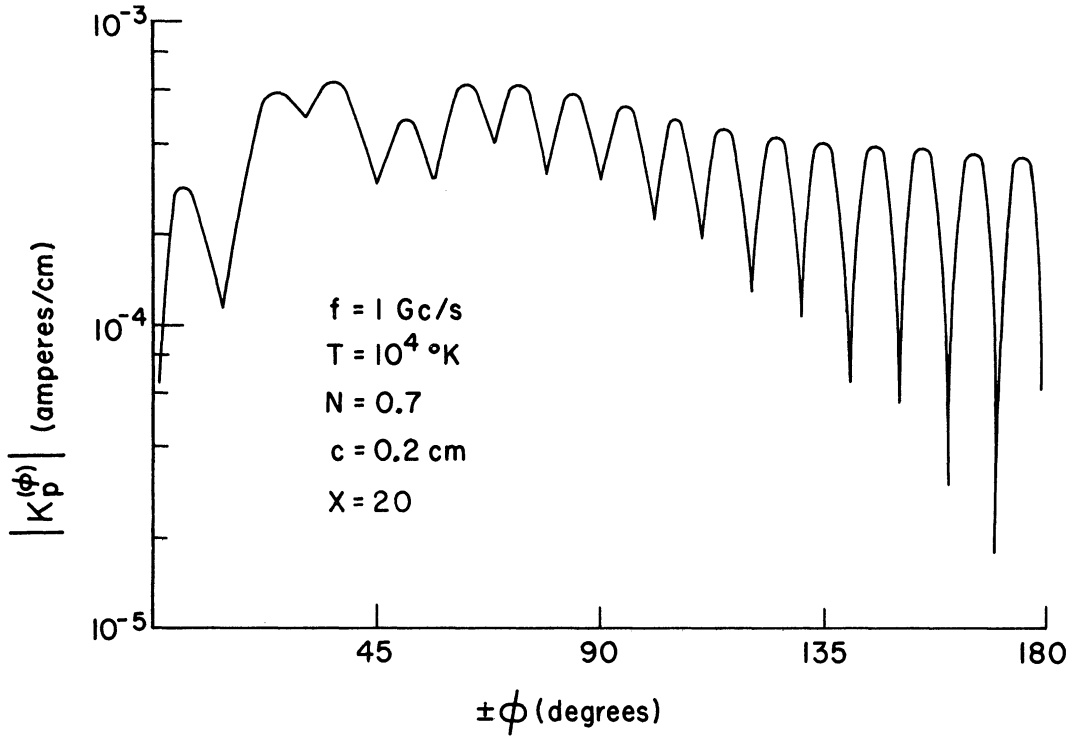

Figure 10. The magnitude of $K_p^{(\varphi)}$ as a function of azimuthal angle φ for normal EK wave incidence, with Φ_c = - 3.06 V, M = 10, and X = 20.

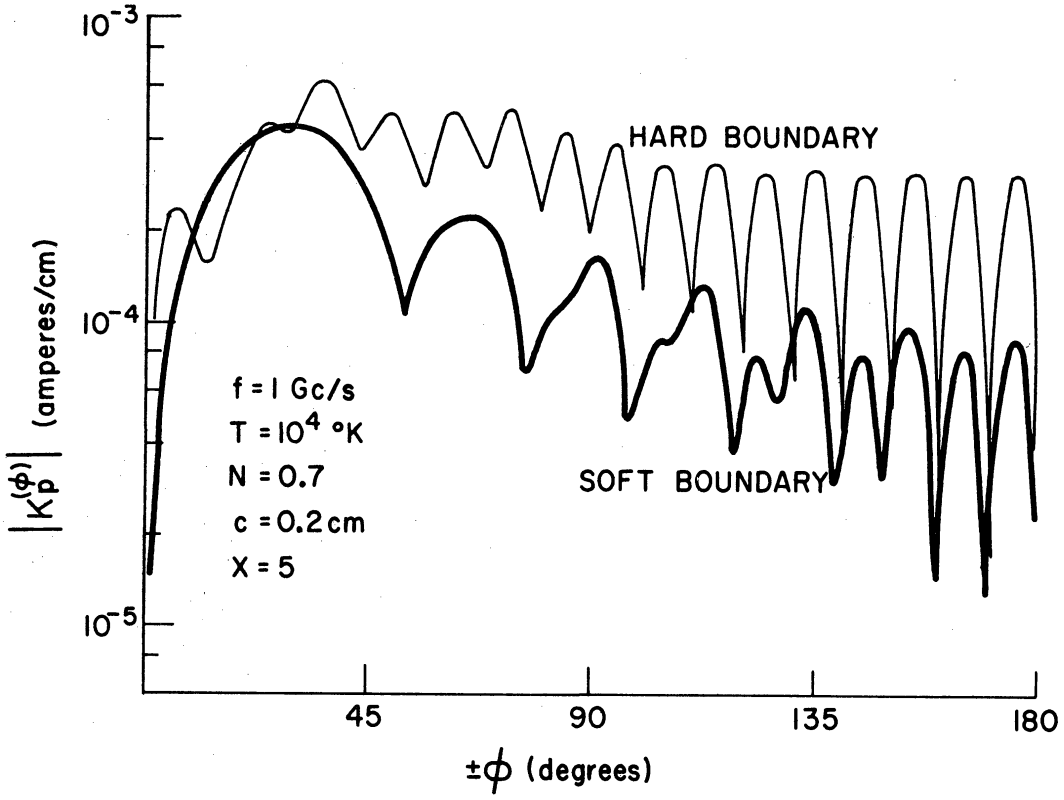

Figure 11. The magnitude of $K_p^{(\varphi)}$ as a function of azimuthal angle φ for normal EK wave incidence, with $\Phi_c = -5.34$ V, M = 2, and X = 5.

angle φ and increased magnitudes, compared with the corresponding curves of figure 6. The current for the soft boundary condition shows the larger increase in magnitude due to the decreased sheath thickness, so that now the current magnitude for the hard boundary is only 2 to 4 times larger than that for the soft boundary. Both curves are quite similar to the curves for the vacuum sheath analysis of figure 7. It is also apparent that decreasing the sheath thickness has an effect similar to increasing the power M, of the potential variation, for the hard boundary, as shown by figures 10 and 11.

II. 3. 2 Incident EM Wave

For normal plane wave incidence, it has been previously pointed out that the TM polarization of the EM wave decouples from the TE polarization of the EM wave and the EK wave. Consequently, only the TE polarization of the EM wave was considered in the numerical calculations for the inhomogeneous sheath. It was found that the current results obtained for TE wave incidence from the inhomogeneous sheath analysis were the same as those of the vacuum sheath analysis given in I, to three significant places, so no numerical results are presented here for TE wave incidence. This outcome tends to strengthen the conclusion reached in I, that the dynamic plasma compressibility and sheath have a negligible effect on the surface currents excited by the EM wave.

II. 3. 3 Linearization Criterion

The maximum allowable potential amplitude $\underline{V}^i$ of the incident plane waves was discussed in I, in connection with the linearized analysis which is used, and found to be given by

$$V_p^i \leq 0.178 \text{ volts} \qquad \text{(I-40a)}$$

$$V_e^i \leq 159 \text{ volts} \qquad \text{(I-40b)}$$

It was remarked in I that (140) represent upper limits on V_e^i and V_p^i, since the field quantities may be expected to be larger than those in the incident plane wave near a scattering obstacle.

We can establish the maximum values of V_e^i and V_p^i more accurately in the present calculations, since the modal dynamic quantities of interest Q_n, and V_n, are obtained as by-products of the numerical solution of (17) to (22) as functions of the radial variable. The Fourier series then lead to the physical quantities of interest, the dynamic electron number density and dynamic electron velocity, which were obtained as functions of the radial variable ρ for 9 equally spaced values of azimuthal angle φ from $\varphi = 0^o$ to $\varphi = 180^o$. The maximum values of these quantities were compared with the static electron number density and rms electron velocity to obtain the maximum allowable value of V_e^i and V_p^i for the inhomogeneous sheath calculations with L = 10.

The values thus obtained for V_e^i and V_p^i were found to depend on the sheath parameters and whether the hard or soft boundary condition was used at the cylinder surface. For the simplest situation, the sheathless case ($\Phi_c = 0$), and the hard boundary condition, (I40) was found to be about 2 times too high for both V_e^i and V_p^i. When the inhomogeneous case was considered, V_e^i obtained from (I40) was found to be about 3×10^2 too high for the hard boundary and 6×10^2 too high for the soft boundary. The value of V_p^i obtained from (I40) was correspondingly about 2×10^2 too high for the the hard boundary and 2×10^3 too high for the soft boundary.

Consequently, since the currents presented in this report for EK wave incidence are calculated with $V_p^i = 1.0$, these current magnitudes must be reduced by a factor of from 10^3 to 10^4 in order to ensure that the linearization is valid. We may observe from this that even though the fields in the uniform plasma may satisfy a desired linearity criterion, the fields in the inhomogeneous sheath may not, especially for the soft boundary condition. This possibility was pointed out by Tidman and Boyd (1962) in connection with wave propagation across a density discontinuity separating two uniform regions of plasma.

II. 4. Summary and Conclusions for Inhomogeneous Sheath Analysis

This investigation has been concerned with finding the surface currents excited by EK and EM plane waves normally incident on a perfectly conducting cylinder at a floating potential in a moderately warm ($T = 10^4\ ^oK$) uniform plasma from which it is separated by an inhomogeneous sheath of variable thickness. The numerical calculations have been performed assuming the cylinder surface to be either perfectly reflecting or perfectly absorbing in relation to the dynamic electron motion at the cylinder surface. One significant aspect of this investigation is the finding that the contribution of the boundary coupling to the surface current excited by the EK wave is approximately 10 times larger than that of the inhomogeneity coupling in the sheath, for a parabolic potential variation in a sheath 20 electron Debye lengths thick. This finding is especially significant since it shows that while the sheath inhomogeneity coupling leading to EK wave surface currents may possibly be neglected in comparison with the contribution of the hard boundary, it establishes an order of magnitude for the surface current which one might expect, even if the hard boundary condition is not

accepted as being physically realistic.

The results obtained here are further significant when compared with the vacuum sheath results of I, in that both the hard and soft boundary condition currents are in quite good quantitative agreement with the currents of I if the vacuum sheath thickness is regarded as a parameter in place of the cylinder surface admittance Y_B. It seems that it may thus be reasonable to characterize the actual inhomogeneous sheath by a vacuum sheath of appropriate thickness and zero surface admittance Y_B as was done in I. When viewed in this light, we see that the vacuum sheath, while admittedly not a physical model of the actual sheath, appears to be a good mathematical approximation to the actual inhomogeneous sheath, at least for normal wave incidence, as far as the surface currents are concerned. The conclusions reached as a consequence of the finds presented in I (which are: (1) the sheath and dynamic plasma compressibility can be neglected when finding the currents excited on a plasma-immersed cylinder by EM waves; (2) the sheath tends to screen the EK wave from the cylinder; and (3) the EK wave is less efficient than the EM wave in exciting surface currents on the cylinder) are thus not altered by the results presented here, though it would be of value to carry out the inhomogeneous sheath calculations for the case of oblique wave incidence, particularly for the EK wave, as a further check on the credibility of the vacuum sheath model. Finally, it should be emphasized that our discussion of the vacuum sheath and inhomogeneous sheath has been concerned with the surface currents produced by the incident wave and that the equivalence of the two models does not hold for the fields in the sheath.

Appendix A: Relation Between the Various Modal Coefficients

The solution of the boundary condition equations arising from the vacuum sheath model for the Fourier coefficients of the scattered, transmitted and reflected fields requires the inversion of the matrix given by (I-24). The matrix was reduced to 3 x 3, with A^S_{n-p}, A^R_{n-m}, and A^R_{n-e} appearing in it as the coefficients to be determined. The advantage of using the coefficients of the reflected waves is that they are required for calculating the surface currents and are related in a simple way to the transmitted wave coefficients which are also needed for this purpose.

The remainder of the coefficients are expressed in terms of these three as

$$A^T_{n-e} = f^{TR}_{ee} A^R_{n-e} \tag{A.1a}$$

$$A^T_{n-m} = f^{TR}_{mm} A^R_{n-m} \tag{A.1b}$$

$$A^S_{n-e} = f^{SR}_{ee} A^R_{n-e} - i^n V^i_e \frac{J_n(\lambda_E s)}{H^{(2)}_n(\lambda_E s)} \tag{A.1c}$$

$$A^S_{n-m} = f^{SR}_{me} A^R_{n-e} + f^{SR}_{mm} A^R_{n-m} - i^n V^i_m \frac{J'_n(\lambda_E s)}{H^{(2)'}_n(\lambda_E s)} \tag{A.1d}$$

Where

$$f_{ee}^{TR} = -\frac{H_n^{(2)'}(\lambda_{Eo}c)}{H_n^{(1)'}(\lambda_{Eo}c)} \tag{A.2a}$$

$$f_{mm}^{TR} = -\frac{H_n^{(2)}(\lambda_{Eo}c)}{H_n^{(1)}(\lambda_{Eo}c)} \tag{A.2b}$$

$$f_{ee}^{SR} = \left(\frac{\lambda_{Eo}}{\lambda_E}\right)^2 \frac{H_n^{(2)}(\lambda_{Eo}s)}{H_n^{(2)}(\lambda_E s)} \left[1 + f_{ee}^{TR} \frac{H_n^{(1)}(\lambda_{Eo}s)}{H_n^{(2)}(\lambda_{Eo}s)}\right] \tag{A.2c}$$

$$f_{me}^{SR} = \frac{\beta n}{sK_E\lambda_E H_n^{(2)'}(\lambda_E s)} \left[f_{ee}^{SR} H_n^{(2)}(\lambda_E s) - f_{ee}^{TR} H_n^{(1)}(\lambda_{Eo} s) - H_n^{(2)}(\lambda_{Eo} s)\right] \tag{A.2d}$$

$$f_{mm}^{SR} = \frac{\lambda_{Eo}\,\eta}{\lambda_E \eta_o} \frac{1}{H_n^{(2)'}(\lambda_E s)} \left[f_{mm}^{TR} H_n^{(1)'}(\lambda_{Eo}s) + H_n^{(2)'}(\lambda_{Eo}s)\right] \tag{A.2e}$$

The dash subscript represents the kind of incident wave, p, e or m and the prime denotes differentiation with respect to argument.

Appendix B: Properties of the Static Sheath

The properties of the static sheath such as electron number density, potential, etc., have been investigated for a wide variety of assumed conditions and various geometries by, for example, Tonks and Langmuir (1929), Allen et. al. (1957), Bernstein and Rabinowitz (1959), Self (1963), Parker (1963) and Laframbois (1964). Our intent here is not to attempt an independent treatment of the sheath for the cylindrical geometry. Instead we wish to incorporate a potential of the form given by (II-7a) together with some results due to Bernstein and Rabinowitz (1959) in order to establish the validity of dropping terms in the static electron velocity from the dynamic equations and to show the accuracy of the Boltzmann distribution for the static electron density variation in the sheath, for the case of a cylinder at floating potential in the plasma. An a priori assumption of the potential variation is reasonable because results presented in some of the sources listed above indicate the correctness of (II-7a). Once the potential is known, the other quantities such as electron density are obtained in a straight-forward manner. Figure B1 shows the static potential as a function of radial position in the sheath, calculated from (II-7a) for various values of the parameter M.

Following Lam's (1964) development of the Bernstein and Rabinowitz (1959) analysis for electrons in a spherical goemetry, we can find for the cylindrical case,

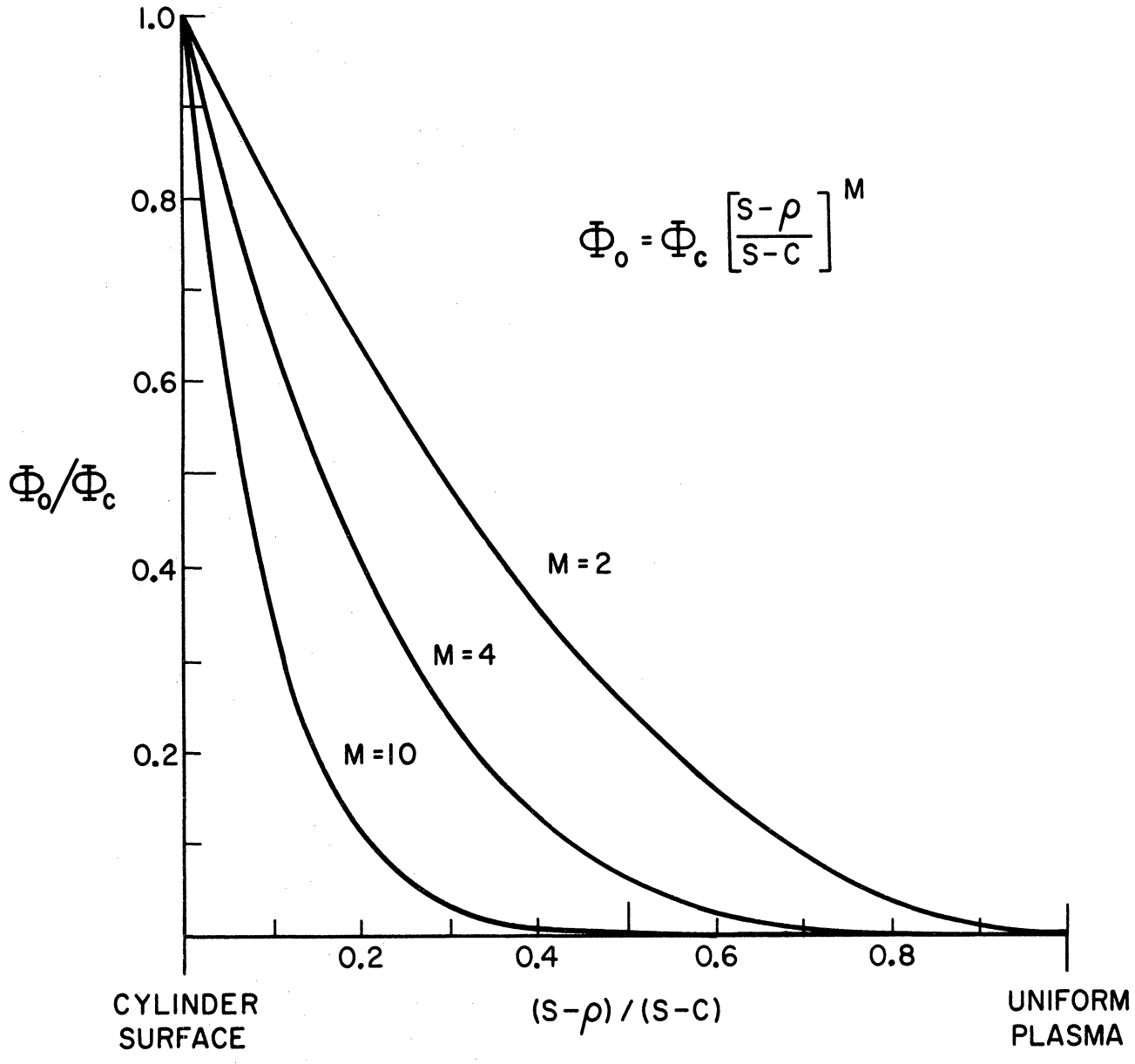

Figure B1. Static potential variation in sheath as a function of radial distance.

$$n_o(\rho) = 8An_\infty \left[\int_0^\infty dE_\parallel \int_{-e\Phi_o}^\infty d E_\perp \int_0^{J_1} dJ F_1 - \frac{1}{2} \int_0^\infty dE_\parallel \int_{-e\Phi_c}^\infty d E_\perp \int_0^{J_2} d J F_1 \right] \tag{B1}$$

where

$$F_1 = \frac{\exp(-2BE_\parallel/m)\exp(-2BE_\perp/m)}{m\sqrt{2mE_\parallel}\,[2m\rho^2(E_\perp+e\Phi_o)-J^2]^{1/2}}$$

$$A = (B/\pi)^{3/2}; \quad B = m/(2kT)$$

$E_\parallel$ and $E_\perp$ are the electron energy components associated with electron motion parallel and perpendicular to the cylinder, and J is the electron angular momentum. J_1 and J_2 are given by

$$J_1 = [2m(E_\perp + e\Phi_o)]^{1/2}\,\rho$$

$$J_2 = [2m(E_\parallel + e\Phi_c)]^{1/2}\,\rho$$

The electron flux is

$$n_o(\rho)v_o(\rho) = \frac{2A}{m^2\rho\sqrt{2m}} \int_0^\infty d E_\parallel \int_{-e\Phi_c}^\infty d E_\perp \int_0^\infty dJ F_2 \tag{B2}$$

with

$$F_2 = \exp(-2BE_\parallel/m)\exp(-2BE_\perp/m)/\sqrt{E_\parallel}$$

After performing the integration over J and $E_\parallel$, there is obtained

$$n_o(\rho) = n_\infty N_e(\rho)\left\{1 - \frac{1}{\pi N_e(\rho)} \int_{Z_c}^\infty e^{-y} \sin^{-1}\left[\frac{c^2}{\rho^2}\left(\frac{y-Z_c}{y-Z_o}\right)\right]^{1/2} dy\right\} \tag{B3}$$

$$v_o(\rho) = \frac{n_\infty}{n_o(\rho)} \frac{c}{\rho\pi}\sqrt{\frac{2kT}{m}} \int_{Z_c}^\infty e^{-y}\sqrt{y-Z_o}\, dy \tag{B4}$$

where

$$Z_c = -e\Phi_c/(kT); \quad Z_o = -e\Phi_o/(kT)$$

$$N_e(\rho) = \exp(-Z_o)$$

We note that the term outside the brackets in (B3) is the Boltzmann distribution, and that the integral portion of (B3) accounts for the modification of the Boltzmann distribution due to the electron flow to the cylinder. It may be seen that the integral term has a maximum value of 0.5 at the cylinder surface, so that the maximum correction to the Boltzmann distribution is a reduction by 0.5. As the radius variable increases to infinity, (B3) approaches the Boltzmann distribution. Numerical calculation performed using (B3) together with the sheath models utilized to obtain the current results presented in this report, showed that (B3) differed from the Boltzmann distribution by less than 5 per cent over the outer 0.8 of the sheath. Consequently, the Boltzmann distribution appears to adequately describe the static electron density variation in the sheath around a cylinder at floating potential in a plasma. These results are illustrated by figures B2 and B3 which show the static electron velocity and density as a function of radial position in the sheath obtained from (B3) and (B4). Also shown are curves of the electron density obtained from the Boltzmann distribution (II-8).

Once we have obtained the static electron velocity and number density, we can determine whether the static velocity terms can be reasonably dropped from (II-2) to (II-6). A straightforward way of determining the relative importance of these terms is to compare them in magnitude with the other terms in the equation which involve the same dynamic quantities. This has the advantage that the dynamic parts of these terms may then be factored out. It is thus of interest to compare the ratios

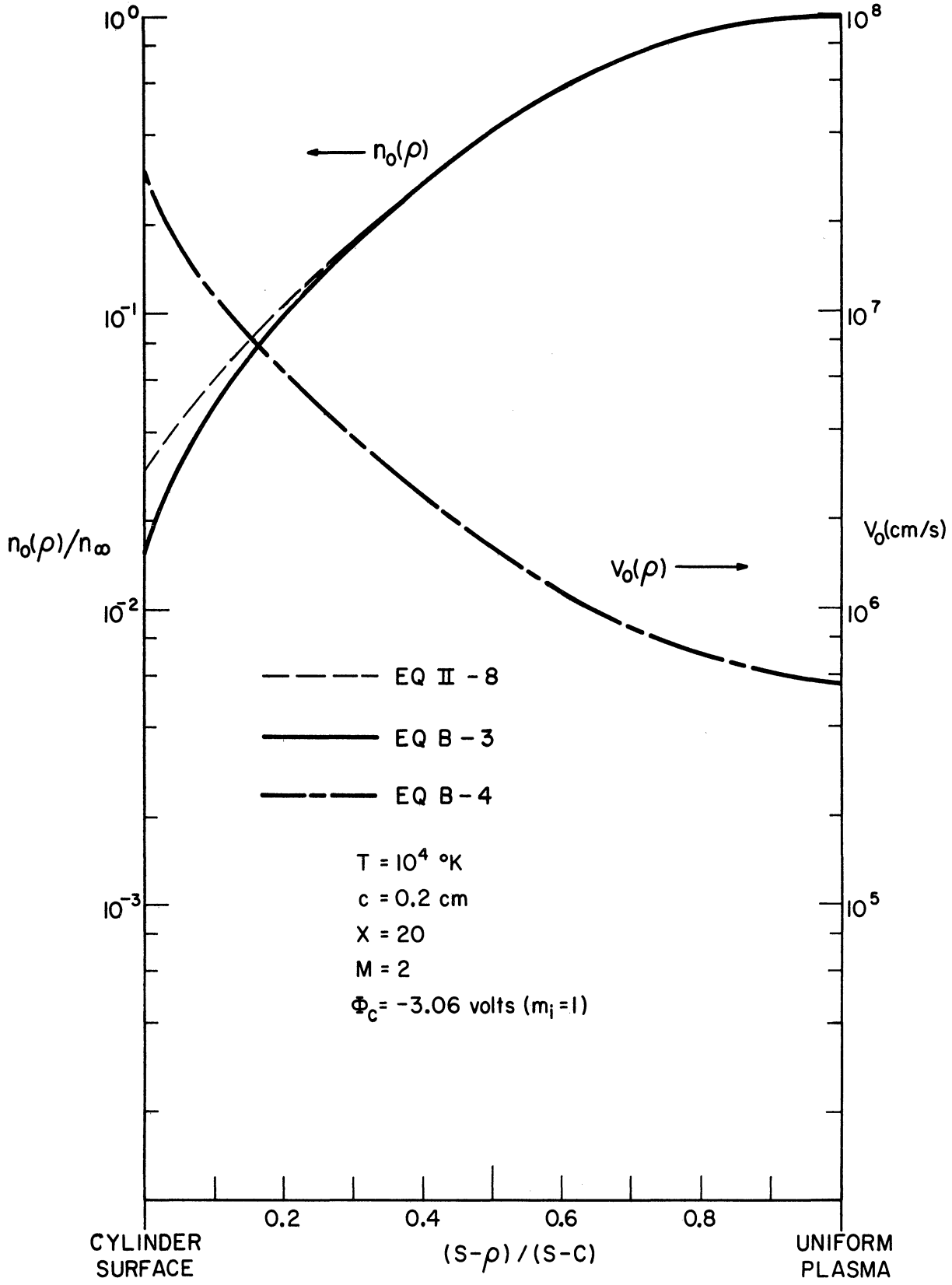

Figure B2. Static Electron density and velocity as a function of radial distance in the sheath for Φ_c = -3.06 volts and M = 2.

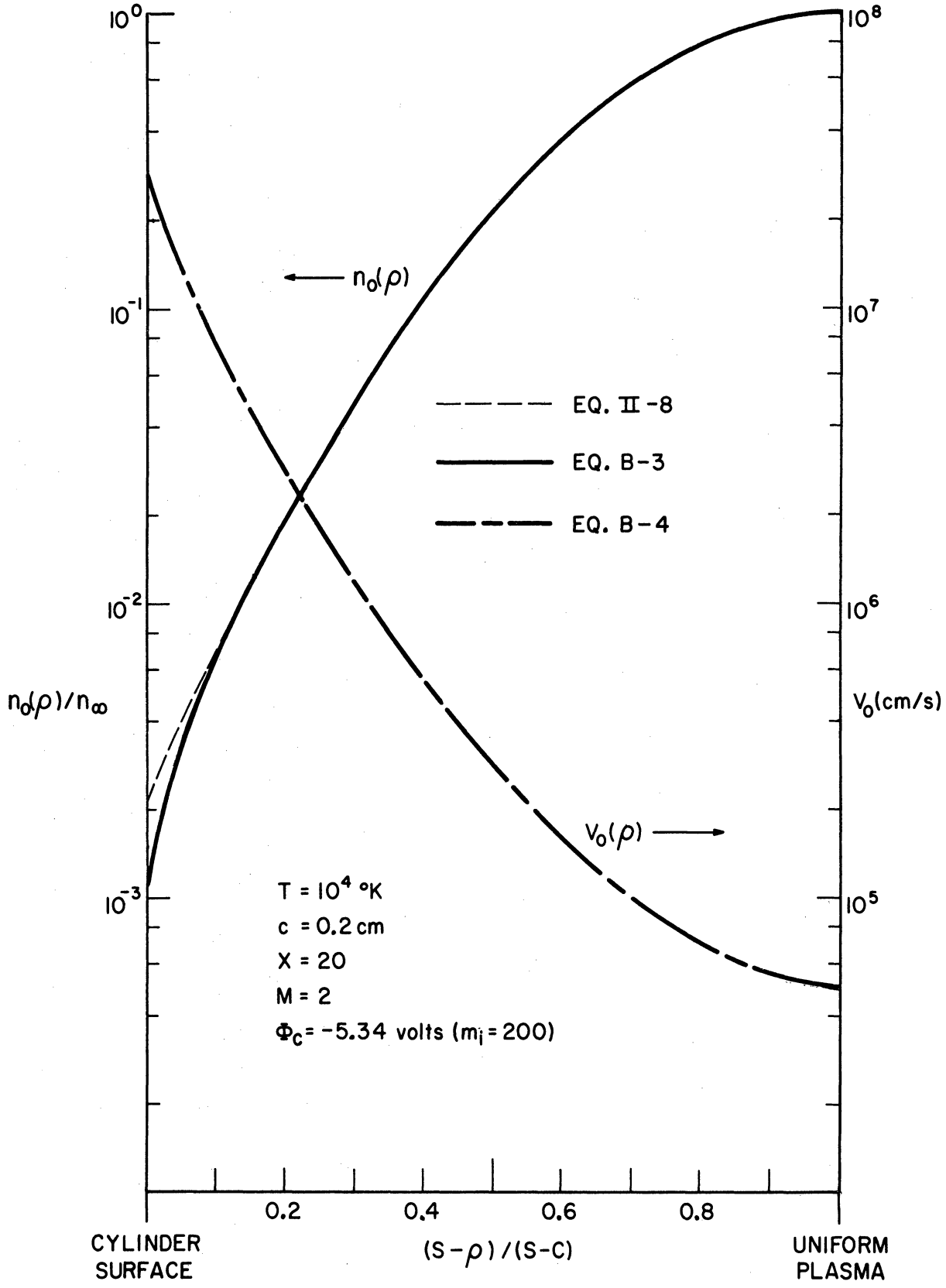

Figure B3. Static electron density and velocity as a function of radial distance in the sheath for Φ_c = 5.34 volts and M = 2.

$$\nabla\cdot(n_1\vec{v}_o) \;:\; i\omega n_1$$

$$(\vec{v}_1\cdot\nabla)\vec{v}_o + (\vec{v}_o\cdot\nabla)\vec{v}_1 \;:\; i\omega\vec{v}_1$$

$$(n_1\vec{v}_o\cdot\nabla)\vec{v}_o \;:\; \frac{e}{m}\, n_1\, \vec{E}_o$$

$$n_1\vec{v}_o \;:\; n_o\,\vec{v}_1$$

which come from (II-2), (II-3), (II-3) and (II-6) respectively. Since we do not have the dynamic solutions, we cannot exactly obtain the radial derivatives of these quantities which appear above. (There are radial derivatives alone because of the static quantities dependence only on ρ.) A good approximation would appear to be

$$\frac{d}{d\rho} = iK$$

where K is the propagation constant of the incident wave. With this assumption, the maximum of the ratios above can be expressed as

$$R_1 = (K|\vec{v}_o| + |\nabla\cdot\vec{v}_o|)/\omega$$

$$R_2 = (K|\vec{v}_o| + |\nabla\cdot\vec{v}_o|)/\omega$$

$$R_3 = \frac{|(\vec{v}_o\cdot\nabla)\vec{v}_o|}{|(e/m)\vec{E}_o|}$$

$$R_4 = K|\vec{v}_o|/\omega$$

In obtaining R_4, the velocity associated with EK wave has been used to cancel the n_1 terms appearing in the numerator.

Since R_2 and R_1 are the same, and R_4 is less than R_1, our task is now to evaluate R_1 and R_3. It is of interest to observe that while R_3

is independent of the frequency, R_1 contains the frequency and can apparently become arbitrarily large as the frequency is decreased. This is not the case however, since we are interested in the region where $\omega_P < \omega$, so that as $\omega \to 0$, ω_P also goes to zero, and the sheath thickness increases proportionately (since the sheath thickness is proportional to $1/\omega_P$). Consequently, since $\vec{v}_o$ is independent of ω_P, $\nabla \cdot \vec{v}_o$ decreases at the same rate as ω decreases, so that these ratios are dependent not on the frequency, but on the ratio of the plasma frequency to the incident wave frequency.

In order to evaluate R_1 and R_3, an expression is required for K, and obviously, if we use $K = K_P$, the ratios will be a maximum. Figure B4 shows R_1 and R_3 for a cylinder potential of -3.04 V ($m_i = 1$), and with M = 2 and M = 4, as a function of radial position in the sheath. We see that these ratios are less than 0.1 over 85 percent of the sheath, with the average value of the largest being 0.058. Similar results are obtained for $m_i = 200$. The omission of terms in the static electron velocity from the dynamic sheath equations, in view of these results would seem to be a very reasonable approximation.

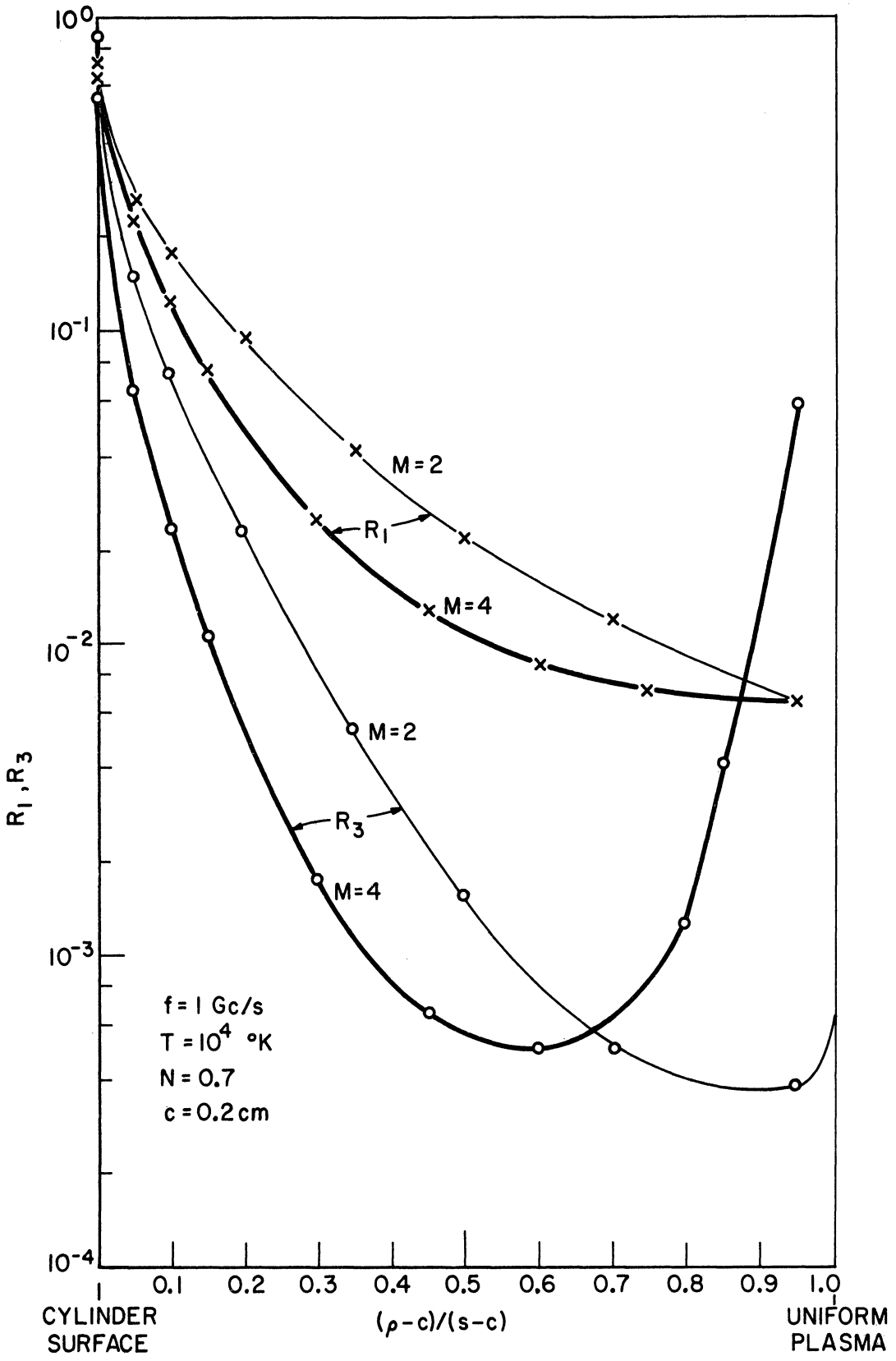

Figure B4. The ratios R_1 and R_3 as a function of radial distance in the sheath, for Φ_c = -3.06 V.

Appendix C: Additional Related Graphs

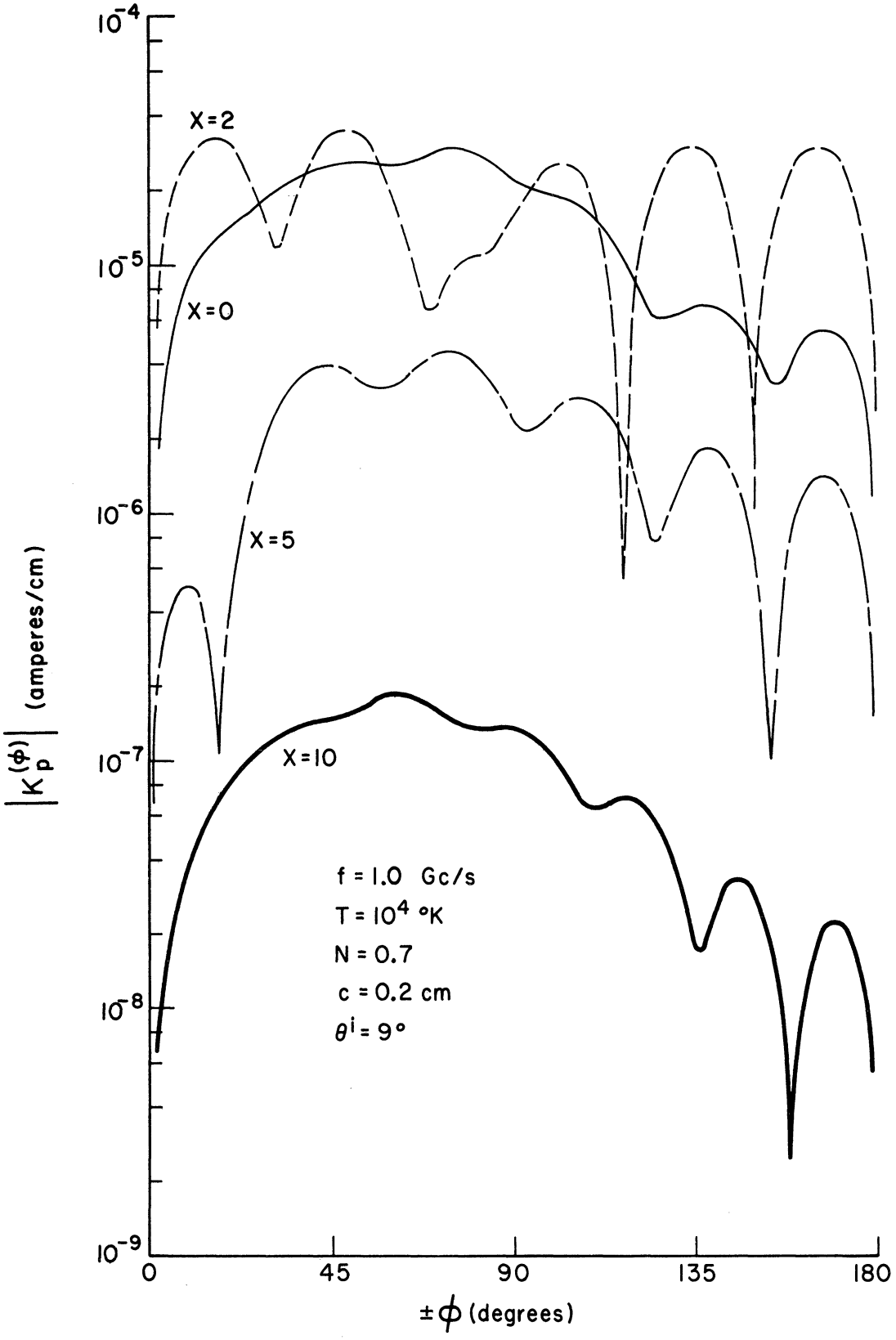

Figure C1. The magnitude of $K_p^{(\varphi)}$ as a function of azimuthal angle for the angle of incidence $\theta^i = 9°$ and the sheath thickness X in Debye lengths a parameter.

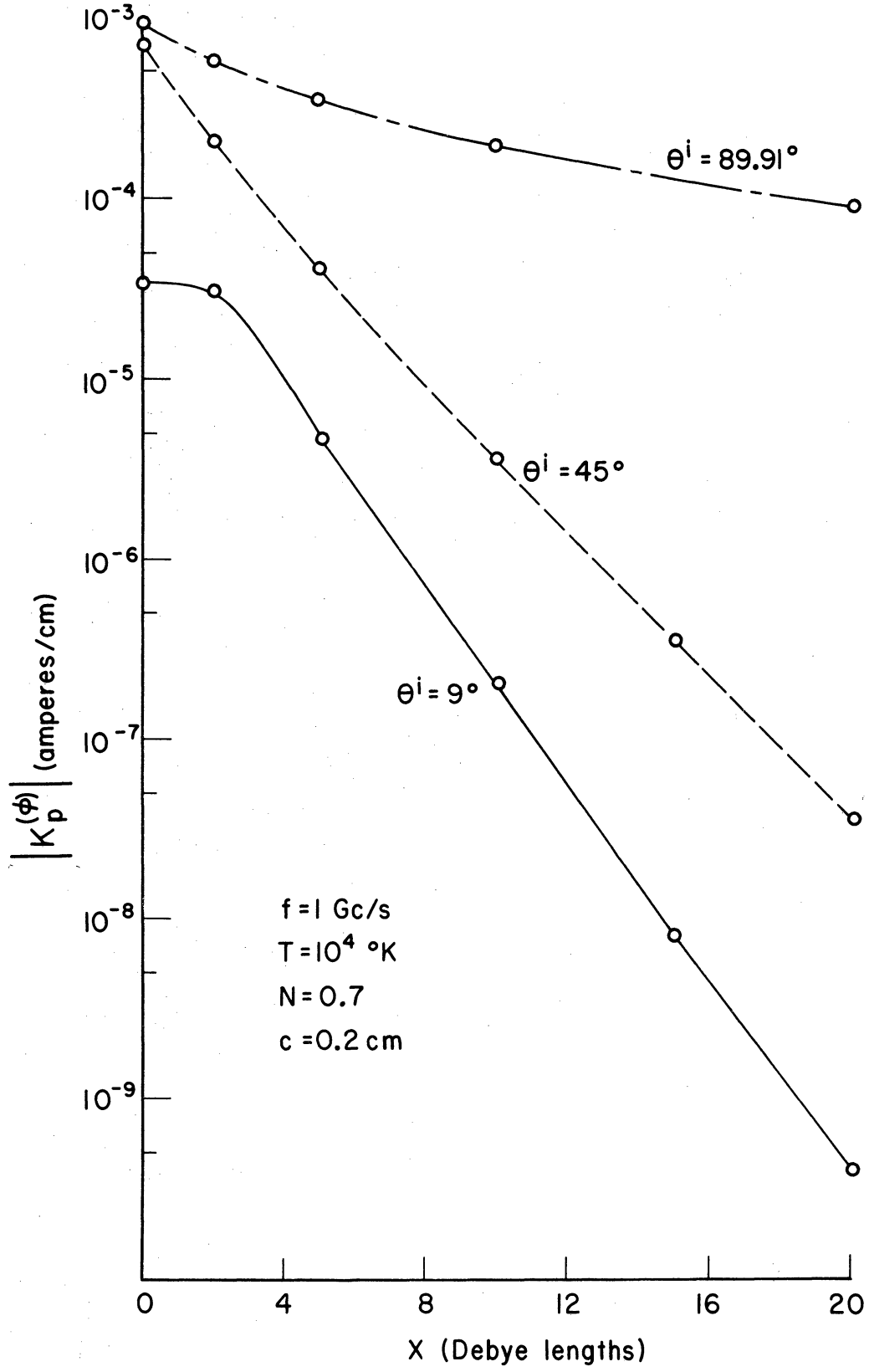

Figure C2. The maximum value of $K_p^{(\varphi)}$ as a function of sheath thickness X with θ^i a parameter.

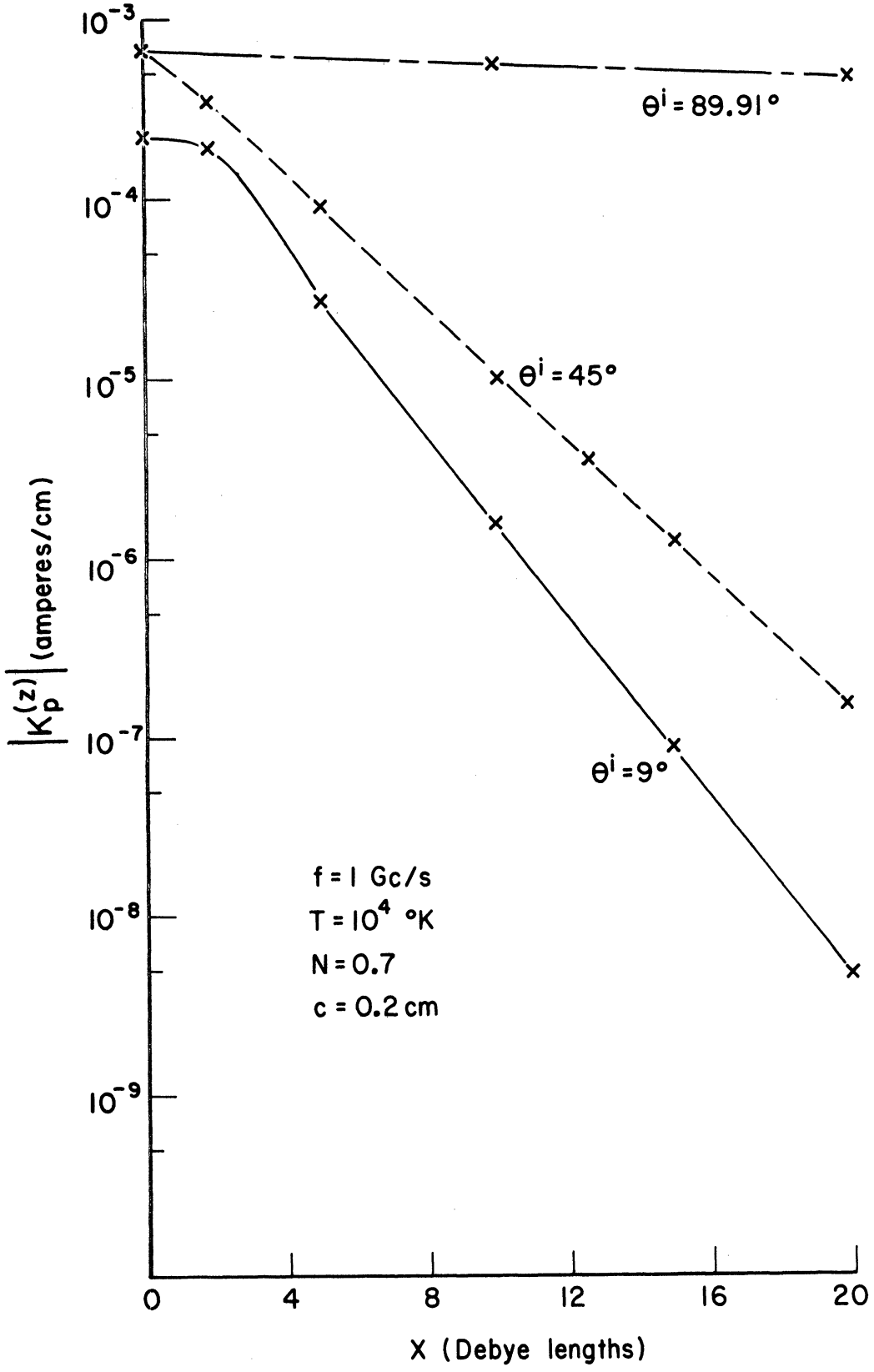

Figure C3. The maximum value of $K_p^{(z)}$ as a function of sheath thickness X with θ^i a parameter.

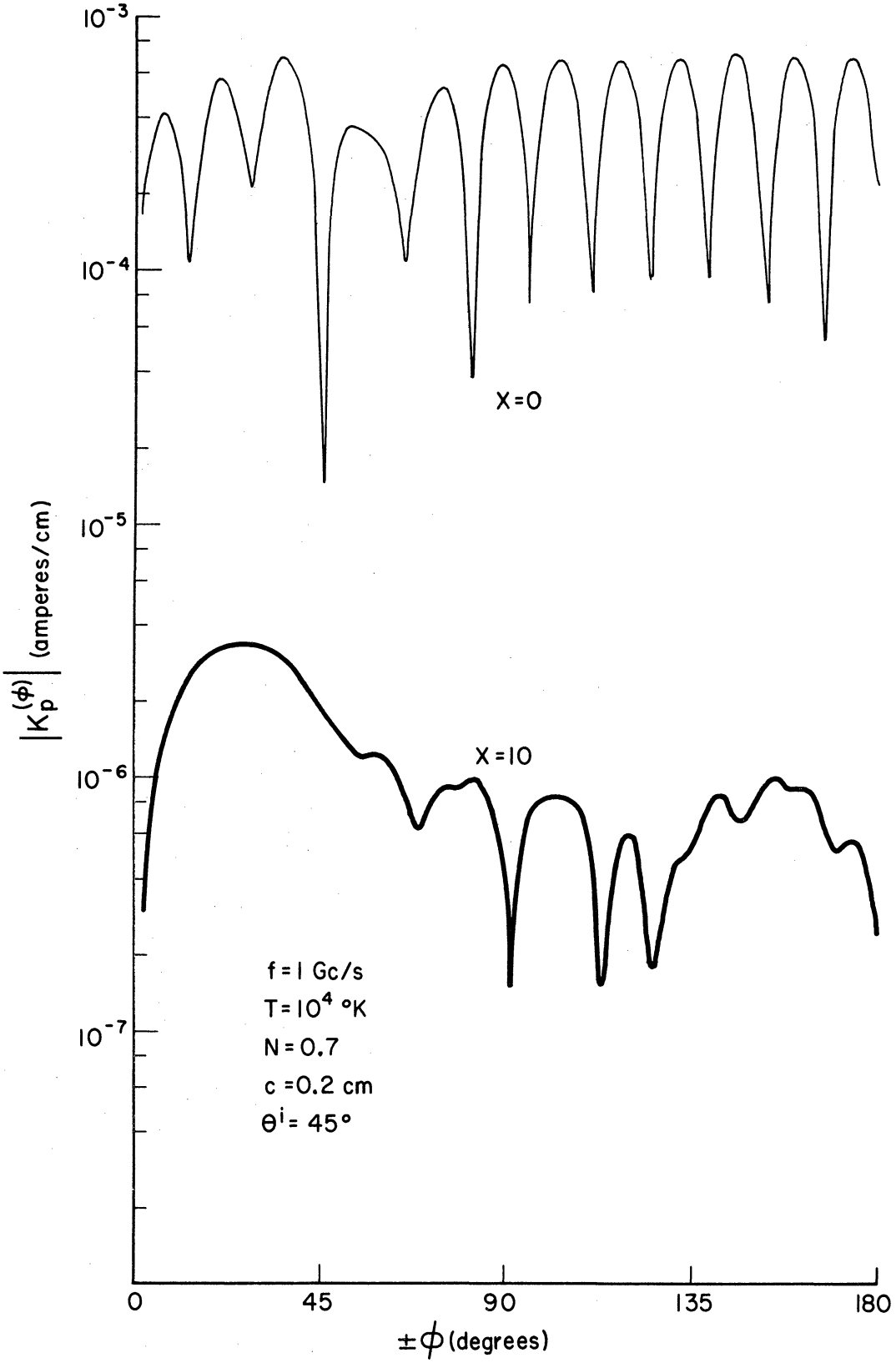

Figure C4. The magnitude of $K_p^{(\varphi)}$ as a function of azimuthal angle φ for N = 0.7 and θ^i = 45°.

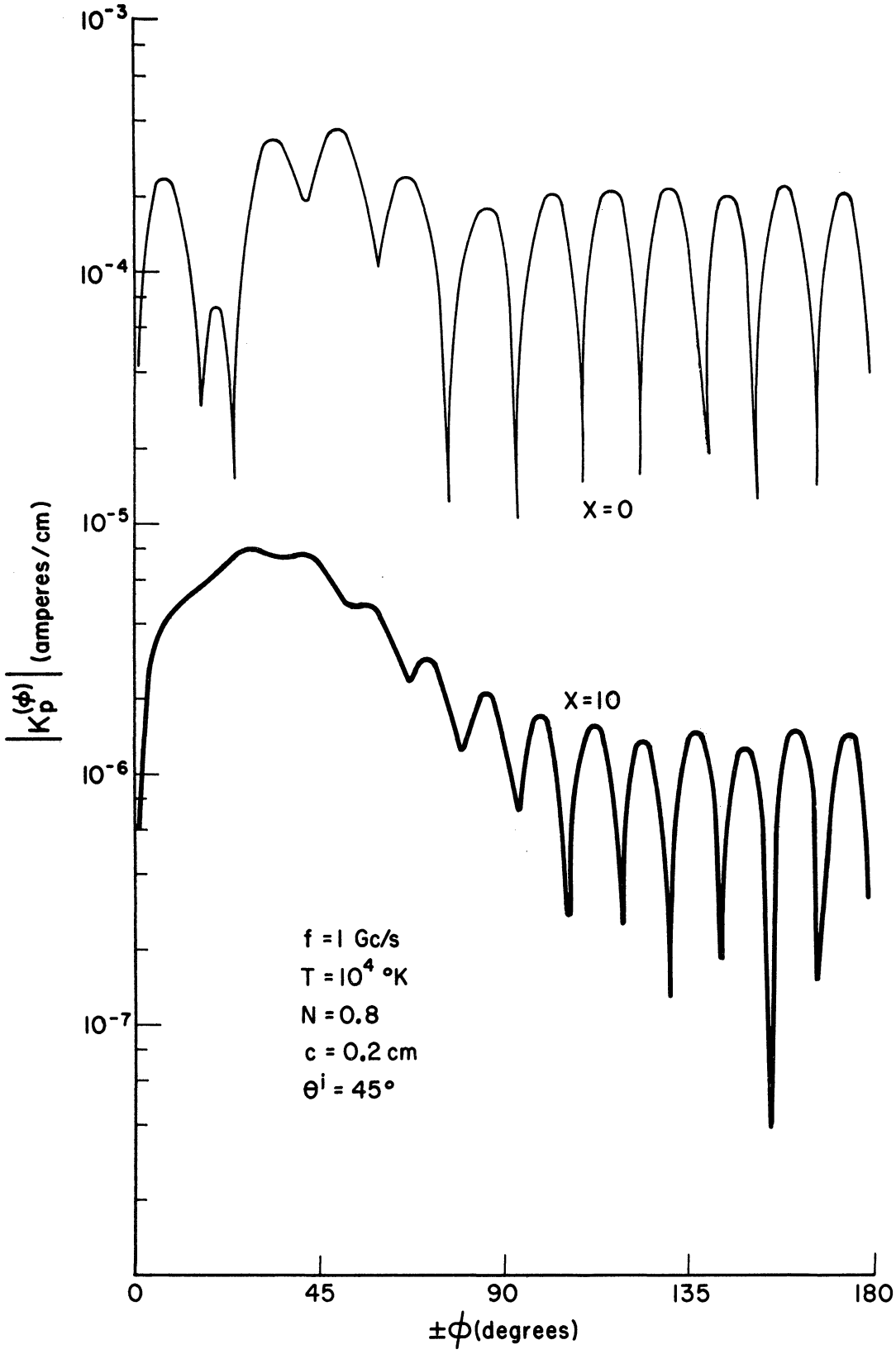

Figure C5. The magnitude of $K_p^{(\varphi)}$ as a function of azimuthal angle φ for N = 0.8 and $\theta^i = 45°$.

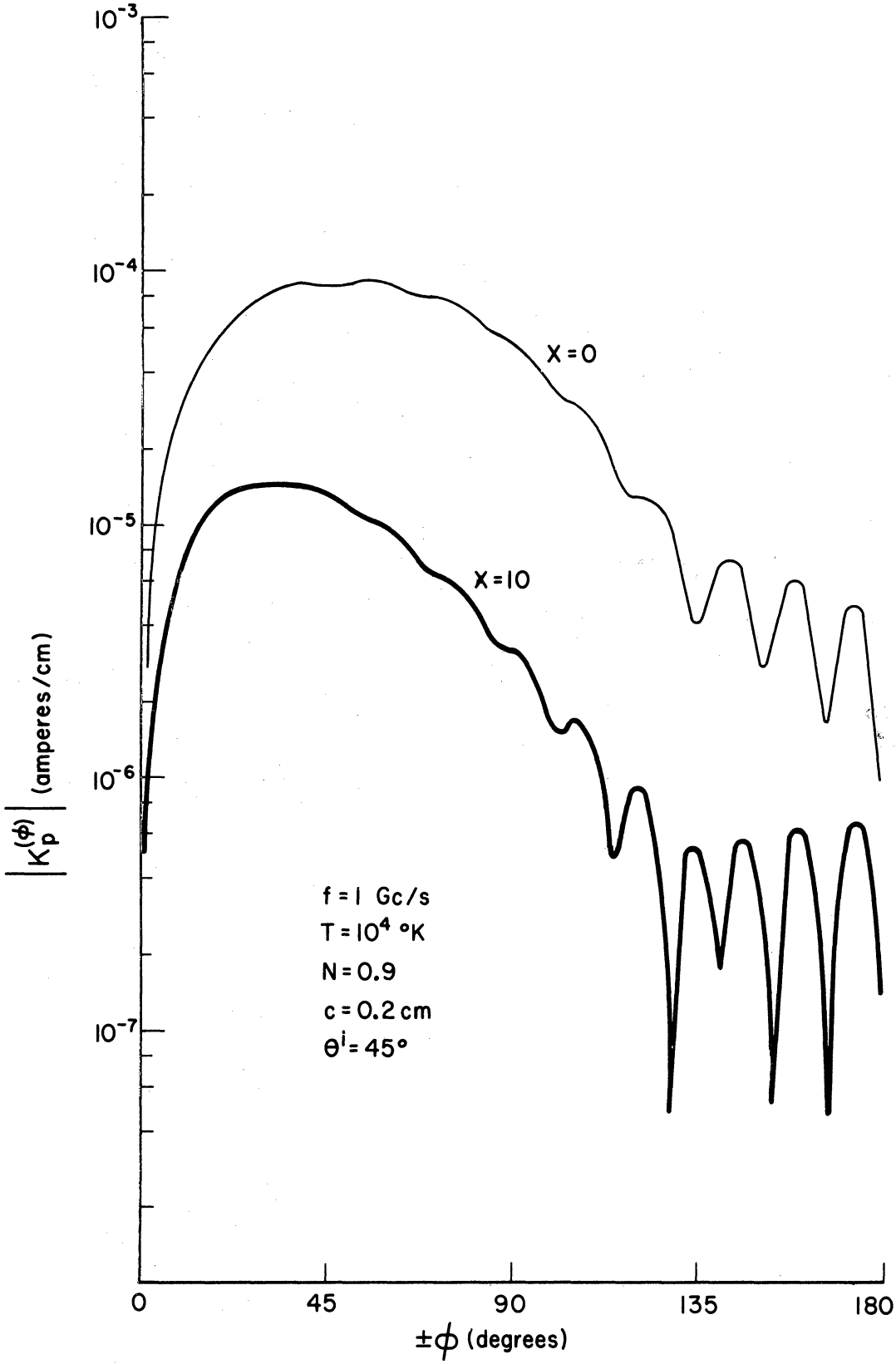

Figure C6. The magnitude of $K_p^{(\varphi)}$ as a function of azimuthal angle φ for N = 0.9 and $\theta^i = 45°$.

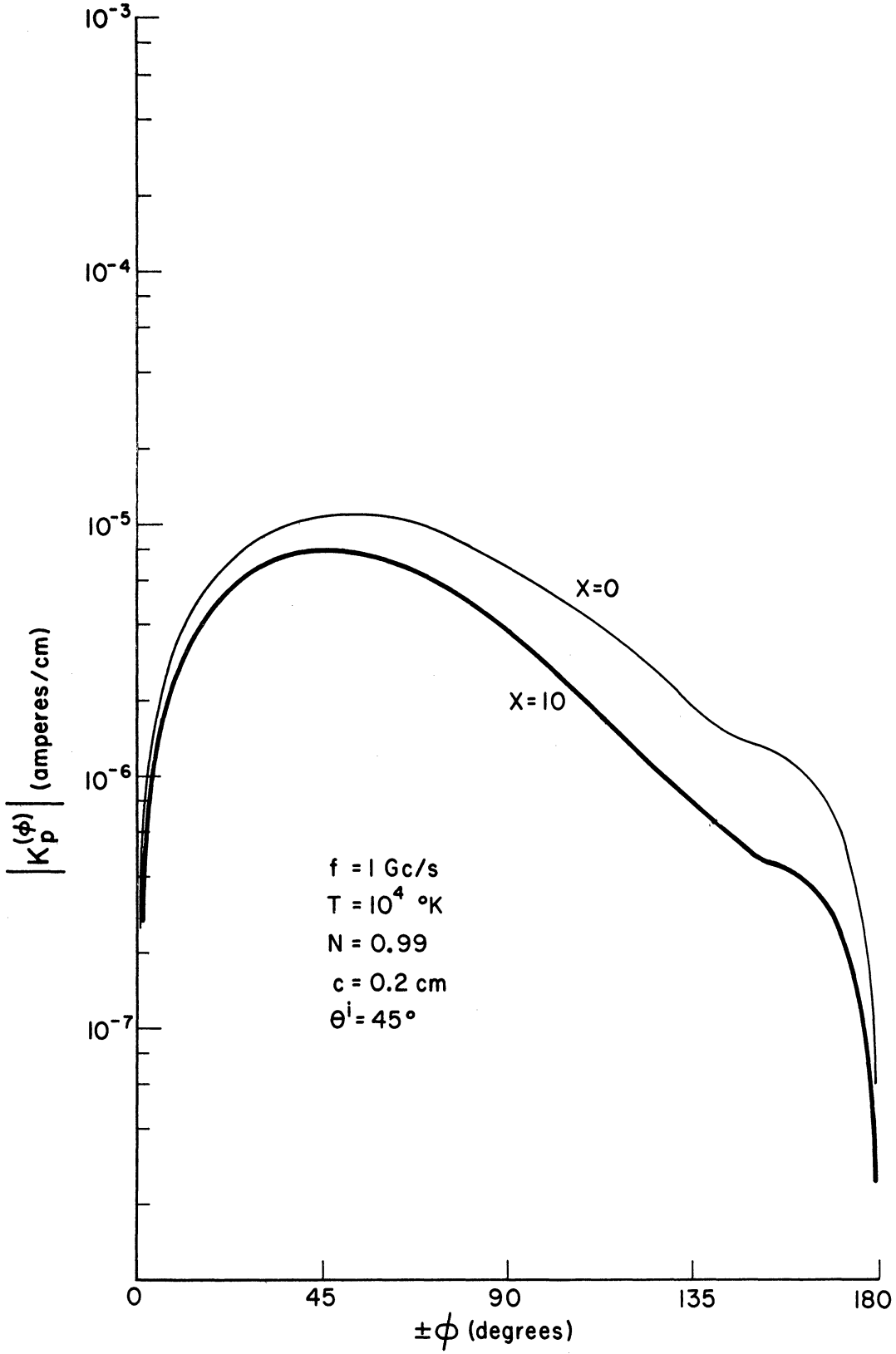

Figure C7. The magnitude of $K_p^{(\varphi)}$ as a function of azimuthal angle φ for N = 0.99 and θ^i = 45°.

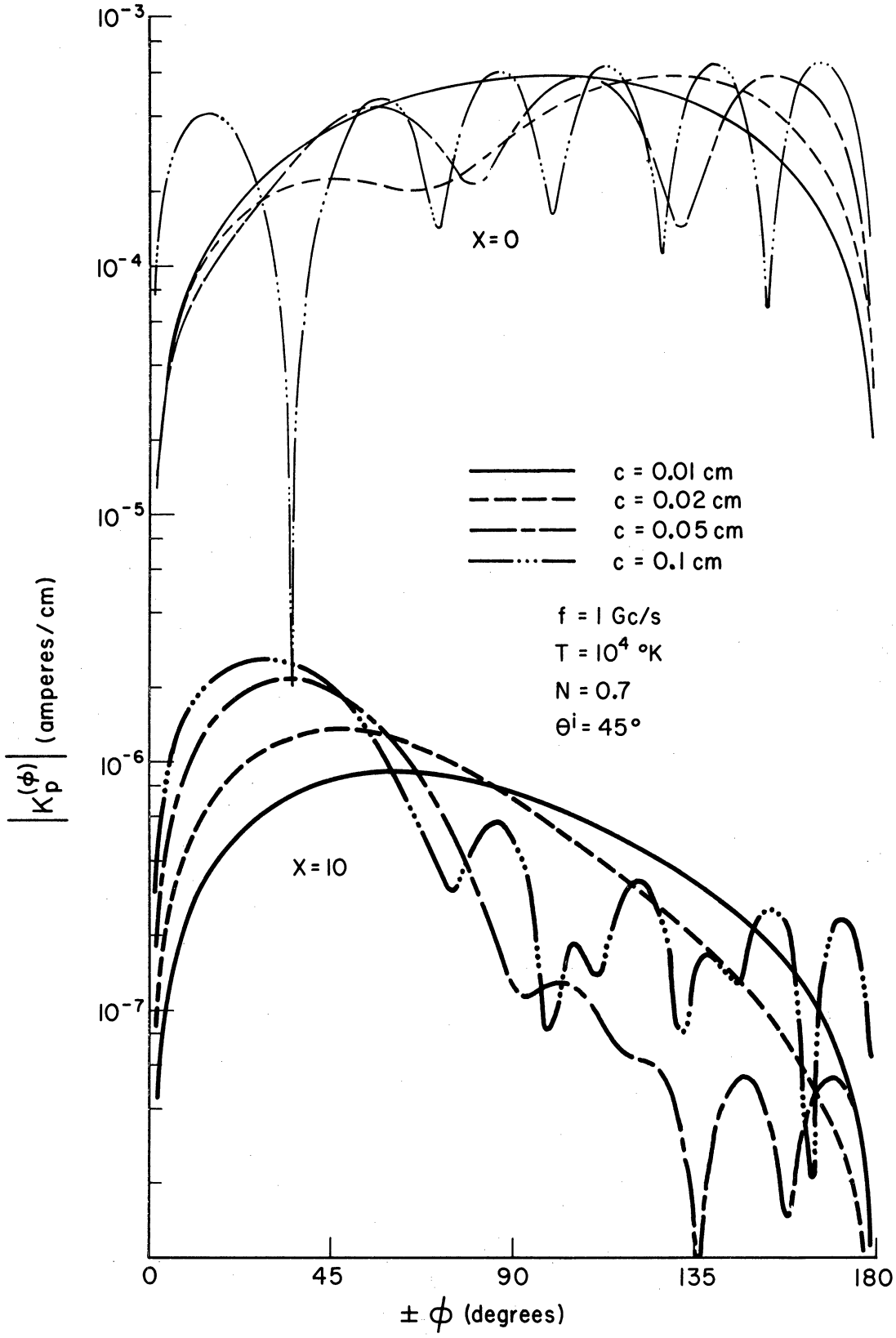

Figure C8. The magnitude of $K_p^{(\varphi)}$ as a function of azimuthal angle φ for $\theta^i = 45°$ with cylinder radius c a parameter.

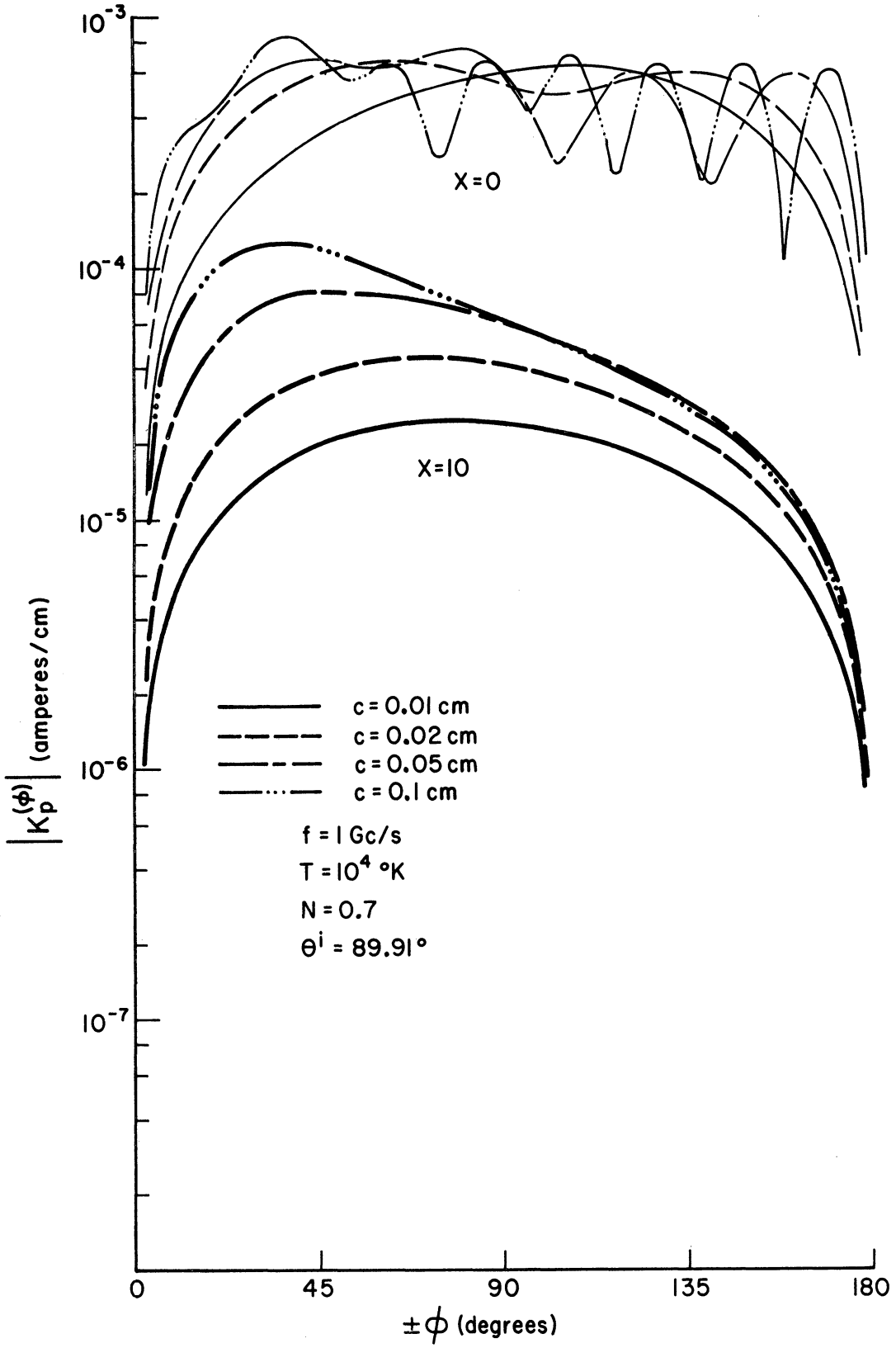

Figure C9. The magnitude of $K_p^{(\varphi)}$ as a function of azimuthal angle φ for θ = 89.91° with cylinder radius c a parameter.

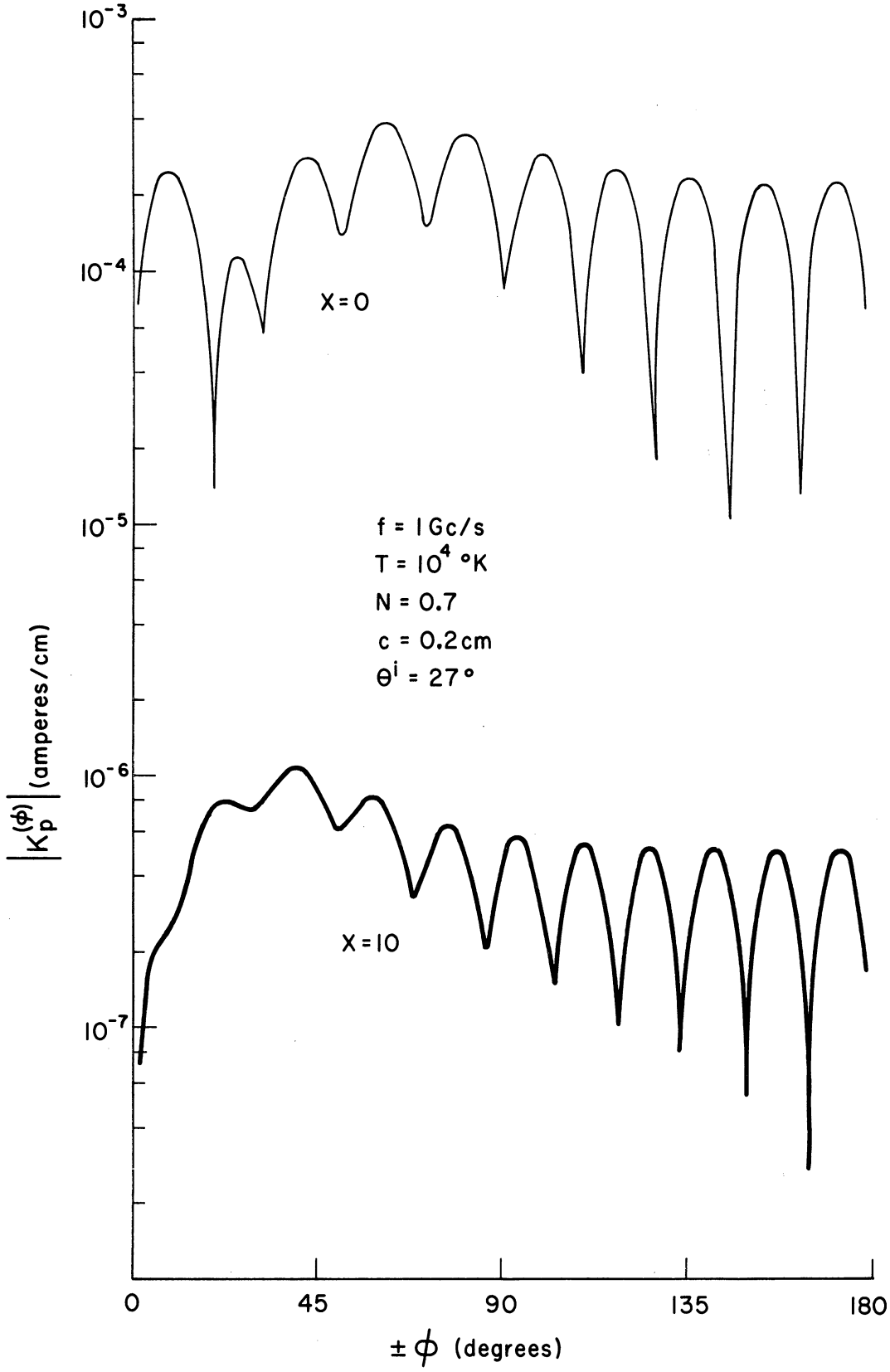

Figure C10. The magnitude of $K_p^{(\varphi)}$ as a function of azimuthal angle φ for θ^i = 27° (0.15π).

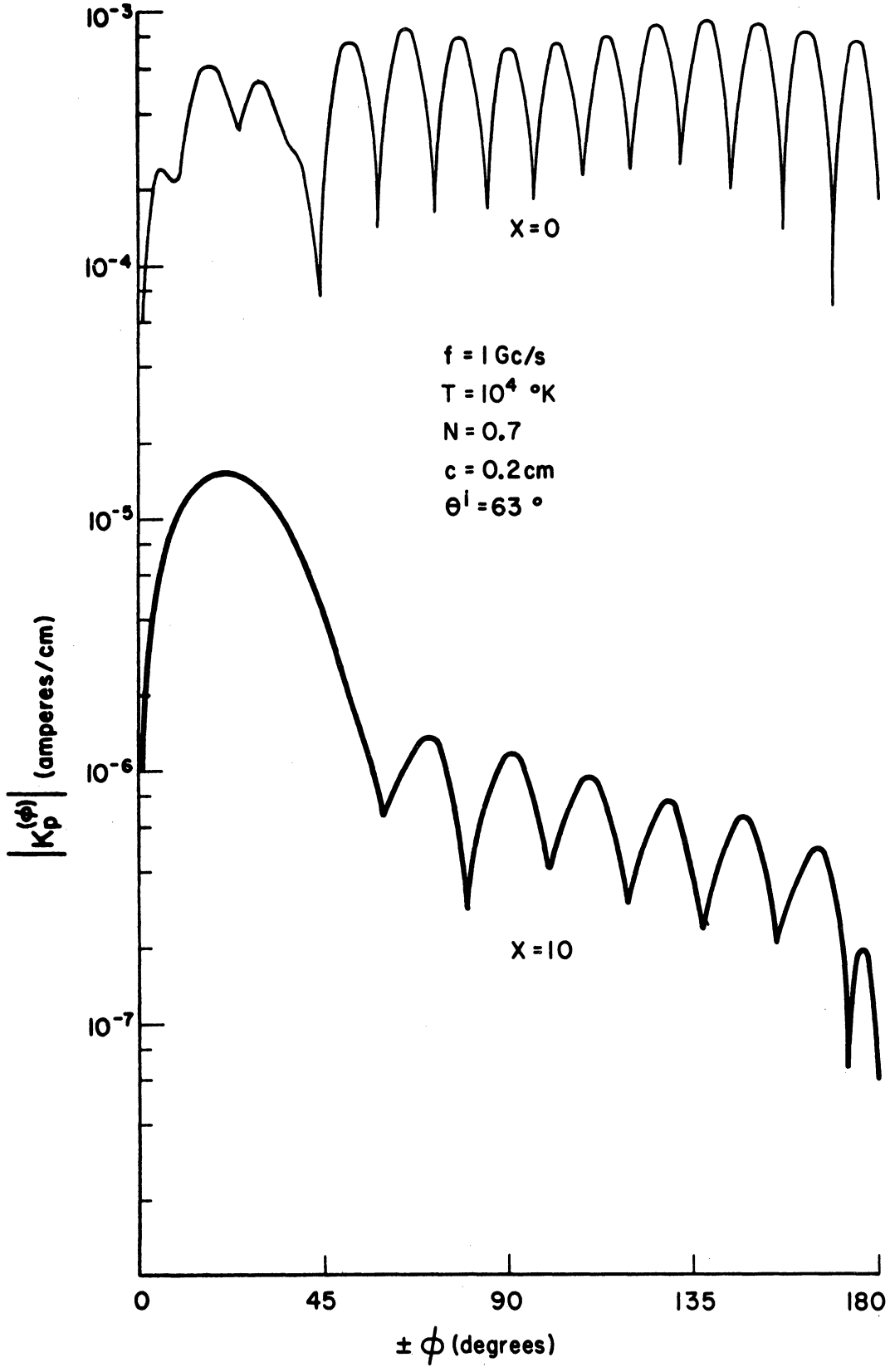

Figure C11. The magnitude of $K_p^{(\varphi)}$ as a function of azimuthal angle φ for θ^i = 63° (0.35π).

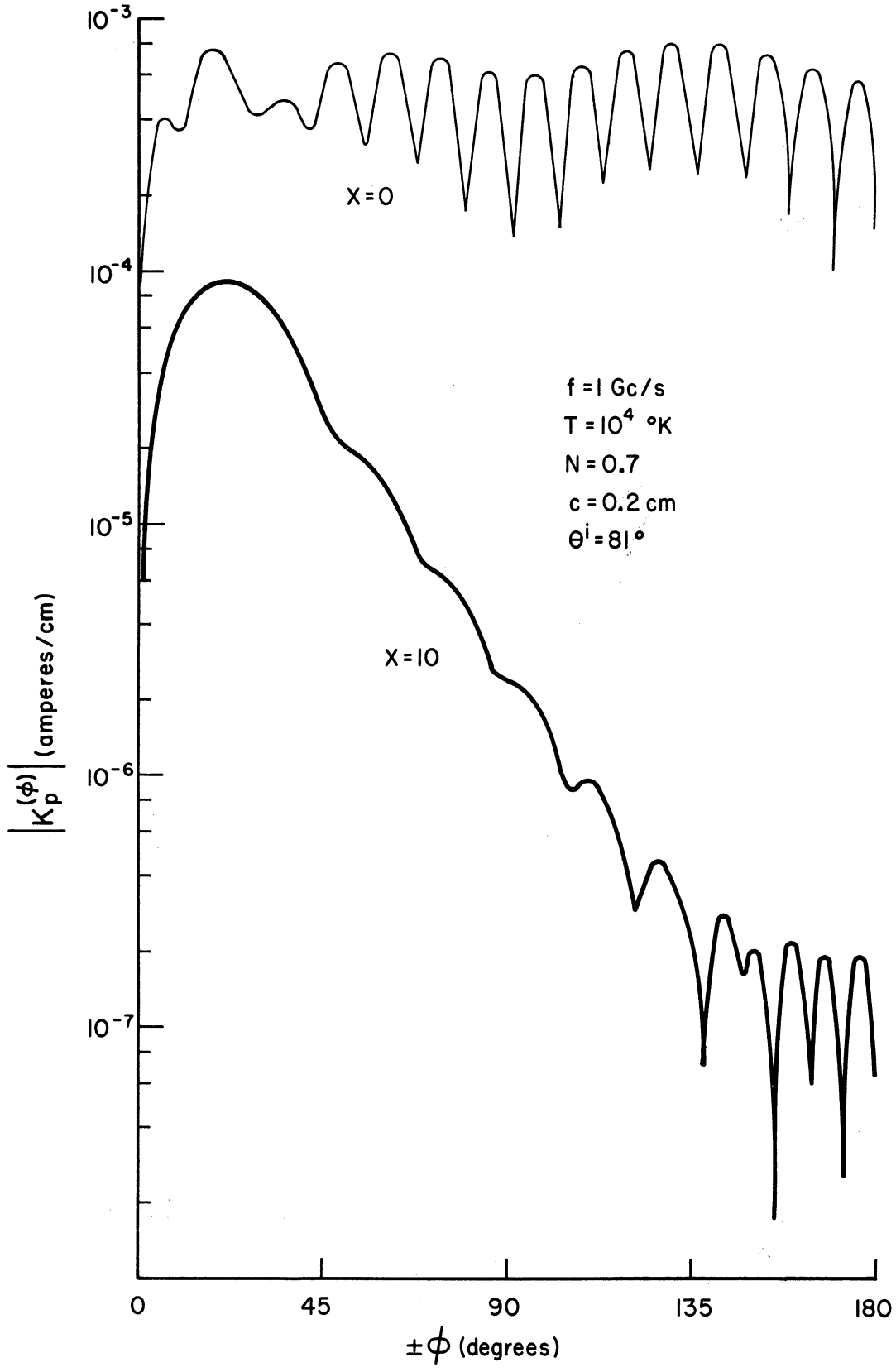

Figure C12. The magnitude of $K_p^{(\varphi)}$ as a function of azimuthal angle φ for θ^i = 81° (0.45π).

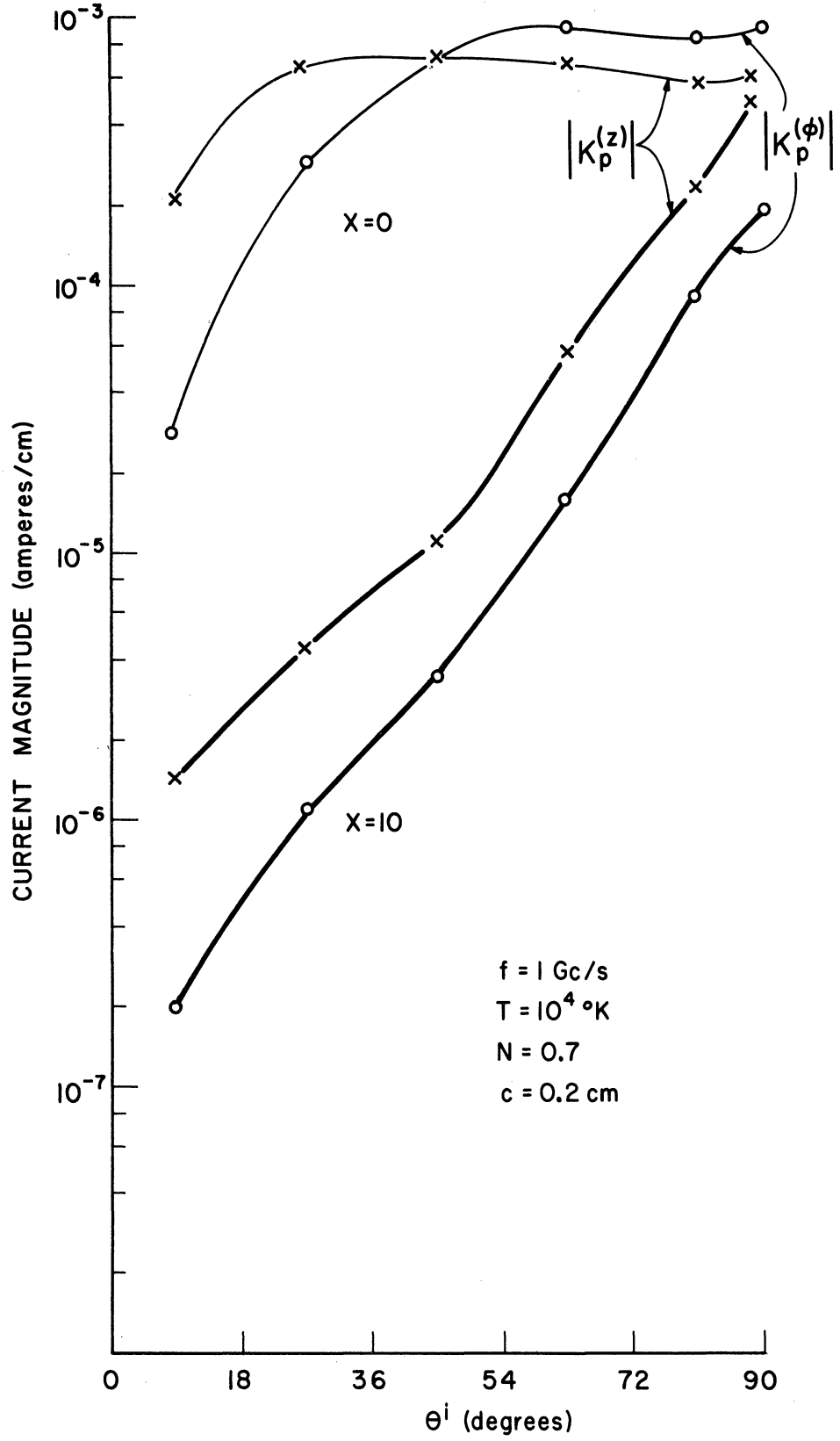

Figure C13. The maximum values of $K_p^{(\varphi)}$ and $K_p^{(z)}$ as a function of angle of incidence θ^i.

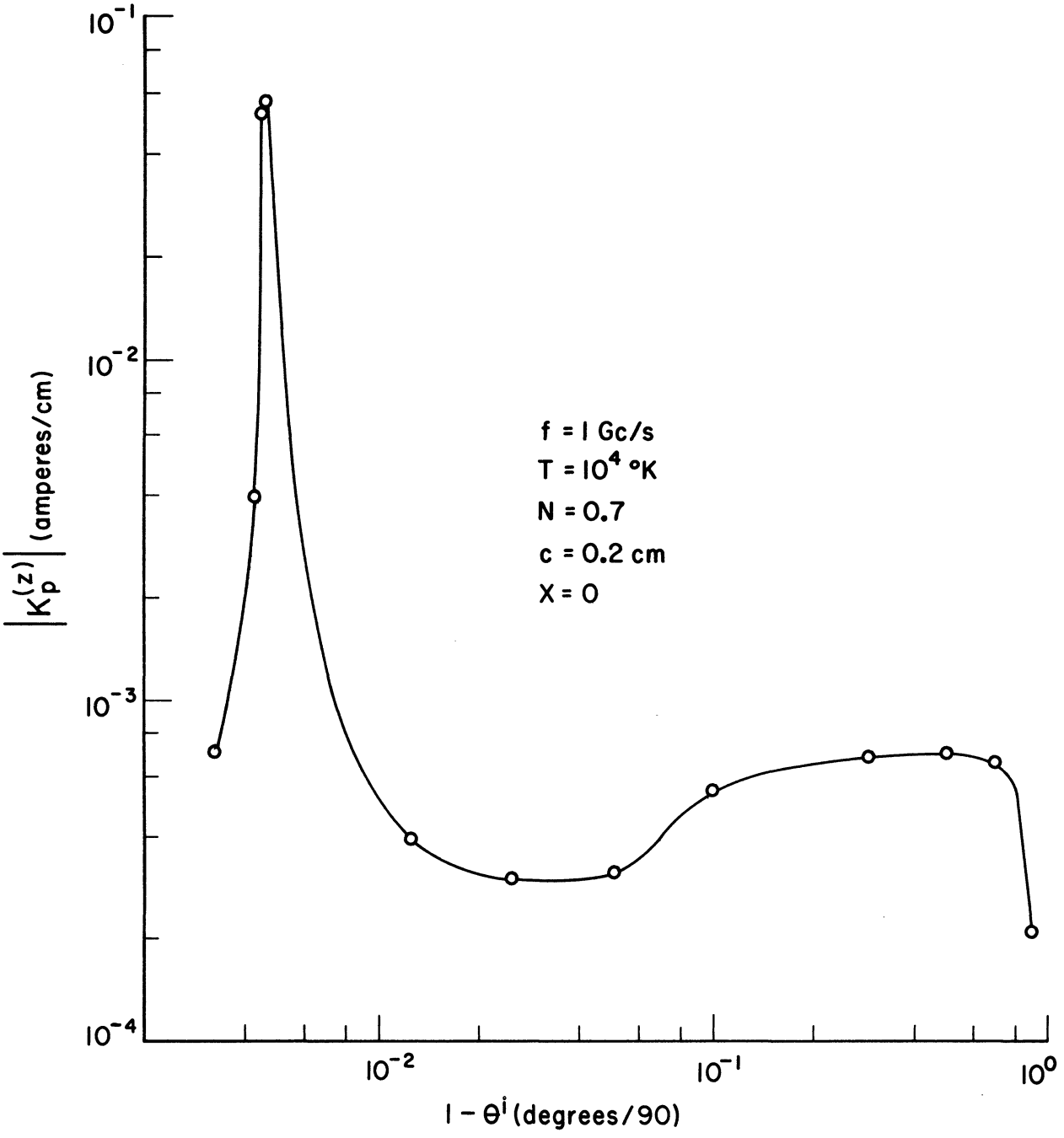

Figure C14. The maximum value of $K_p^{(z)}$ as a function of angle of incidence showing the spike near $\theta^i = 90°$.

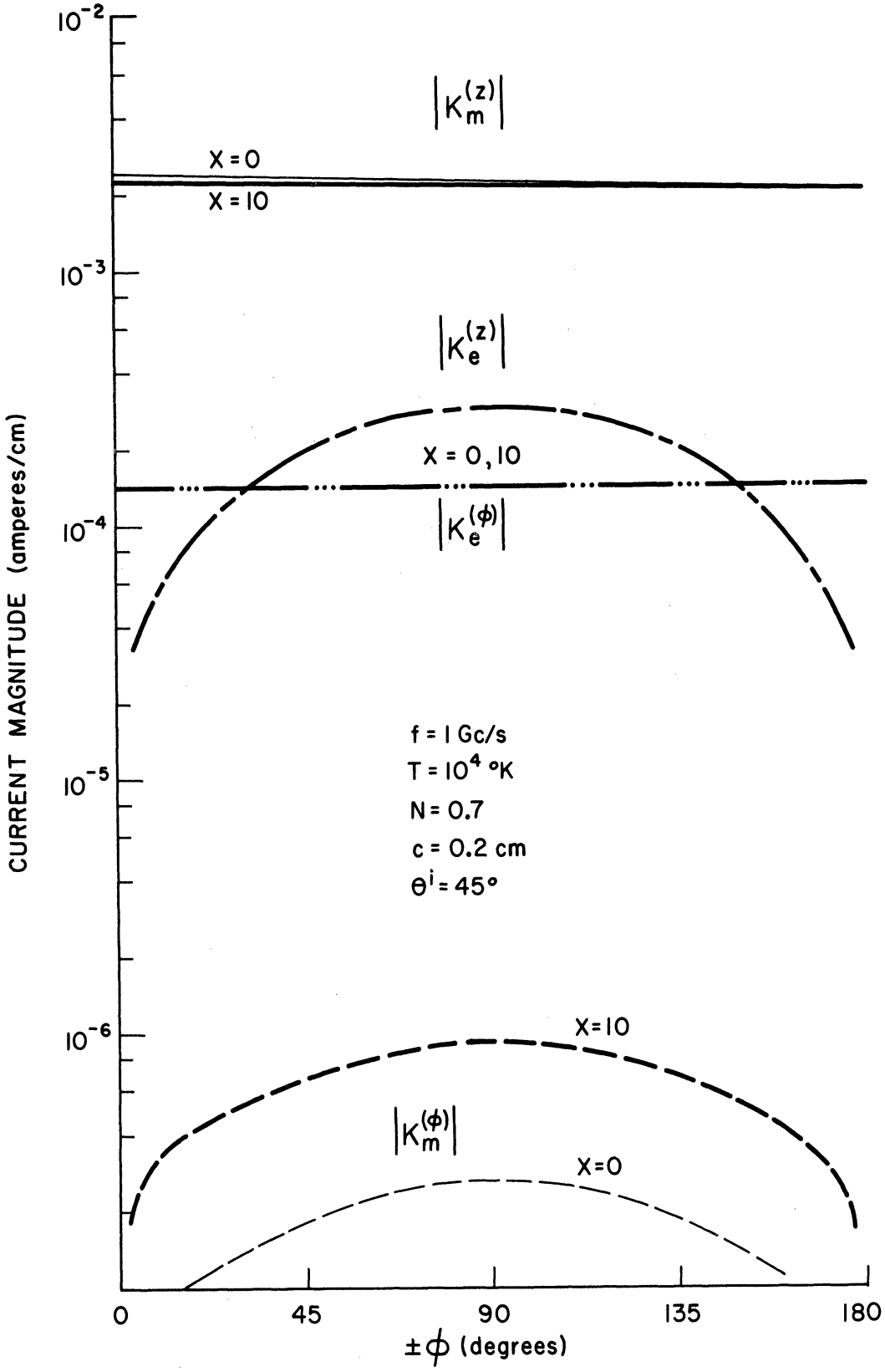

Figure C15. The magnitude of the currents excited by the EM wave as a function of azimuthal angle φ for $\theta^i = 45°$.

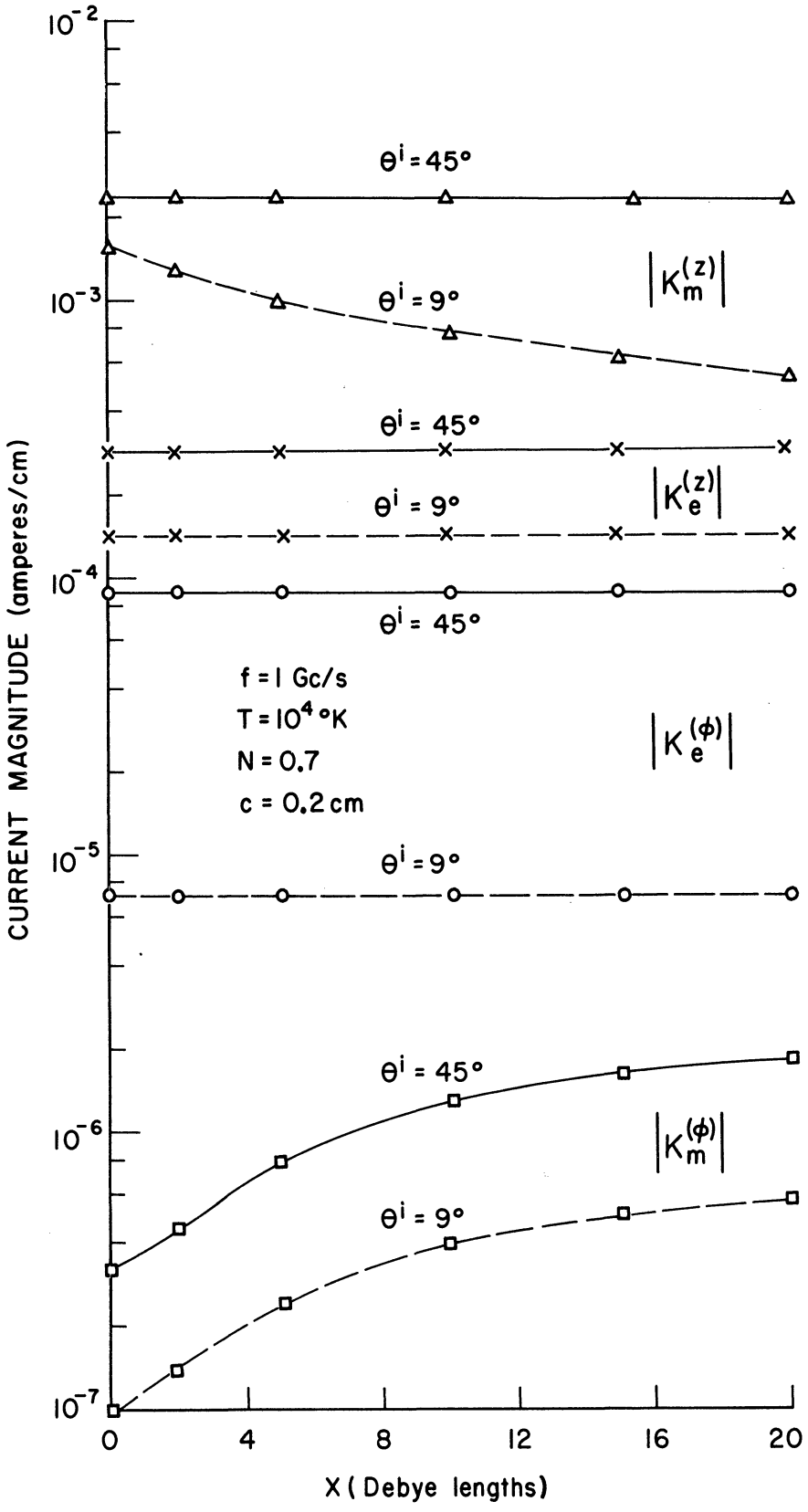

Figure C16. The magnitude of the maximum current values excited by the EM wave as a function of sheath thickness X.

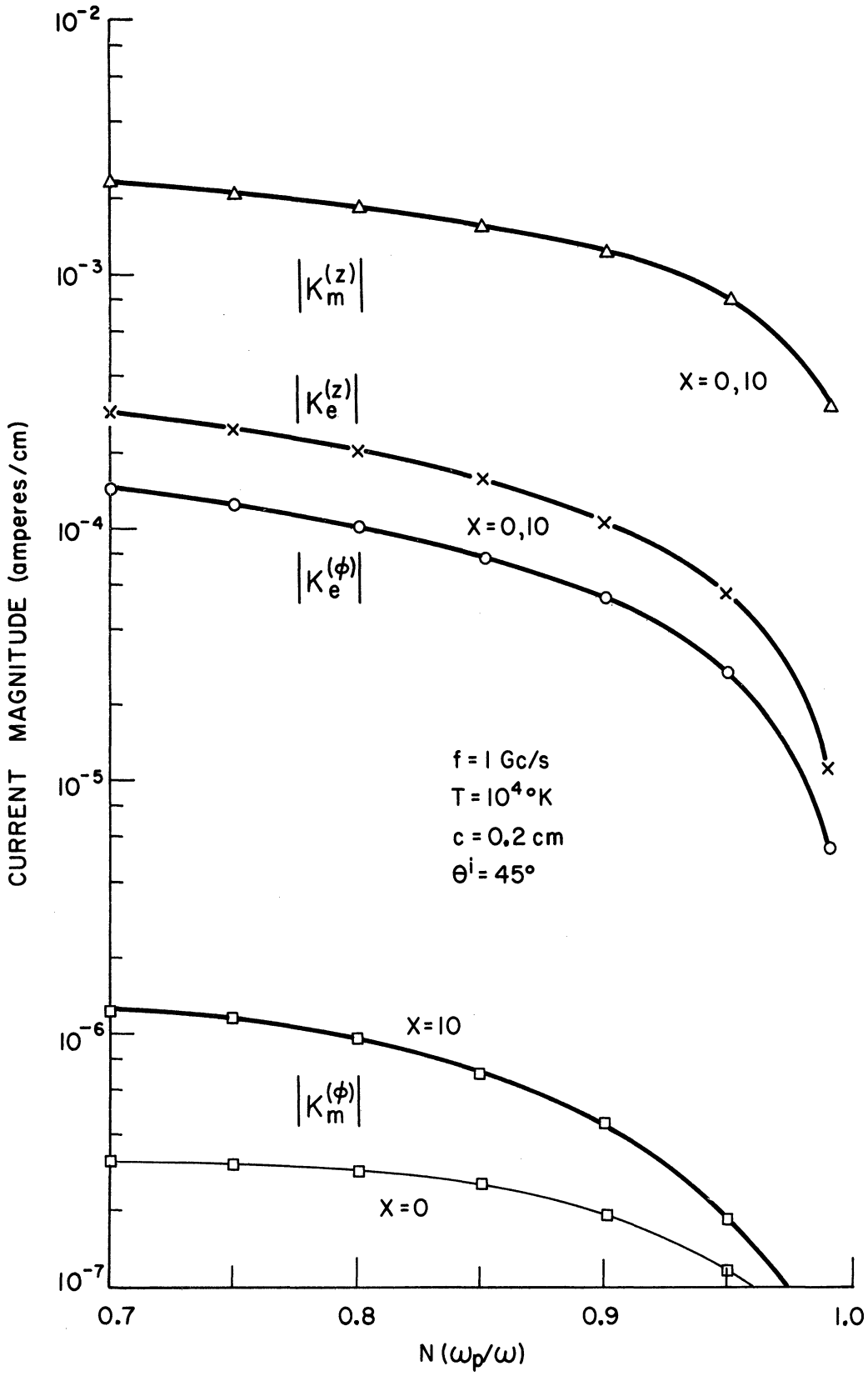

Figure C17. The magnitude of the maximum current values excited by the EM wave as a function of N.

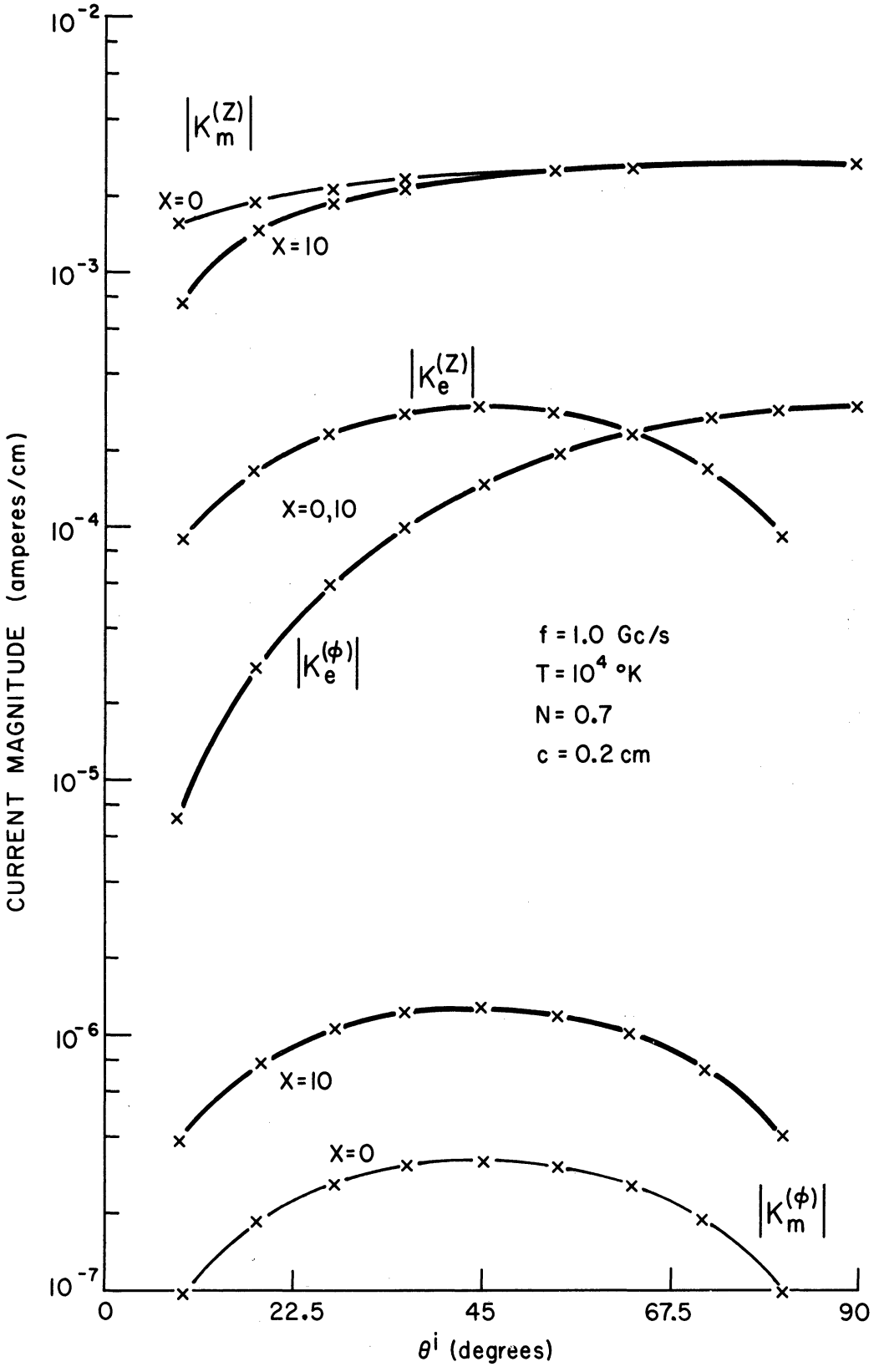

Figure C18. The magnitude of the maximum current values excited by the EM wave as a function of angle of incidence θ^i.

References

Allen, J. E., R. L. F. Boyd and P. Reynolds (1957), "The Collection of Positive Ions by a Probe Immersed in a Plasma, "Proc. Phy. Soc. of London 70, Pt. 3, 297-304.

Bernstein, I. B. and I. N. Rabinowitz (1959), Theory of Electrostatic Probes in a Low-Density Plasma, Phys. of Fluids 2, 112-121.

Chen, K. M. (1961) et. al., Studies in Non-Linear Modeling III: On the Interaction of Electromagnetic Fields with Plasma, Radiation Laboratory, Ann Arbor, Michigan Report 4134-2-F.

Collatz, L. (1960), The Numerical Treatment of Differential Equations Springer-Verlag, Berlin.

Cohen, M. H. (1962), Radiation in a Plasma III: Metal Boundaries Phys. Rev. 126, 398-404.

Field, G. B. (1956), Radiation by Plasma Oscillations, Astrophys. Journal 124, 555-570.

Fox, L. F., (1957), The Numerical Solution of Two-Point Boundary Problems in Ordinary Differential Equations, Oxford Press.

Gabor, D., E. A. Ash and D. Dracott (1955) Langmuir's Paradox, Nature 176, 916-919.

Gierke, E., W. Ott and F. Schwirzke (1961) Proc. Fifth Internat. Conf. on Ionized gases, Munich, Vol. 2, 1412.

Harp, R. and G. S. Kino (1963), Experiments on the Plasma Sheath, VIth International Conference on Ionization Phenomena in Gases, Paris France.

Hessel, A., N. Markuvitz and J. Shmoys (1962), Scattering and Guided Waves at an Interface Between Air and a Compressible Plasma, IRE Trans. AP-10, 48-54.

Hessel, A., and J. Shmoys (1962), Excitation of Plasma Waves by a Dipole in a Homogeneous Isotropic Plasma, Proc. Symposium on Electromagnetic and Fluid Dynamics of Gaseous Plasma, 173-183, (Polytechnic Press of Polytechnic Institute of Brooklyn, New York).

Hok, G. (1958), Electrokinetic and Electromagnetic Noise Waves in Electronic Waveguides, Proc. of Symp. on Electronic Wave Guides (Polytechnic Press of the Polytechnic Institute of Brooklyn).

Kritz, A. H. and D. Mintzer (1960), Propagation of Plasma Waves Across a Density Discontinuity, Phys. Rev. 117, 382-386.

Laframbois, J. (1964), Theory of Electrostatic Probes in Collisionless Plasma at Rest, Fourth International Symposium on Rarified Gases, Toronto.

Lam, S. H. (1964), The Langmuir Probe in a Collisionless Plasma, Aeronautical Eng. Dept., Princeton University Report No. 681.

Miller, E. K. (1965), The Excitation of Surface Currents on a Plasma-Immersed Cylinder by Incident Electromagnetic and Electrokinetic Waves, Ph. D. Thesis, University of Michigan.

Parker, J. V. (1963), Collisionless Plasma Sheath in Cylindrical Geometry, Phys. of Fluids 6, 1657-1658.

Parker, J. V., J. C. Nickel and R. W. Gould (1964), Reasonance Oscillations in a Hot Nonuniform Plasma, Phys. of Fluids 7, 1489-1500.

Self, S. A. (1963), Exact Solution of the Collisionless Plasma Sheath Equation, Phys. of Fluids 6, 1762-1768.

Seshadri, S. R., I. L. Morris and R. J. Mailoux (1964), Scattering by a Perfectly conducting Cylinder in a Compressible Plasma, Canadian J. of Physics, 42, No. 3, 465-576.

Seshadri, S. R. (1965a), Radiation in a Warm Plasma from an Electric Dipole with a Cylindrical Column of Insulation, IEEE, Trans. AP-13, No. 4, 613-629.

Seshadri, S. R. (1965b), Infinite Cylindrical Antenna Immersed in a Warm Plasma, IEEE, Trans. AP-13, No. 5, 789-799.

Tidman, D. A. and J. M. Boyd (1962), Radiation by Plasma Oscillations Incident on a Density Discontinuity, Phys. of Fluids 5, 213-218.

Tonks, L. and I. Langmuir (1929), General Theory of the Plasma of an Arc, Phys. Rev. 34, 876.

Wait, J. R. (1964a), Theory of a Slotted Sphere Antenna Immersed in a Compressible Plasma, Part I, Radio Sci. J. Res. NBS/USNC-URSI 68P, 1127-1136.

Wait, J. R. (1964b), Theory of a Slotted Sphere Antenna Immersed in a Compressible Plasma, Part II, Radio Sci. J. Res. NBS/USNC-URSI 68P, 1137-1143.

Wait, J. R. (1965a), On Radiation of Electromagnetic and Electroacoustic Waves in a Plasma, Appl. Sci. Res., Section B. Vol. 12, p. 1.

Wait, Jr. R. (1965b), Scattering of Electromagnetic and Electroacoustic Waves by a Cylindrical Object in a Compressible Plasma, Radio Sci. J. Res. NBS/USNC-URSI 69D, No. 2, 247-256.

Yildiz, A. (1963), Scattering of Plane Plasma Waves from a Plasma Sphere, Nuovo Cimento 30, 1182-1207.